TE
278
.S69
1991

FACTORS AFFECTING DETERIORATION OF TRANSVERSE CRACKS IN JOINTED REINFORCED CONCRETE PAVEMENTS

Final Report - Year 1

Prepared for

Michigan Department of Transportation
and
Great Lakes Center for Truck Transportation Research
University of Michigan Transportation Research Institute
U. S. Department of Transportation

by
Mark B. Snyder
and
Zafar I. Raja

LIBRARY
M.D.O.T.
RESEARCH LABORATORY
MATERIALS & TECHNOLOGY
DIVISION

Michigan State University
Department of Civil and Environmental Engineering
East Lansing, Michigan 48824-1226

January, 1991

FACTORS AFFECTING DETERIORATION OF TRANSVERSE CRACKS IN JOINTED REINFORCED CONCRETE PAVEMENTS

Final Report - Year 1

Prepared for

Michigan Department of Transportation
and
Great Lakes Center for Truck Transportation Research
University of Michigan Transportation Research Institute
U. S. Department of Transportation

by
Mark B. Snyder
and
Zafar I. Raja

Michigan State University
Department of Civil and Environmental Engineering
East Lansing, Michigan 48824-1226

January, 1991

ACKNOWLEDGEMENTS

This work was sponsored by the Michigan Department of Transportation and the Great Lakes Center for Truck Transportation, which is administered by the University of Michigan Transportation Research Institute for the Federal Highway Administration.

The following persons are gratefully acknowledged for their contributions to this research effort:

Mr. C.J. Arnold and Dr. Gail Grove of the Michigan Department of Transportation Materials and Technology Division for their expertise and assistance throughout the project;

Dr. Frank Hatfield of the Michigan State University Department of Civil and Environmental Engineering for his assistance in the structural design and analysis (both static and dynamic) of the project test stand;

Mr. J.C. Brenton, the MSU Civil and Environmental Engineering lab technician, whose fabricating, welding, and general scavenging expertise helped us out of more than one tight spot;

Mr. Mickey McGhee and Mr. Steve Lemons of Holloway Construction for their generous cooperation in the processing of the recycled aggregates that were necessary

for the project work;

Mr. Dave Fredline, Mr. Scott Johnson and the other employees at the Michigan DOT Grand Ledge maintenance facility who assisted in transporting materials to and from the recycling plant;

Mr. Bob George of MTS and the people at the MTS "HELPLINE" for their guidance in setting up and operating the truck load simulation portion of the test stand;

Dr. Gary Cloud of the Michigan State University Department of Metallurgy, Mechanics, and Materials Science for lending his expertise in the selection and use of strain gages to this project;

All of the graduate and undergraduate students who hauled literally tons of aggregate, cement, fresh concrete, and broken concrete, and assisted in the design, erection, and maintenance of the test stand components, and performed other dirty little tasks too numerous to mention. These people include Ramez Butros, Doug Gatrell, "Edward" Hua Guo, Julia Hoogerwerf, Jer-Wen Hsu, Dave Jeakle, Shamshad Khan, Ken Kucel, Gary Mekjian, Michael Miller, Fred Nazar, Jeni Nolan, Greg Soehnlen, Keith Ward, Jack Wheatley, Brad Weiferich, and Geoff Wilkie.

DISCLAIMER

The opinions, findings, and conclusions expressed or implied in this publication are those of the authors and are not necessarily those of the Michigan State Transportation Commission, the Michigan Department of Transportation, or the Great Lakes Center for Truck Transportation Research.

TABLE OF CONTENTS

	page
ABSTRACT	1
INTRODUCTION	2
BACKGROUND	3
TEST EQUIPMENT	6
Test Specimen Loading System	6
Test Specimen Tensioning System	12
Test Specimen Support System	12
LOAD SIMULATION	13
Loading due to Truck Traffic	13
Loading due to Environment	15
INSTRUMENTATION AND DATA COLLECTION	16
TEST MATERIALS	19
Artificial Foundation	19
Portland Cement Concrete Slabs	20
TEST PROCEDURE	23
TEST RESULTS	28
Effect of Type of Coarse Aggregate	30
Effect of Gradation of Coarse Aggregate	33
Effect of Treatment of Coarse Aggregate	35
CONCLUSIONS AND RECOMMENDATIONS	40
REFERENCES	43
APPENDIX: LOAD-DEFLECTION HISTORIES OF TEST SPECIMENS	46

LIST OF TABLES

Table		page
1.	Laboratory Study Factors	5
2.	Mix Characteristics and Concrete Properties	21
3.	Physical Characteristics of Concrete Aggregates	21
4.	Coarse Aggregate Gradation of 6A Materials	24
5.	Coarse Aggregate Gradation of 17A Material	24
6.	Coarse Aggregate Gradation of 4A Material	25

LIST OF FIGURES

Figure		page
1.	Test Matrix A	7
2.	Test Matrix B	8
3.	Test Matrix C	9
4.	Test Stand	10
5.	Test Specimen Loading System	11
6.	Test Specimen Tensioning System	11
7.	Load Profile	14
8.	Test Specimen Instrumentation	17
9.	Test Control and Data Acquisition Setup	18
10.	Strength Gain Curves of the Test Specimens	22
11.	A View of a Failed Specimen	29
12.	Effect of Coarse Aggregate Type on the Relation Between LTE% and Number of Load Cycles	31
13.	Exposed Crack Faces of Small Test Specimens, Varying Coarse Aggregate Type, 6A Gradation Materials	32
14.	Effect of Coarse Aggregate Type on the Relation Between Peak Deflection and Number of Load Cycles	34
15.	Effect of Coarse Aggregate Gradation on the Relation Between LTE% and Number of Load Cycles	36
16.	Effect of Coarse Aggregate Treatment on the Relation Between LTE% and Number of Load Cycles	38
17.	Exposed Crack Face of 100% Recycled Gravel Concrete Specimen After Loading	39

LIST OF FIGURES (Continued)

Figure		page
A-1.	Load and Deflection Curves for 6A Virgin Gravel Slab after Cycle # 1	47
A-2.	Load and Deflection Curves for 6A Virgin Gravel Slab after Cycle # 1,000	48
A-3.	Load and Deflection Curves for 6A Virgin Gravel Slab after Cycle # 2,000	49
A-4.	Load and Deflection Curves for 6A Virgin Gravel Slab after Cycle # 5,000	50
A-5.	Load and Deflection Curves for 6A Virgin Gravel Slab after Cycle # 20,000	51
A-6.	Load and Deflection Curves for 6A Virgin Gravel Slab after Cycle # 50,000	52
A-7.	Load and Deflection Curves for 6A Virgin Gravel Slab after Cycle # 100,000	53
A-8.	Load and Deflection Curves for 6A Virgin Gravel Slab after Cycle # 300,000	54
A-9.	Load and Deflection Curves for 6A Virgin Gravel Slab after Cycle # 600,000	55
A-10.	Load and Deflection Curves for 6A Virgin Gravel Slab after Cycle # 900,000	56
A-11.	Load and Deflection Curves for 6A Virgin Limestone Slab after Cycle # 1	57

LIST OF FIGURES (Continued)

Figure		page
A-12.	Load and Deflection Curves for 6A Virgin Limestone Slab after Cycle # 1,000	58
A-13.	Load and Deflection Curves for 6A Virgin Limestone Slab after Cycle # 2,000	59
A-14.	Load and Deflection Curves for 6A Virgin Limestone Slab after Cycle # 5,000	60
A-15.	Load and Deflection Curves for 6A Virgin Limestone Slab after Cycle # 10,000	61
A-16.	Load and Deflection Curves for 6A Virgin Limestone Slab after Cycle # 20,000	62
A-17.	Load and Deflection Curves for 6A Virgin Limestone Slab after Cycle # 50,000	63
A-18.	Load and Deflection Curves for 6A Virgin Limestone Slab after Cycle # 100,000	64
A-19.	Load and Deflection Curves for 6A Virgin Limestone Slab after Cycle # 300,000	65
A-20.	Load and Deflection Curves for 6A Virgin Limestone Slab after Cycle # 600,000	66
A-21.	Load and Deflection Curves for 6A Virgin Limestone Slab after Cycle # 900,000	67
A-22.	Load and Deflection Curves for 6A Virgin Limestone Slab after Cycle # 1,500,000	68

LIST OF FIGURES (Continued)

Figure		page
A-23.	Load and Deflection Curves for 6A Virgin Slag Slab after Cycle # 1	69
A-24.	Load and Deflection Curves for 6A Virgin Slag Slab after Cycle # 1,000	70
A-25.	Load and Deflection Curves for 6A Virgin Slag Slab after Cycle # 2,000	71
A-26.	Load and Deflection Curves for 6A Virgin Slag Slab after Cycle # 5,000	72
A-27.	Load and Deflection Curves for 6A Virgin Slag Slab after Cycle # 10,000	73
A-28.	Load and Deflection Curves for 6A Virgin Slag Slab after Cycle # 20,000	74
A-29.	Load and Deflection Curves for 6A Virgin Slag Slab after Cycle # 50,000	75
A-30.	Load and Deflection Curves for 6A Virgin Slag Slab after Cycle # 100,000	76
A-31.	Load and Deflection Curves for 6A Virgin Slag Slab after Cycle # 250,000	77
A-32.	Load and Deflection Curves for 17A Virgin Gravel Slab after Cycle # 1	78
A-33.	Load and Deflection Curves for 17A Virgin Gravel Slab after Cycle # 1,000	79

LIST OF FIGURES (Continued)

Figure	page
A-34. Load and Deflection Curves for 17A Virgin Gravel Slab after Cycle # 2,000	80
A-35. Load and Deflection Curves for 17A Virgin Gravel Slab after Cycle # 5,000	81
A-36. Load and Deflection Curves for 17A Virgin Gravel Slab after Cycle # 10,000	82
A-37. Load and Deflection Curves for 17A Virgin Gravel Slab after Cycle # 20,000	83
A-38. Load and Deflection Curves for 17A Virgin Gravel Slab after Cycle # 50,000	84
A-39. Load and Deflection Curves for 17A Virgin Gravel Slab after Cycle # 100,000	85
A-40. Load and Deflection Curves for 17A Virgin Gravel Slab after Cycle # 300,000	86
A-41. Load and Deflection Curves for 17A Virgin Gravel Slab after Cycle # 600,000	87
A-42. Load and Deflection Curves for 17A Virgin Gravel Slab after Cycle # 900,000	88
A-43. Load and Deflection Curves for 6A 100% Recycled Gravel Slab after Cycle # 1	89
A-44. Load and Deflection Curves for 6A 100% Recycled Gravel Slab after Cycle # 1,000	90

LIST OF FIGURES (Continued)

Figure	page
A-45. Load and Deflection Curves for 6A 100% Recycled Gravel Slab after Cycle # 2,000	91
A-46. Load and Deflection Curves for 6A 100% Recycled Gravel Slab after Cycle # 5,000	92
A-47. Load and Deflection Curves for 6A 100% Recycled Gravel Slab after Cycle # 10,000	93
A-48. Load and Deflection Curves for 6A 100% Recycled Gravel Slab after Cycle # 20,000	94
A-49. Load and Deflection Curves for 6A 100% Recycled Gravel Slab after Cycle # 50,000	95
A-50. Load and Deflection Curves for 6A 100% Recycled Gravel Slab after Cycle # 100,000	96
A-51. Load and Deflection Curves for 6A 100% Recycled Gravel Slab after Cycle # 300,000	97
A-52. Load and Deflection Curves for 50-50 Recycle Blend Slab after Cycle # 1	98
A-53. Load and Deflection Curves for 50-50 Recycle Blend Slab after Cycle # 1,000	99
A-54. Load and Deflection Curves for 50-50 Recycle Blend Slab after Cycle # 5,000	100
A-55. Load and Deflection Curves for 50-50 Recycle Blend Slab after Cycle # 10,000	101

LIST OF FIGURES (Continued)

Figure page

A-56. Load and Deflection Curves for 50-50 Recycle Blend Slab after Cycle # 20,000 102

A-57. Load and Deflection Curves for 50-50 Recycle Blend Slab after Cycle # 50,000 103

A-58. Load and Deflection Curves for 50-50 Recycle Blend Slab after Cycle # 100,000 104

A-59. Load and Deflection Curves for 50-50 Recycle Blend Slab after Cycle # 300,000 105

A-60. Load and Deflection Curves for 50-50 Recycle Blend Slab after Cycle # 350,000 106

FACTORS AFFECTING DETERIORATION OF TRANSVERSE CRACKS IN JOINTED REINFORCED CONCRETE PAVEMENTS

By

Mark B. Snyder[1] and Zafar I. Raja[2]

ABSTRACT

Jointed Reinforced Concrete Pavement (JRCP) develops transverse cracks as the drying and thermal shrinkage of the concrete is resisted by friction with the supporting layers. These cracks deteriorate with time and traffic due to loss of aggregate-interlock load transfer capacity. However, rapid deterioration of these cracks has been observed on some recently-constructed projects in Michigan. This rapid crack deterioration leads to accelerated maintenance requirements and shortened service lives.

This research report describes the first year of a laboratory investigation to determine the relative effects of a few selected factors (coarse aggregate type, gradation, and treatment) on transverse crack deterioration in JRCP. The work described herein focused on the development, execution, collection and analysis of load transfer data from the testing of a series of large-scale pavement test specimens that were

---

[1]Principal Investigator: Assistant Professor, Department of Civil and Environmental Engineering, Michigan State University, A349 Engineering Building, East Lansing, MI 48824-1226.

[2]Associate Investigator: Graduate Research Assistant, Department of Civil and Environmental Engineering, Michigan State University, A349 Engineering Building, East Lansing, MI 48824-1226.

subjected to repeated applications of loads simulating the passage of heavy truck traffic.

Test results indicate that slabs cast using crushed limestone and natural gravel graded to meet Michigan Department of Transportation (MDOT) specification 6A (1.5 in. [4 cm] top size, coarser gradation) perform comparably while specimens cast using similarly graded slag deteriorate much more rapidly. The use of more finely graded gravels meeting MDOT specification 17A (1.0 in. [2.5 cm] top size, finer gradation) resulted in a performance only slightly worse than that of the larger gravel. Finally, specimens using 100% recycled gravel concrete (6A Gradation) or a blend of recycled gravel concrete (6A Gradation) and large crushed limestone (MDOT Gradation 4A: 2.5 in. [6 cm] top size) performed only slightly better than the slag specimen. Test results also suggest that the amount of temperature steel currently used in Michigan JRCP (0.17% by area of concrete) may be insufficient to endure the combined effects of repeated truck traffic and environmental loads.

INTRODUCTION

Jointed reinforced concrete pavement (JRCP) typically develops transverse cracks over the first several years of its service life as contractions of the slab (caused by combinations of drying and thermal shrinkage) are restrained by friction between the slab and supporting layers. Transverse cracks may also be initiated by combinations of curling, warping, and

load-related stresses. Most JRCP designs rely on aggregate or grain interlock to transfer shear loads across these cracks. The loss of aggregate interlock due to opening of these cracks permits increased slab deflections, and may be accompanied by the infiltration of water and the intrusion of incompressibles into the cracks. These, in turn, lead to pumping and crack deterioration through faulting and spalling. Continued pumping eventually leads to a loss of slab support, which greatly increases load-related stresses in the slab and can result in fatigue cracking. Thus, transverse cracks must exhibit good long-term load transfer characteristics to minimize the development and severity of the distresses described above.

This research report describes a portion of a laboratory investigation to determine the effects of a few selected factors on JRCP transverse crack performance. The research program included development and execution of a laboratory experiment involving the collection and analysis of load transfer data from the testing of a series of large-scale pavement test specimens that were subjected to repeated applications of loads simulating the passage of heavy truck traffic.

BACKGROUND

The Michigan Department of Transportation (MDOT) has reconstructed several major Interstate projects (using recycled concrete as aggregates) since 1983 [1]. It was recently observed that some of these newer JRCP were exhibiting rapid transverse

crack deterioration (spalling and faulting), which may lead to increased maintenance requirements and shortened service lives. A preliminary evaluation of the causes of deterioration of these cracks suggested that the use of small-sized recycled concrete aggregates might be a major contributor to the crack deterioration [2].

Tests of the gravel used in the original construction had shown it to have poor freeze-thaw durability. In order to improve the durability of the new pavement sections, the coarse aggregate produced by recycling old pavement sections was crushed to a smaller top size (1.0 in. [2.5 cm] or less, in accordance with MDOT gradation 17A). This course of action was chosen in accordance with the concept that the propensity of an aggregate to manifest durability-related distress is diminished by reducing its average particle size. However, reduction in coarse aggregate top size may adversely affect the aggregate interlock load transfer characteristics of the crack faces. Moreover, coarse aggregates produced by recycling concrete may also exhibit very different bonding characteristics with cement paste due to local variations in the water-cement ratio caused by the non-uniform (and sometimes high) moisture absorption characteristics of these aggregates. Thus, these aggregates may fracture differently (and more readily) than virgin aggregates, producing unusual crack face textures. This theory may help explain why cores taken by MDOT at cracks along some of the previously described prematurely damaged projects have shown very straight vertical crack faces with very little roughness or

meander.

In addition to above factors, a large number of other factors have been identified which may have an impact on the rate of deterioration of transverse cracks in JRCP [3,4]. However, *the scope of the first year of this study was limited to include only coarse aggregate-related factors* due to financial and time restraints. Discussions with MDOT researchers suggested consideration of the variables and test levels shown in table 1.

Table 1: Laboratory Study Factors

Variable	Test Level		
	1	2	3
CA Type	Gravel	Limestone	Slag
CA Gradation	6A	17A	-
CA Treatment	Virgin	Recycle Blend	100% Recycled

Notes:
1. 6A gradation - (1.5 in. [4 cm] top size, coarser gradation)
2. 17A gradation - (1.0 in. [2.5 cm] top size, finer gradation)
3. Recycle blend - 50-50 blend of 6A recycled gravel concrete with 4A (2.5 in. [6 cm] top size) crushed limestone
4. 100% recycled gravel concrete - graded to meet MDOT 6A specification

A full-factorial, unreplicated experimental design using these variables and test levels would require 18 test specimens. Since it was desirable to obtain preliminary measures of the main effects of these variables as quickly as possible, it was decided that this work effort should focus on a few selected cells. An unreplicated comparative experiment was designed for laboratory testing to provide an indication of the three main effects of the variables described above (figures 1-3).

TEST EQUIPMENT

For this research it was necessary to develop equipment to apply repetitive loads of known magnitude across a transverse crack in a manner closely simulating field loading conditions. A test setup was developed similar to the apparatus used in the joint load transfer research conducted by Teller and Cashell in the 1950's [5], Colley and Humphrey in the 1960's [6], Ball and Childs, and Ciolko and Colley in the 1970's [7,8]. The test stand (shown in figure 4) consists of three basic components and is described below:

Test Specimen Loading System

The test stand allows the application of a known repetitive load profile to the test specimen. This is accomplished using a pair of hydraulic actuators (11-kip [5000-kg] capacity) which react against a structural steel frame (see figure 5). The load

MATRIX A

CA TYPE	GRAVEL	X
	LIMESTONE	X
	SLAG	X

Notes:
1. X = Test cell being tested under matrix A
2. All coarse aggregates conform to MDOT gradation 6A
3. Foundation modulus = 100 psi/in.
4. Slab tension = 3500 lb/ft width [51 KN/m width] (modelling an assumed coefficient of friction = 1.5, slab length = 41 ft. [12.5 m], crack face depth = 9 in. [23 cm])
5. Longitudinal steel = 0.17% by area of concrete

Figure 1: Test Matrix A

MATRIX B

CA GRADATION	6A	A
	17A	X

Notes:
1. A = Test cell first filled in matrix A
2. X = Test cell being tested under matrix B
3. Foundation modulus = 100 psi/in.
4. Slab tension = 3500 lb/ft width [51 KN/m width] (coefficient of friction = 1.5, slab length = 41 ft. [12.5 m], crack face depth = 9 in. [23 cm])
5. Longitudinal steel = 0.17% by area of concrete

Figure 2: Test Matrix B

MATRIX C

CA TREATMENT	VIRGIN	A
	RECYCLE BLEND	X
	100% RECYCLED	X

Notes:
1. A = Test cell first filled in matrix A
2. X = Test cell being tested under matrix C
3. Foundation modulus = 100 psi/in.
4. Slab tension = 3500 lb/ft width [51 KN/m width] (coefficient of friction = 1.5, slab length = 41 ft. [12.5 m], crack face depth = 9 in. [23 cm])
5. Longitudinal steel = 0.17% by area of concrete

Figure 3: Test Matrix C

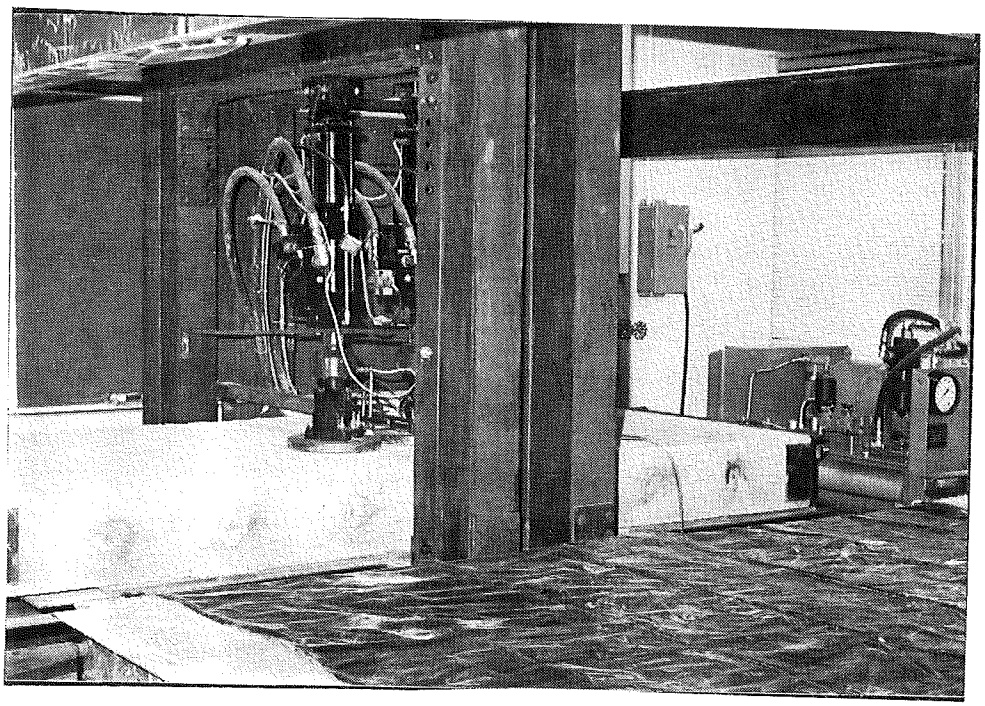

Figure 4: Test Stand

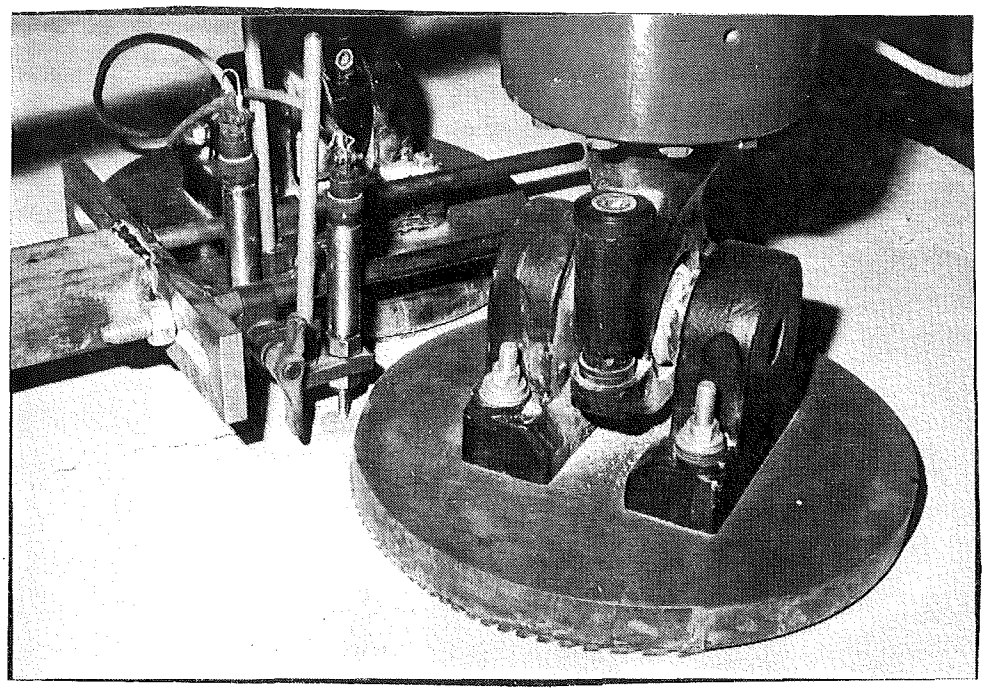

Figure 5: Test Specimen Loading System

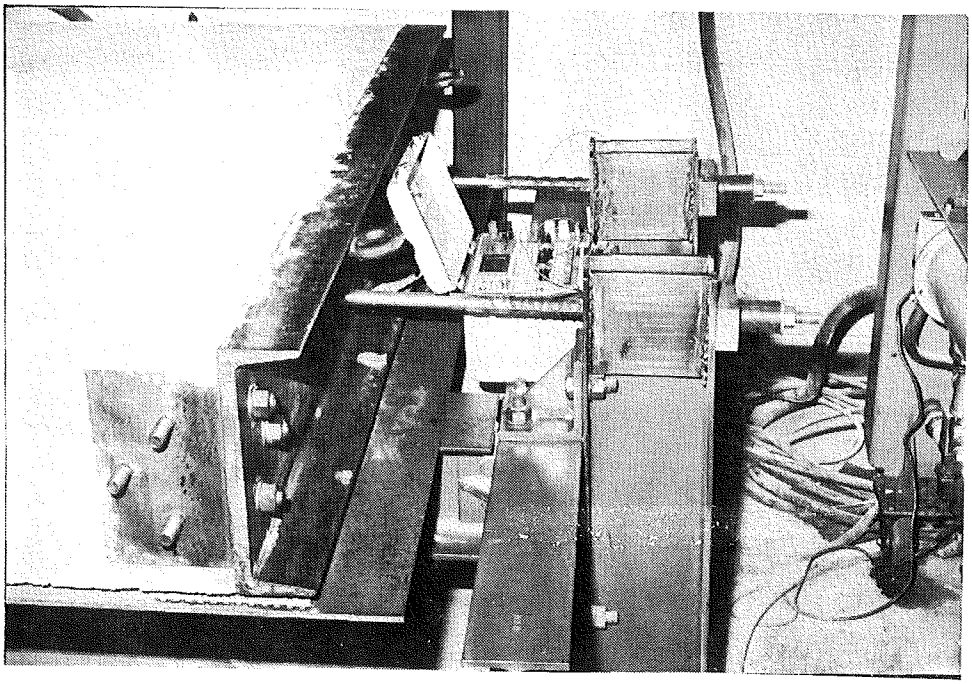

Figure 6: Test Specimen Tensioning System

is transmitted to the test specimen by a pair of 12 in. [30 cm] diameter, 1.0 in. [2.54 cm] thick steel plates, each resting on a 1/4 in. [5/8 cm] contact rubber pad. The plates are positioned on each side of the crack with their centers 7 in. [18 cm] from the crack and 18 in. [46 cm] from the slab edge.

Test Specimen Tensioning System

The test stand allows the slabs to be placed in tension prior to and during testing to simulate the effects of resistance to thermal and drying shrinkage and restraint caused by improperly functioning load transfer dowel bars at transverse joints in the field. To induce tension, two steel rods with threaded ends anchored in each end of the slab are connected through threaded couplings to crossplates at the end columns (see figure 6). Tightening the nuts on the threaded ends places the slab in tension; this tension is carried through steel at the transverse crack. This system also helps to reduce movement of the slabs under dynamic loads and helps to simulate the continuity of longer slabs in the field.

Test Specimen Support System

The test stand provides approximately uniform support for the specimen through the use of an artificial foundation (neoprene vibration isolation padding) resting on a steel plate which is supported by structural steel sections. The steel

sections are connected to the reaction frame in such a way that the test frame absorbs the simulated truck loadings in tension

In addition, test specimen casting frames, a handling frame (for transporting the large slabs in the laboratory), and a cracking frame (for inducing transverse cracks in the specimens) were designed, fabricated, and erected for this research work.

LOAD SIMULATION

Loading due to Truck Traffic

The hydraulic actuators were programmed to apply a sequence of load pulses to rubber contact pads (simulating 12 in. [30 cm] tire imprint areas) on the approach and leave sides of the crack to simulate field loading conditions for the outer wheel path of a highway pavement. The maximum applied load was 9000 lbs [40 KN] (one-half of a standard 18000-lb [80 KN] single-axle load). Throughout repetitive loading, a minimum static load of 500 lbs [2.3 KN] was applied through each actuator to maintain contact between the load plates and the slab throughout the test program.

A composite sinusoidal load profile was generated (using MTS T/RAC software) to simulate a wheel crossing the crack at 55 mph [88 km/hr] (figure 7). To simulate a wheel approaching a crack, the load applied to the the approach side is increased from the static load to the peak dynamic load in 0.0125 seconds. The load on the approach side is then reduced to the static load while

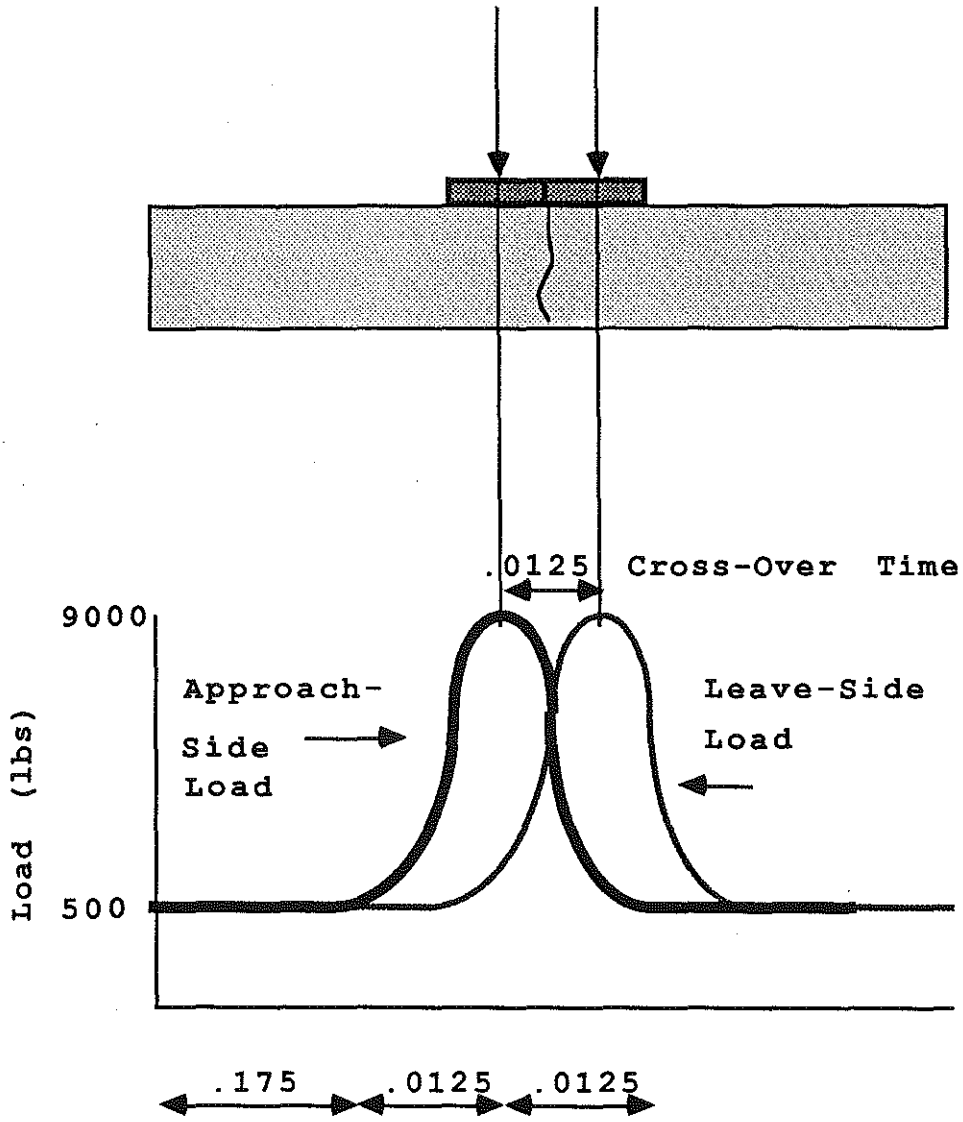

Not to Scale

Note: 1 lb = 0.4536 kg

Figure 7: Load Profile

the load on the departure side is simultaneously increased from the static load to the peak dynamic load in 0.0125 seconds. This cross-over interval of 0.0125 second would permit a tire making a 12 in. [30 cm] imprint and travelling 55 mph [88 km/hr] to move completely across the crack. To simulate a wheel moving away from the crack, the load on the departure side is reduced to the static load in 0.0125 second while the approach load is held at the static load. The static load is then maintained for 0.175 second before the cycle is repeated. Thus, one full load cycle takes 0.2 second, resulting in a load application frequency of 5 Hz. This allows the application of 432,000 load cycles per day.

Loading due to Environment

Each test specimen is placed in tension just prior to testing to simulate the effects of foundation frictional resistance to thermal and drying shrinkage and restraint caused by improperly functioning load transfer dowel bars at transverse joints in the field. This slab tension may open the transverse cracks, exacerbating the effects of repeated heavy loads. The amount of tension was computed from subgrade drag theory for an assumed coefficient of frictional resistance of 1.5 and for a 9 in. [23 cm] slab measuring 41 ft [12.5 m] in length by 4.5 ft [1.4 m] wide. A tension of approximately 16000 lbs [71.3 KN] (3500 lbs/ft width) [51 KN/m width] was induced in the test specimens by adjusting the two tensioning bars embedded in each

test specimen and monitoring tension bar strain with the strain gages.

INSTRUMENTATION AND DATA COLLECTION

Test specimens were instrumented for measurements of crack openings, deflections under loading, and tensile strains (tensioning). Instrument locations are shown in figure 8. Gage plugs and a vernier caliper were used to monitor crack openings. Linearly variable deflection transducers (LVDT's) were used for measuring deflections on either side of the crack. General purpose CEA-series strain gages were used to measure strain in the tensioning bars, thereby monitoring the amount of tension in the specimen.

All testing and data collection operations were controlled using a 286-based personal computer equipped with a data acquisition system (Metrabyte I/O board and Labtech Notebook software). This system was connected directly to the hydraulic actuator control panel (MTS T/RAC controller) and signal conditioners. The arrangement, shown in figure 9, allowed the coordinated control of both hydraulic actuators, as well as the collection of load data from both actuators and deflection data from two external LVDT's. The load and deflection data were collected following the completion of 1, 2000, 5000, 10000, 20000, 50000, 100000, 300000, 600000, 900000, and 1500000 load applications. Each data collection channel was sampled 250 times per load cycle (about 1 sample per channel every 0.0008

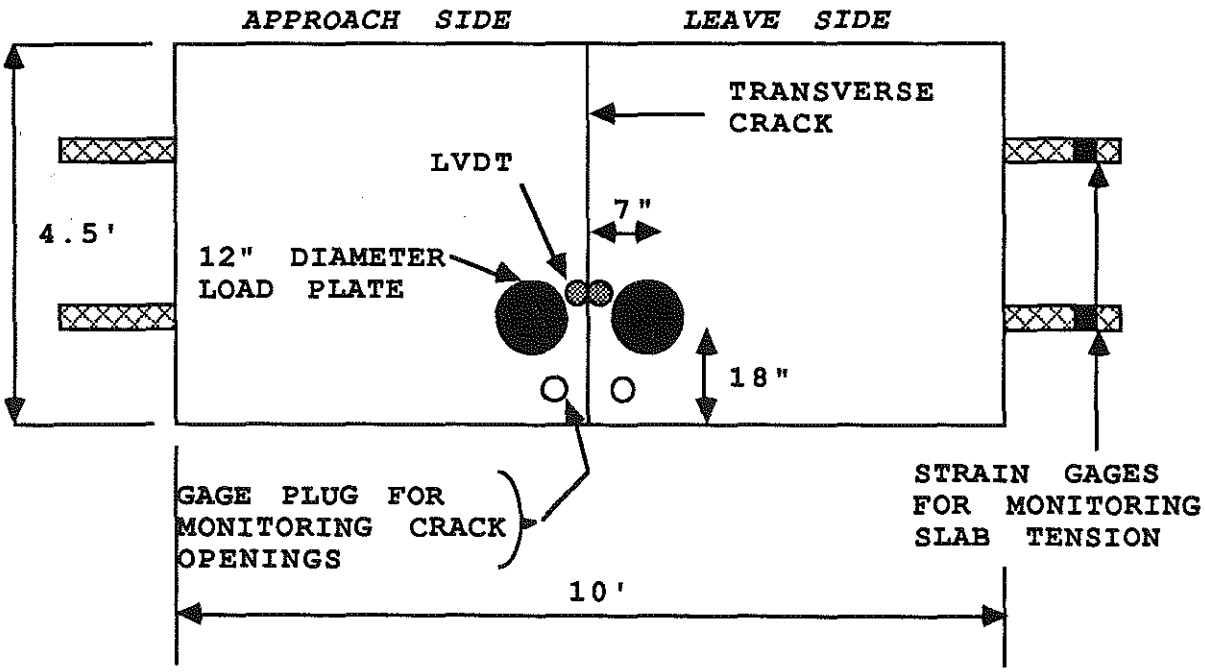

Note: 1 in = 2.54 cm

1 ft = 0.3048 m

Figure 8: Test Specimen Instrumentation

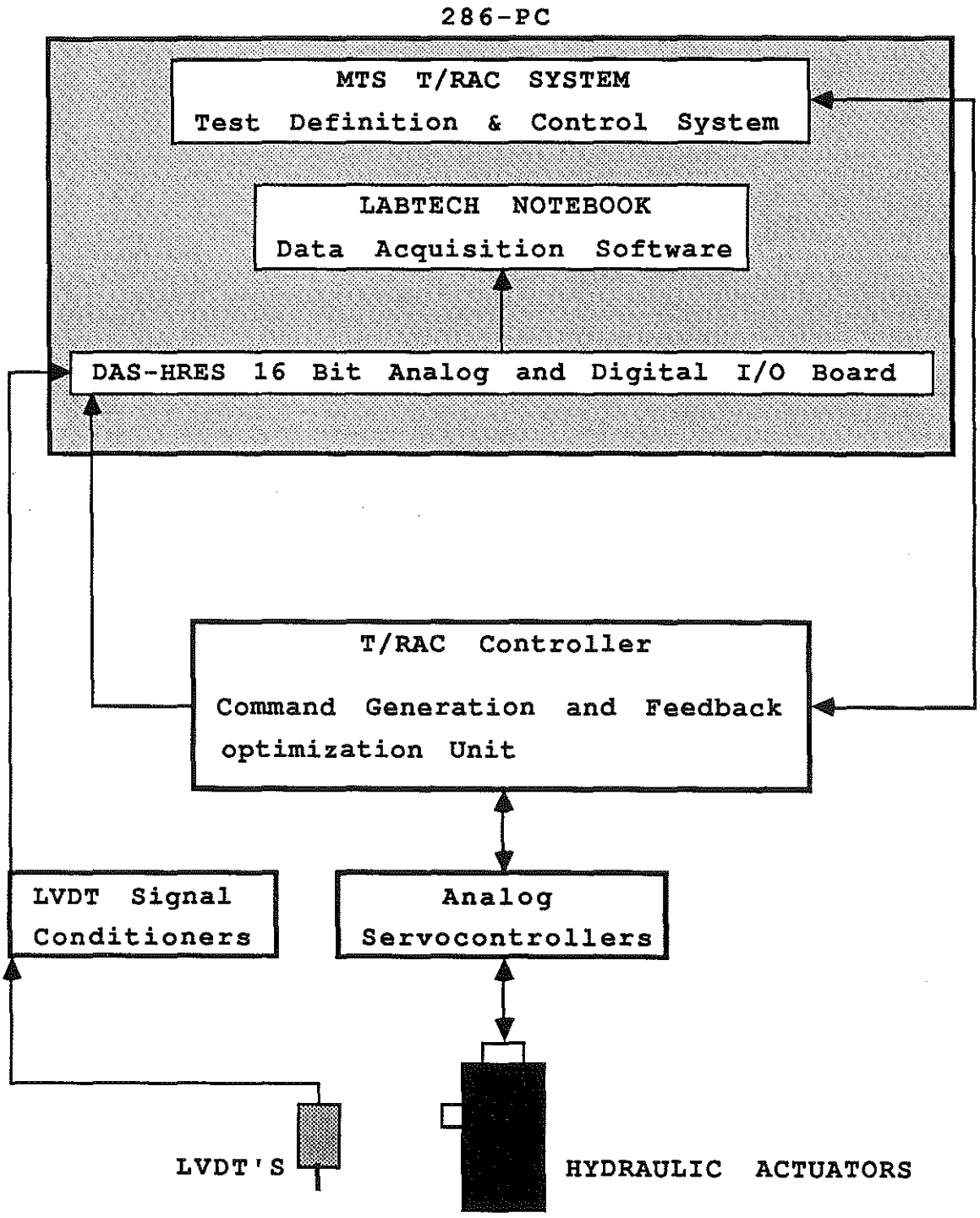

Figure 9: Test Control and Data Acquisition Setup

seconds). Each data collection stage lasted one second (5 load cycles). This sampling rate and stage duration provided sufficiently close data points for plotting smooth curves and identifying peak loads and deflections (see APPENDIX A). In this report, unless otherwise noted, all data pertaining to loads and relative deflections are based on the average of 5 sets of measurements.

TEST MATERIALS

Artificial Foundation

Each test specimen was provided approximately uniform support through the use of an artificial foundation (FABCEL vibration isolation padding rated at specific "k" values). Since it is difficult to reproduce foundation properties accurately and consistently using real granular materials and this can introduce variability in test results, it was decided to use artificial material for the foundation support. FABCEL is a high quality neoprene, molded into scientifically designed pads measuring 18" x 18" x 5/16" [46 cm x 46 cm x 3/4 cm]. The pad surfaces have molded recessed offset-cells to allow the neoprene to deform under load while maintaining lateral stability. Desired levels of foundation support are achieved by providing various thickness and type combinations of these pads. Three layers of FABCEL-25 were used to provide a foundation with a simulated modulus of subgrade reaction of approximately 100

psi/in [27 Kpa/m] under the entire test specimen.

Portland Cement Concrete Slabs

The test specimens were PCC slabs measuring approximately 10 ft [12.5 m] long by 4.5 ft [1.4 m] wide and 9 in. [23 cm] thick at the crack. The cracks were of the plane-of-weakness type where load transfer is achieved solely by aggregate interlock. Each specimen contained 8 ft x 4 ft [2.8 m x 1.2 m] of smooth steel wire mesh reinforcment (0.17% by area of concrete longitudinally) placed 3 in. [7.5 cm] below the slab surface. This reinforcment was typical of the size, quantity and type used in Michigan JRCP construction.

The test program required the design of six concrete mixes. Mix designs provided by MDOT (mortar voids method of proportioning) were used as a starting point for trial batching to reach a final mix design (target slump 2-3 inches, air content 6-7 percent). Type I portland cement was used in each mix (cement factor of approximately six sacks per cubic yard of concrete). Air entrainment was provided through the addition of Microair air-entraining admixture. Table 2 shows the mix characteristics and other properties of the test specimens. Figure 10 shows the average age-strength relationship of compression cylinders cast from the same mixes as the six test specimens.

Three types of virgin coarse aggregates were used in the concrete. One was natural gravel with rounded particles and

Table 2: Mix Characteristics and Concrete Properties

Test Specimens	Mix Proportions (oven-dry weights) CA:FA:WATER:CEMENT	Entrained Air %	Compressive Strength (28-days) psi
6A Virgin Gravel	1966:1079:235:554	6.4	5681
6A Virgin Limestone	1817:1240:245:560	5.4	5295
6A Virgin Slag	1808:1297:305:744	6.7	5954
17A Virgin Gravel	1878:1163:283:548	6.0	4294
100% Recycled	1559:1209:263:523	6.7	4780
50-50 Recycle Blend	1682:1137:272:545	6.7	5352

Table 3: Physical Characteristics of Concrete Aggregates

AGGREGATE	SPECIFIC GRAVITY	ABSORPTION (24hr) PERCENT
Sand	2.62	2.20
6A Virgin Gravel	2.61	0.90
4A/6A Virgin Limestone	2.60	0.66
6A Virgin Slag	2.41	3.71
17A Virgin Gravel	2.61	0.90
100% 6A Recycled Gravel	2.40	4.66
50-50 Recycle Blend	2.50	2.92

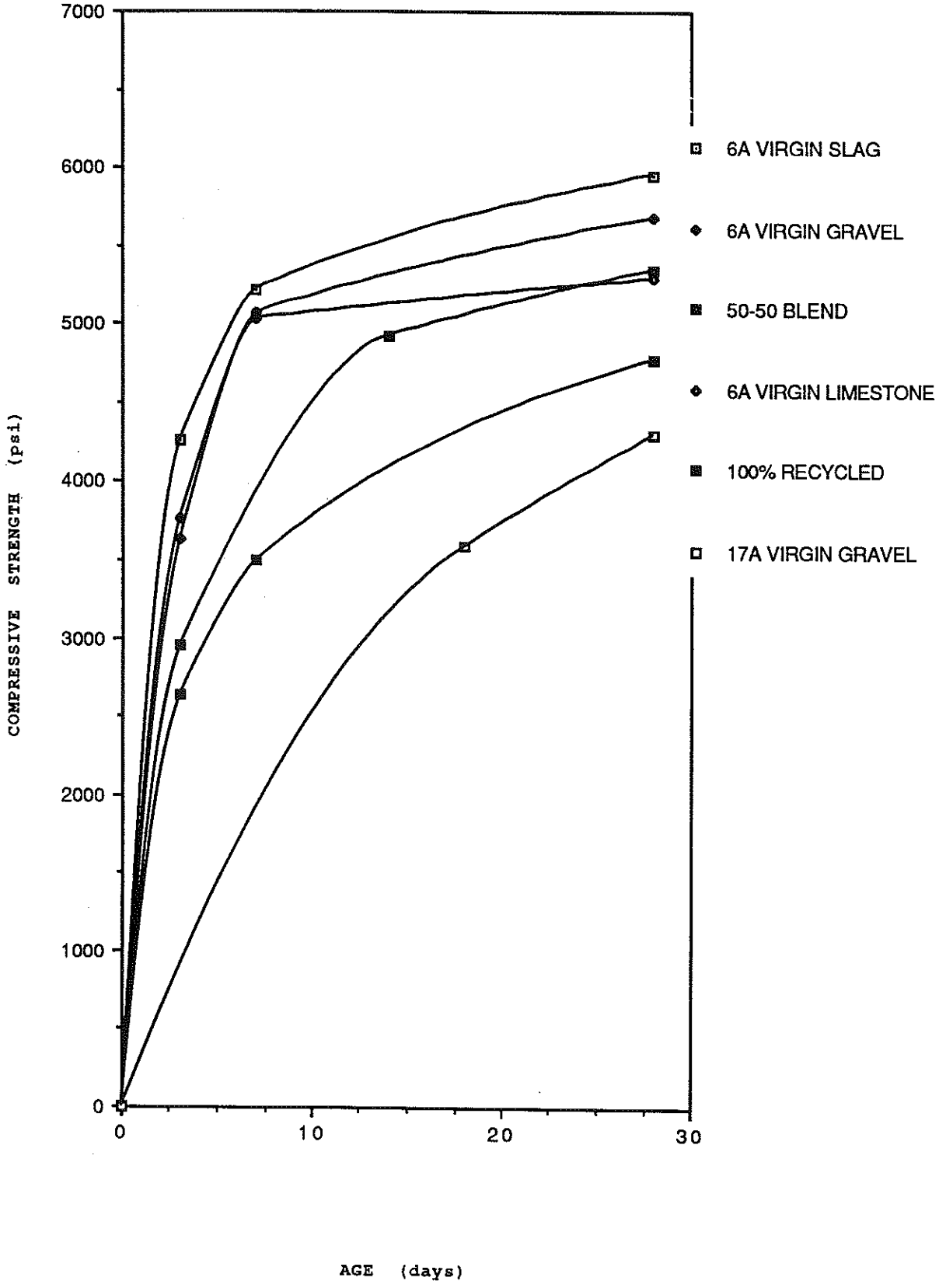

Figure 10: Strength-Gain Curves of the Test Specimens

smooth surfaces. The second aggregate was crushed limestone with angular edges and relatively rough surfaces. The third type was slag with rounded particles and rough surfaces. Physical characteristics of the three aggregates are shown in table 3.

Two different coarse aggregate gradations were used, designated as MDOT specification 6A (1.5 in. [4 cm] top size, coarser gradation) and MDOT specification 17A (1.0 in. [2.5 cm] top size, finer gradation). The grading requirements for these designations along with actual gradations of the materials are given in tables 4 and 5. Test specimens incorporating recycled concrete were produced by breaking and crushing slabs cast using 6A gravel in commercial crushers, and then sieving, grading and reblending this recycled material for use in test specimens. The 100% recycled test specimen was graded to meet MDOT specification 6A. The 50-50 recycled blend specimen contained coarse aggregate composed of a blend of 50% (by weight) recycled gravel concrete graded to meet MDOT specification 6A and 50% virgin crushed limestone graded to meet MDOT specification 4A (2.5 in. [6 cm] top size). The 4A gradation requirements and actual 4A material gradation are presented in table 6.

TEST PROCEDURES

Casting

The concrete was mixed under careful laboratory control. First the coarse aggregates were sieved and blended (as

Table 4: Coarse Aggregate Gradation of 6A Materials

SIEVE SIZE	TOTAL PERCENT PASSING				
	6A Spec	6A Limestone	6A Gravel	6A Slag	6A Recycled
1.5 in	100%	100	100	100	100
1.0 in	95-100%	98	98	100	97
1/2 in	30-60%	38*	38	60	42
No. 4	0-8%	2	4	2	4

Note: *Gradation test run in the lab show only 16% passing 1/2 in sieve for 6A crushed Limestone

Table 5: Coarse Aggregate Gradation of 17A Material

SIEVE SIZE	TOTAL PERCENT PASSING	
	17A Spec	17A gravel
1.0 in	100%	100%
3/4 in	90-100%	100%
1/2 in	50-75%	56%
No. 4	0-8%	6%

Table 6: Coarse Aggregate Gradation of 4A Material

SIEVE SIZE	TOTAL PERCENT PASSING	
	4A Spec	4A Limestone
2.5 in	100%	82
2.0 in	95-100%	47
1.5 in	65-90%	9
1.0 in	10-40%	2
1/2 in	0-20%	-
3/8 in	0-5%	-

required) to meet the appropriate gradation requirements. Then the coarse and fine aggregates were left in the laboratory to air dry. Tests were run to determine coarse and fine aggregate absorption capacities, unit weights and moisture contents. Trial batches were made to develop a final mix design for each test specimen. Prior to actual mixing, moisture contents of the aggregates were again determined to adjust the mix water.

The size of the test specimens and the capacity of the available drum mixers required mixing the concrete in a continuous stream of small batches to prevent the formation of cold joints. For each batch, one-half of coarse aggregates, fine aggregates and water were blended first, followed by the addition of cement, the remaining one-half of the water (with air-entraining admixture), coarse aggregates and fine aggregates. The mixer was operated for five minutes after the addition of the final component.

Concrete was hauled to the structural steel form in wheel barrows, where it was consolidated with a shaft-type vibrator. Each specimen was cast according to a schedule that generally

---

*The first two specimens (6A gravel and 6A limestone) were tested at 55 days and 52 days, respectively due to difficulties in getting the test program to operate properly. According to Troxell, Davis and Kelly [16] concrete made with 1.5 in. [4 cm] aggregates; 6 sacks cement per cu yd; and cured under standard conditions typically experiences a 9 percent gain in compressive strength between 28 and 55 days of curing. Thus, these specimens could have gained another 500 psi in compressive strength. However, actual increase in strength is expected to be less than this because of exposure to air after 28-days which may retard the hydration process due to drying.

allowed testing to begin after 28 days of curing*. Specimens were cured in the laboratory under polyethelene sheets.

Cracking

The transverse crack was forced near midslab after approximately 18 hrs. of curing. A removable metal joint insert (1/4 in. x 1 in. [5/8 cm x 2.5 cm] tall) was used at the bottom of the 10 in. [25 cm] slab to form a plane-of-weakness at the midslab. The slab was cracked full-depth along the weakened plane by jacking one-half of the slab and frame while clamping the other half to the cracking frame. A hinge mounted on top of the casting frame assured a tensile mode of fracture.

Loading

After 28 days of curing, each test specimen was moved to the test stand while still in the structural channel casting form, which was equipped with lifting loops. The slabs were held securely in the form during cracking and transportation by short steel studs, which were welded to the insides of the form around its perimeter. After each specimen was placed and centered on the test stand, the casting form was removed. This procedure ensured that the temperature steel was not over stressed prior to loading.

Tension was induced in the specimens as described previously. LVDT's were then set to zero, the data acquisition

system was initialized, and the repetitive loading was begun.

Load-deflection data were collected at the intervals described earlier. Each test was run until the temperature steel ruptured (see figure 11). During the test, applied loads and slab tension were monitored and adjusted as needed.

TEST RESULTS

The ability of transverse cracks to transfer load is a major factor in the structural performance of the crack and the surrounding slab fragments. In this study, the ability to transfer load was evaluated by comparing the deflections of the two slab fragments using the definition presented below:

$$\%LTE = d_{UL}/d_L \qquad \text{(Eq. 1)}$$

where

%LTE = percent load transfer efficiency

d_{UL} = deflection of unloaded side of the crack

d_L = deflection of the loaded side of the crack

Note that in the above formula, the maximum load transfer that can be achieved is 100%. This is obtained when the two sides deflect an equal amount. On the other extreme, if the two sides move with complete independence, the load transfer efficiency would be zero.

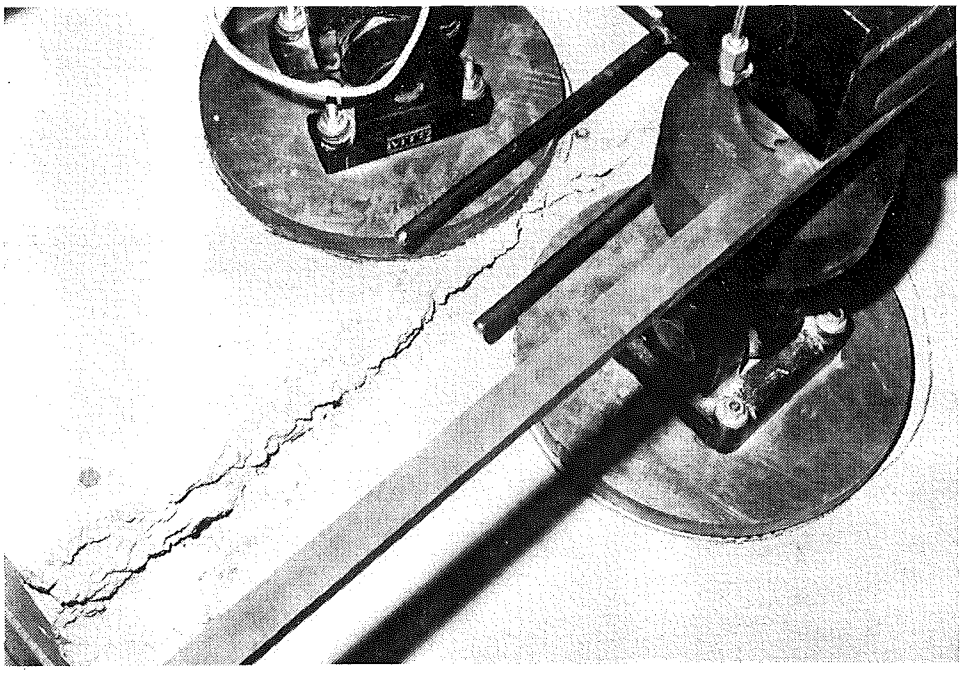

Figure 11: A View of a Failed Specimen

Effect of Type of Coarse Aggregate

The effect of type of coarse aggregate on aggregate interlock load transfer characteristics of transverse cracks was studied by comparing the performance of three test specimens, each containing a different type of coarse aggregate meeting the MDOT 6A gradation specifications. The three types of aggregates used were crushed limestone, gravel and slag. Figure 12 summarizes some of the test results for these materials. Detailed results are presented in the APPENDIX.

The results show that specimens containing crushed limestone and gravel coarse aggregates started with and retained higher load transfer efficiencies than the specimen containing slag coarse aggregate. This difference in performance is probably due to the different textures of the crack faces of these specimens, as illustrated in figure 13. It is seen that the specimens containing crushed limestone and gravel have rougher crack faces (more large protrusions and macrotexture) than the specimen containing slag. This is due to the fact that slag aggregate apparently fractured at the time of crack development, whereas limestone and gravel pulled out through the loss of bond, thus resulting in rougher crack faces.

It is possible that the test results are biased due to differences in the three coarse aggregate gradations. Table 4 indicates that, although all three materials meet the requirements of MDOT gradation designation 6A, the slag is somewhat finer than either the limestone or gravel. It is also

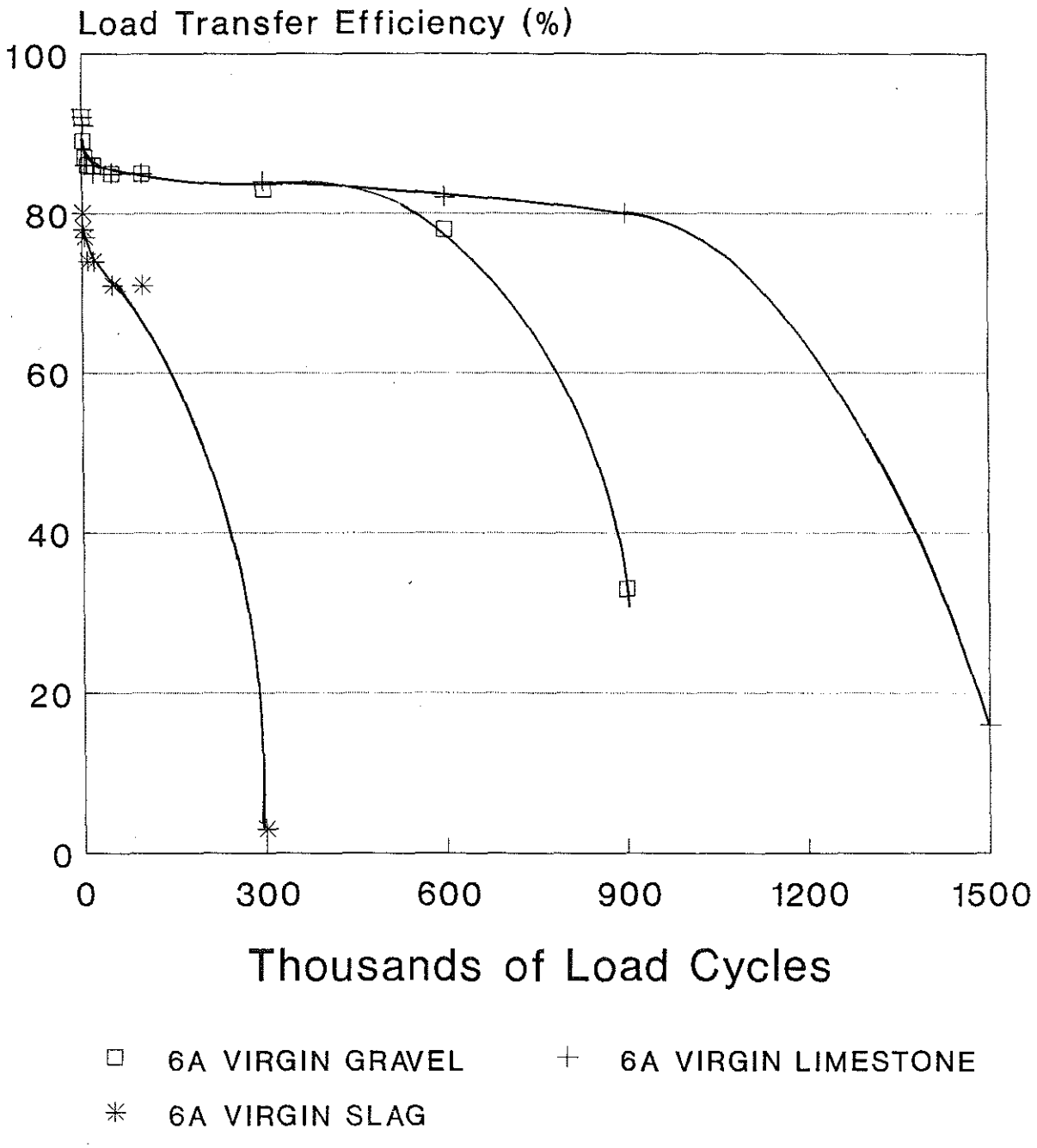

Figure 12: Effect of Coarse Aggregate Type on the Relation Between LTE% and Number of Load Cycles

Crushed Limestone

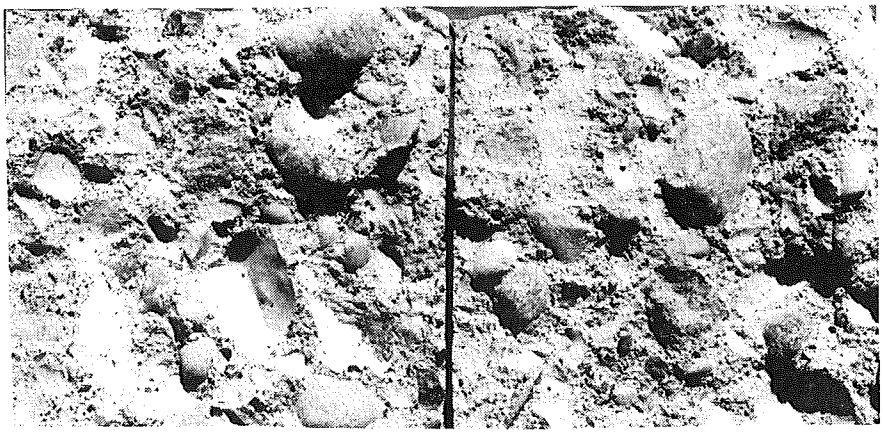

Gravel

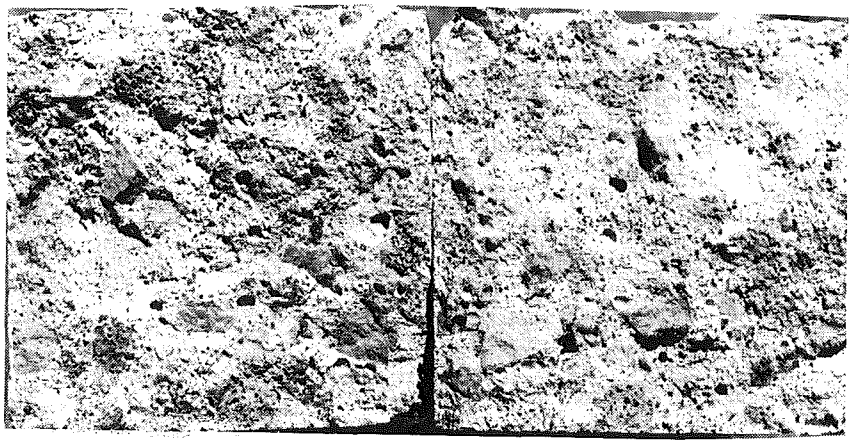

Slag

Figure 13: Exposed Crack Faces of Small Test Specimens, Varying Coarse Aggregate Type, 6A Gradation Materials

possible that the results were affected by the slight differences in mix designs and strengths between the three test slabs (see table 2). However, it seems most likely that the observed differences in performance (endurance of load transfer efficiency) are mainly due to differences in the crack face texture (see figure 13) and coarse aggregate particle strengths. The highly porous slag particles were obviously of lower strength and produced crack faces with little macrotexture. These conclusions should be verified in future tests through the use of more comparably graded aggregates and identical curing conditions for each specimen.

Figure 14 shows the approach side peak deflections of the three test specimens after repeated loading. The crushed limestone specimen exhibited lower deflections than the gravel or slag at all times. Similarly, the gravel generally performed better than the slag. Although the temperature reinforcement eventually ruptured in all three cases, the crushed limestone concrete was able to endure a significantly higher number of load repetitions than the other two specimens. This better endurance is probably due at least in part to the relatively low deflections that are attributable to the angularity of the crushed particles, which increase the sliding resistance of the crack faces.

Effect of Gradation of Coarse Aggregate

The effect of coarse aggregate gradation on load transfer

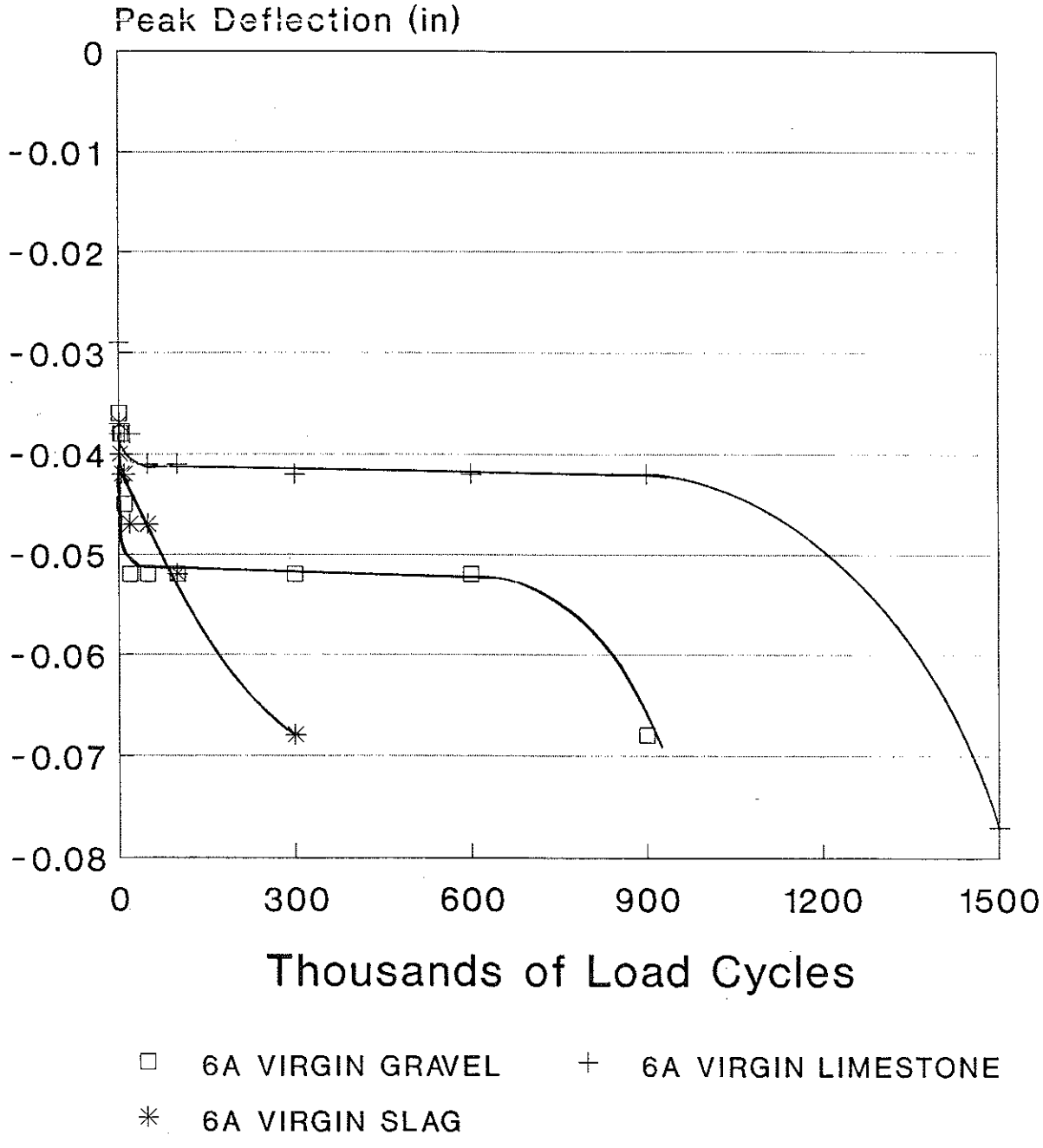

Figure 14: Effect of Coarse Aggregate Type on the Relation Between Peak Deflection and Number of Load Cycles

characteristics of transverse cracks was studied by comparing the results of two specimens, one cast using coarsely graded gravel (6A Gradation: 1.5 in. [4 cm] top size) and the other cast using more finely graded gravel (17A Gradation: 1.0 in. [2.5 cm] top size). The test results are summarized in figure 15 (detailed results are presented in the Appendix). The results show that for initial loading cycles (up to 20,000 cycles) both test specimens performed comparably. As the number of load cycles increased, the load transfer efficiency of the 17A gravel test specimen dropped slightly. This is probably due to the small size of coarse aggregates which, after initial attrition or abrasion of the crack faces, requires a larger vertical displacement of the two slab fragments to make a contact and transfer load. However, this increase in looseness was not large enough to produce immediate failure, as evidenced by the fact that the 17A gravel test specimen was able to endure a number of load cycles comparable to that of the 6A gravel test specimen before the steel reinforcement eventually ruptured.

Effect of Treatment of Coarse Aggregate

The effect of treatment of coarse aggregate on aggregate interlock load transfer characteristics of transverse cracks was studied by comparing the performance of three test specimens, each containing a different treatment of coarse aggregate. The three treatments of aggregates included virgin gravel aggregates (MDOT gradation 6A), 100% recycled gravel concrete aggregates

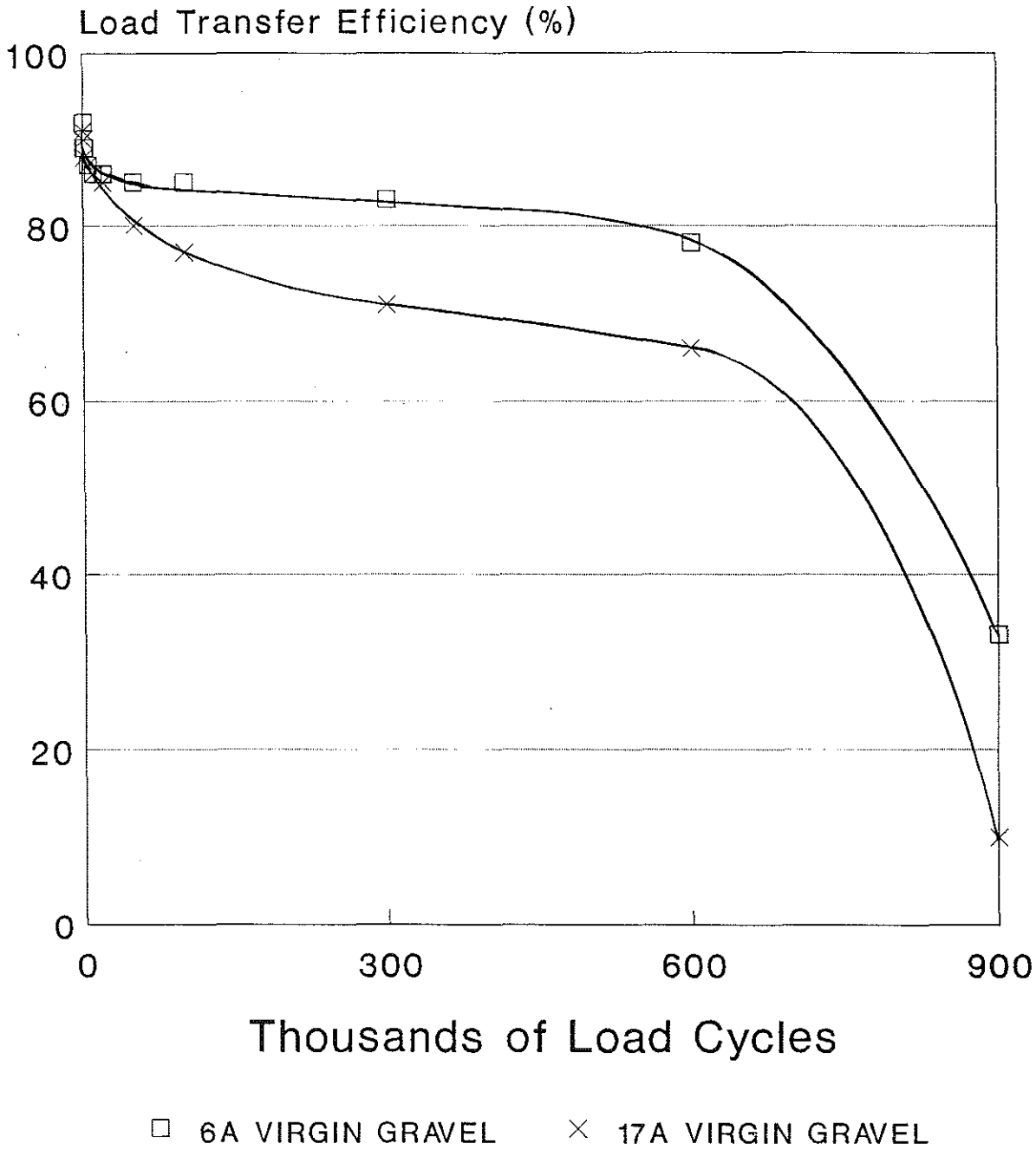

Figure 15: Effect of Coarse Aggregate Gradation on the Relation Between LTE% and Number of Load Cycles

(MDOT gradation 6A), and a 50-50 blend of recycled gravel concrete (MDOT gradation 6A) and large virgin limestone (MDOT gradation 4A) aggregates. Figure 16 summarizes the test results of these treatments (details are presented in the Appendix).

The results show that the specimen containing virgin coarse aggregates performed considerably better than the other two test specimens which contained recycled concrete as coarse aggregates. The examination of the crack faces of the 100% recycled specimen revealed that very few pull outs of aggregate particles existed (see figure 17). The reason for this condition is probably related to the mode of fracture of recycled concrete aggregates. Coarse aggregates produced by recycling concrete consist of two materials (i.e., cement mortar and original aggregate) bonded together. At the time of crack development, recycled concrete aggregates apparently often fracture at the old bond interface, thus resulting in the above condition. Furthermore, the use of comparable quantities of recycled aggregate results in nearly a 50% reduction in the actual number of virgin coarse aggregate particles in the mix. If the shear transfer characteristics of the slab depend upon the number and quality of virgin aggregate particles at the crack interface, it stands to reason that concrete utilizing only recycled concrete aggregates may fare poorly.

The unexpected poor performance of 50-50 recycle blend specimen may also be attributable to a reduction in the number of virgin aggregate particles at the crack face (see figure 18). Not only are there fewer virgin particles present because of the

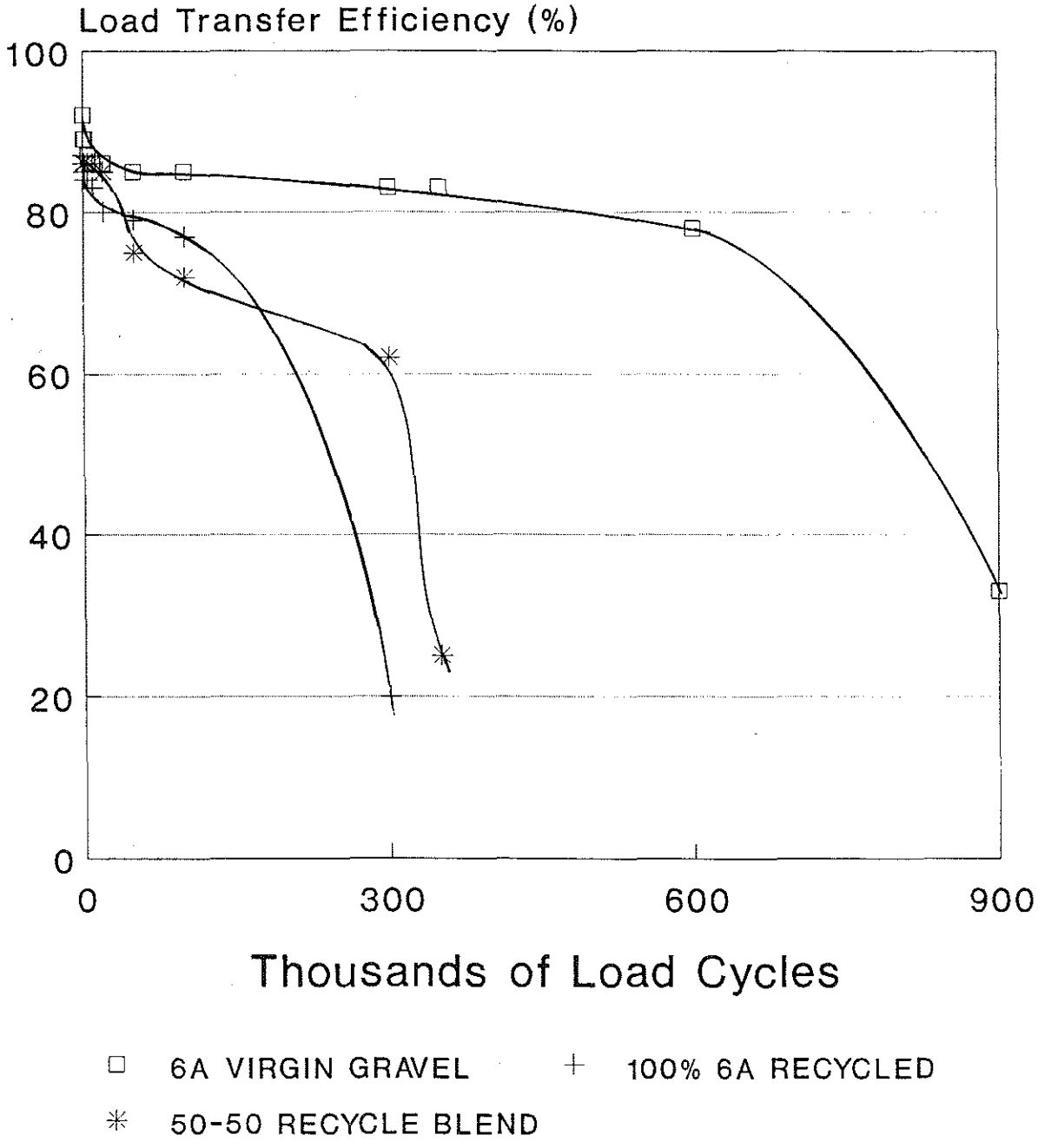

Figure 16: Effect of Coarse Aggregate Treatment on the Relation Between LTE% and Number of Load Cycles

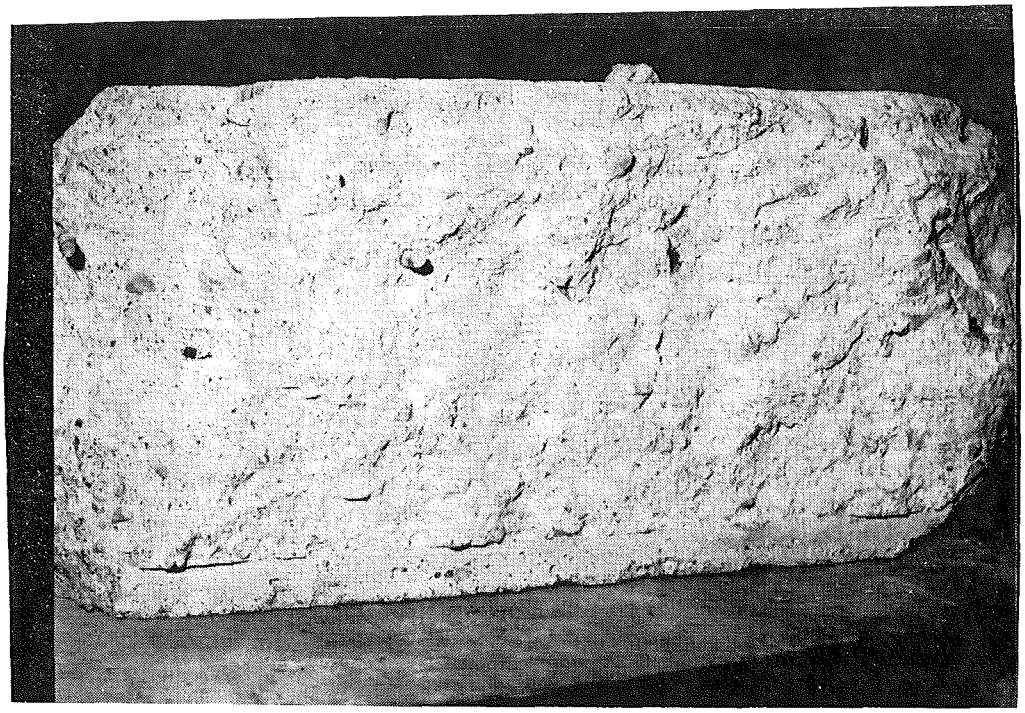

Figure 17: Exposed Crack Face of 100% Recycled Gravel Concrete Specimen After Loading

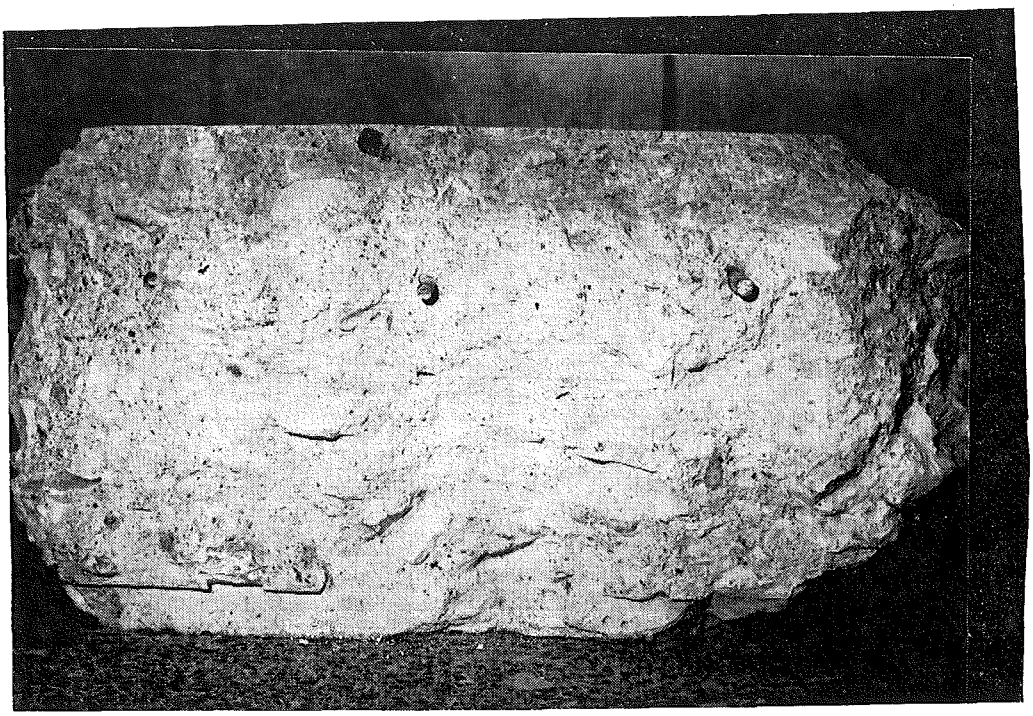

Figure 18: Exposed Crack Face of 50-50 Recycled Blend Specimen After Loading

use of recycled concrete materials, but the use of an equal weight of large aggregate also results in a smaller number of particles (although the few that are present are large enough to provide significant interlock for some time). The distribution of particles that protrude from the crack face can be fairly widespread, as seen in figure 18.

It should also be noted that during transportation of this specimen (50-50 recycle blend) from the cracking frame to the test stand, one of the lifting ropes broke, causing one end of the specimen to drop a distance of about 2 in. [5 cm]. This may have contributed to the observed performance since initial load transfer efficiency of this specimen was also low compared to all other specimens except one (6A virgin slag).

It is recommended that this test cell (50-50 recycle blend) should be replicated in future tests to determine whether the observed results were caused by the accidental handling or were truly indicative of the performance of this mixture.

CONCLUSIONS, FINDINGS AND RECOMMENDATIONS

The following primary conclusions were drawn from the results of this laboratory study:

1. When the type of coarse aggregate (gravel, limestone or slag) was varied while holding all other variables approximately constant, load transfer efficiency and endurance was significantly higher for 6A limestone and 6A gravel than for 6A slag.

2. When all other variables were held constant, transverse crack load transfer efficiency and endurance decreased (but only slightly) when the coarse aggregate gradation was changed from 6A (1 in. nominal top size) to 17A (3/4 in. nominal top size)

3. The use of 100% recycled 6A gravel concrete as coarse aggregates decreased the load transfer efficiency and endurance considerably as compared to concrete made using virgin 6A gravel.

4. The use of the blend of 50% virgin 4A (2 in. nominal top size) limestone and 50% recycled 6A gravel concrete as coarse aggregate decreased the load transfer efficiency and endurance considerably as compared to concrete made using virgin 6A gravel.

Other related findings and recommendations are summarized below:

1. Aggregate interlock load transfer efficiency of reinforced transverse cracks decreases with increasing load cycle applications. It was observed that load transfer efficiency (LTE) typically drops by 3 to 8 percent during initial load cycle applications (5000 load cycles or fewer); LTE then typically remains approximately constant until the longitudinal steel begins to yield, after which it drops sharply.

2. The aggregate interlock load transfer capacity of transverse cracks is related to the texture of the crack face. The crack face texture is primarily a function of the type, size, and number of coarse aggregate particles at the crack face and the mode of fracture. It was observed that specimens in which crack

developed around the aggregate (i.e., virgin crushed stone and virgin gravel) developed higher initial load transfer efficiencies and were able to maintain this higher level over a considerably larger number of load cycles than specimens in which the crack developed through the aggregate (i.e., virgin slag and recycled aggregates).

3. Although the unexpected poor performance of the 50-50 recycle blend (6A recycled gravel concrete with 4A virgin limestone) concrete might be due to inadequate numbers of virgin coarse aggregate particles at the crack face or due to slab handling difficulties, there is enough concern about the results of this particular specimen to recommend replicating the test in future experimentation.

4. One of the unexpected findings of this study is the relatively early rupture of steel in all six test specimens. Although this laboratory test is rigorous in nature in that each test specimen is under adverse loading conditions (i.e., combined tension and shear) constantly, it is possible that current longitudinal steel quantities (0.17% percent by area of concrete) are inadequate for the combined tension and shear loading conditions encountered in the field. Further testing should include variations of steel quantities.

5. Several other factors are likely to affect transverse crack performance. These include variations in slab tension, type of steel reinforcement (smooth wire vs deformed wire), and foundation support. These factors should also be considered in future testing.

REFERENCES

1. McCarthy, G.J., and MacCreery, W.J., "Michigan Department of Transportation Recycles Concrete Freeways," Proceedings Third International Conference on Concrete Pavement Design and Rehabilitation, Purdue University, April 23-25, 1983, W. Lafayette, IN., pp. 643-647.

2. Darter, M. I., "Initial Evaluation of Michigan JRCP Crack Deterioration," a report prepared for Michigan Concrete Paving Association, December, 1988, Revised February, 1989, Mahomet, IL 61853.

3. Snyder, M. B., "Factors Affecting Transverse Crack Deterioration in JRCP," a research proposal to the Michigan Department of Transportation, Department of Civil and Environmental Engineering, Michigan State University, July, 1989, E. Lansing, MI 48824-1226.

4. Raja, Z.I., and Snyder, M.B., "Factors Affecting Transverse Crack Deterioration in JRCP," a paper prepared for presentation at the 1991 Annual Meeting of the Transportation Research Board, Washington, D.C.

5. Teller, L.W., and Cashell, H.D., "Performance of Dowelled Joints Under Repetitive Loading," Bulletin 217, Highway Research Board, Washington, D.C., 1959.

6. Colley, B.E., and Humphrey, H.A., "Aggregate Interlock at Joints in Concrete Pavements," Highway Research Record No. 189, Highway Research Board, National Research Council, Washington, D.C., 1967, pp. 1-18.

7. Ball, C. G., and Childs, L.D., "Tests of Joints for Concrete Pavements," Research and Development Bulletin RD026.01P, Portland Cement Association, Skokie, IL, 1975.

8. Ciolko, A. T., Nussbaum, P. J., and Colley, B. E., "Load Transfer of Dowel Bars and Star Lugs," Final Report, Construction Technology Laboratories, Skokie, IL, 1979.

9. Benkelman, A.C., "Tests of Aggregate Interlock at Joints and Cracks," Engineering News Record, Vol. III, No. 8, August 24, 1933, New york, N.Y., pp. 227-232.

10. Nowlen, W.J., "Influence of Aggregate Properties on Effectiveness of Interlock Joints in Concrete Pavements," Journal of the PCA, Research and Development Laboratories, Vol. 10, No. 2, May 1968, pp. 2-8

11. Sutherland, E.C., and Cashell, H.D., "Structural Efficiency of Transverse Weakened-Plane Joints," Public Roads, Vol. 24, No. 4, April-May-June 1945.

12. Older, C., "Efficiency of Aggregate interlock in Concrete Roads," Engineering News Record, Vol. III, No. 8, November 23, 1933, New York, N.Y., pp 615-616.

13. Poblete, M., Valenzuela, R., and Salsilli, R., "Load Transfer in Undowelled Transverse Joints of PCC Pavements," Transportation Research Record 1207, Transportation Research Board, National Research Council, Washington, D.C. 1988.

14. Ioannides, A. M., and Korovesis, G. T., "Aggregate Interlock: Pure-Shear Load Transfer Mechanism," paper prepared for presentation at the 1990 Annual Meeting of the Transportation Research Board, Washington, D.C.

15. Snyder, M. B., "Dowel Load Transfer Systems for Full-Depth Repairs of Jointed Portland Cement Concrete Pavements," Ph.D. Thesis, University of Illinois at Urbana-Champaign, 1988.

16. Troxell, G.E., Davis, H.E., and Kelly, J.W., Composition and Properties of Concrete, second edition, McGraw-Hill Book Company, N.Y., 1968, pp 238-247.

APPENDIX

LOAD AND DEFLECTION CURVES FOR THE TEST SPECIMENS

6A VIRGIN GRAVEL
CYCLE # 1

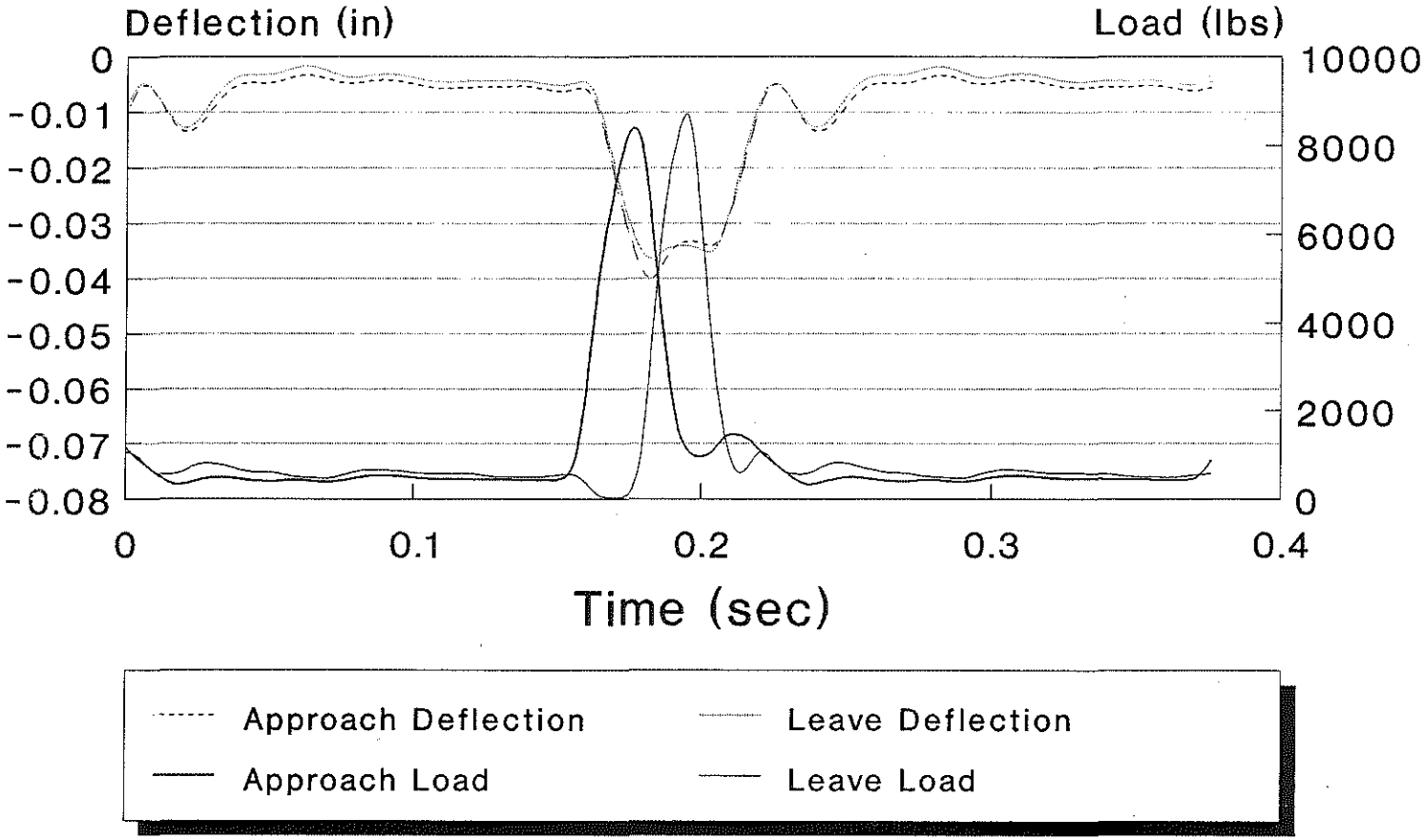

Figure A-1: Load and deflection curves for 6A virgin gravel slab after cycle # 1.

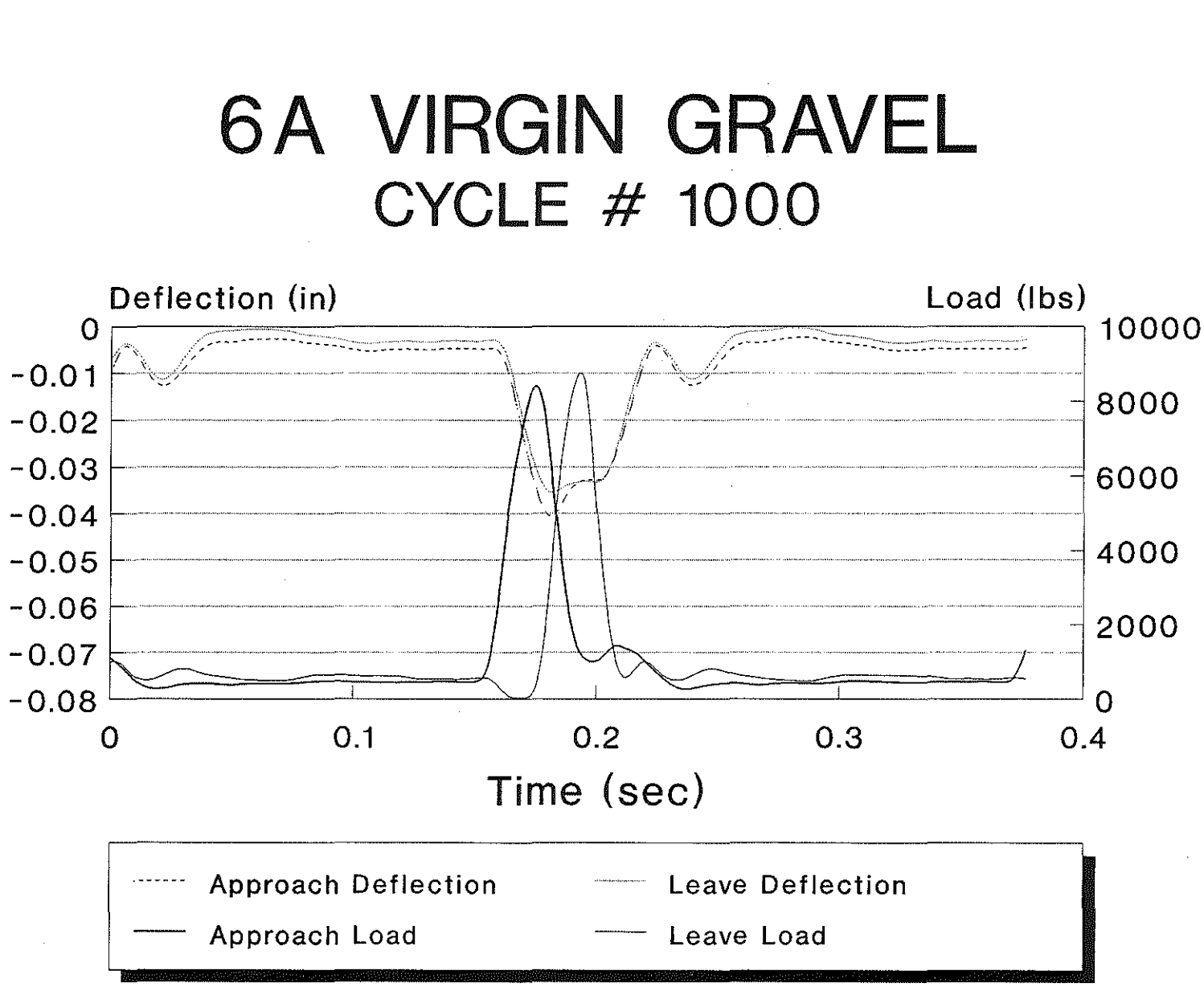

Figure A-2: Load and deflection curves for 6A virgin gravel slab after cycle # 1,000.

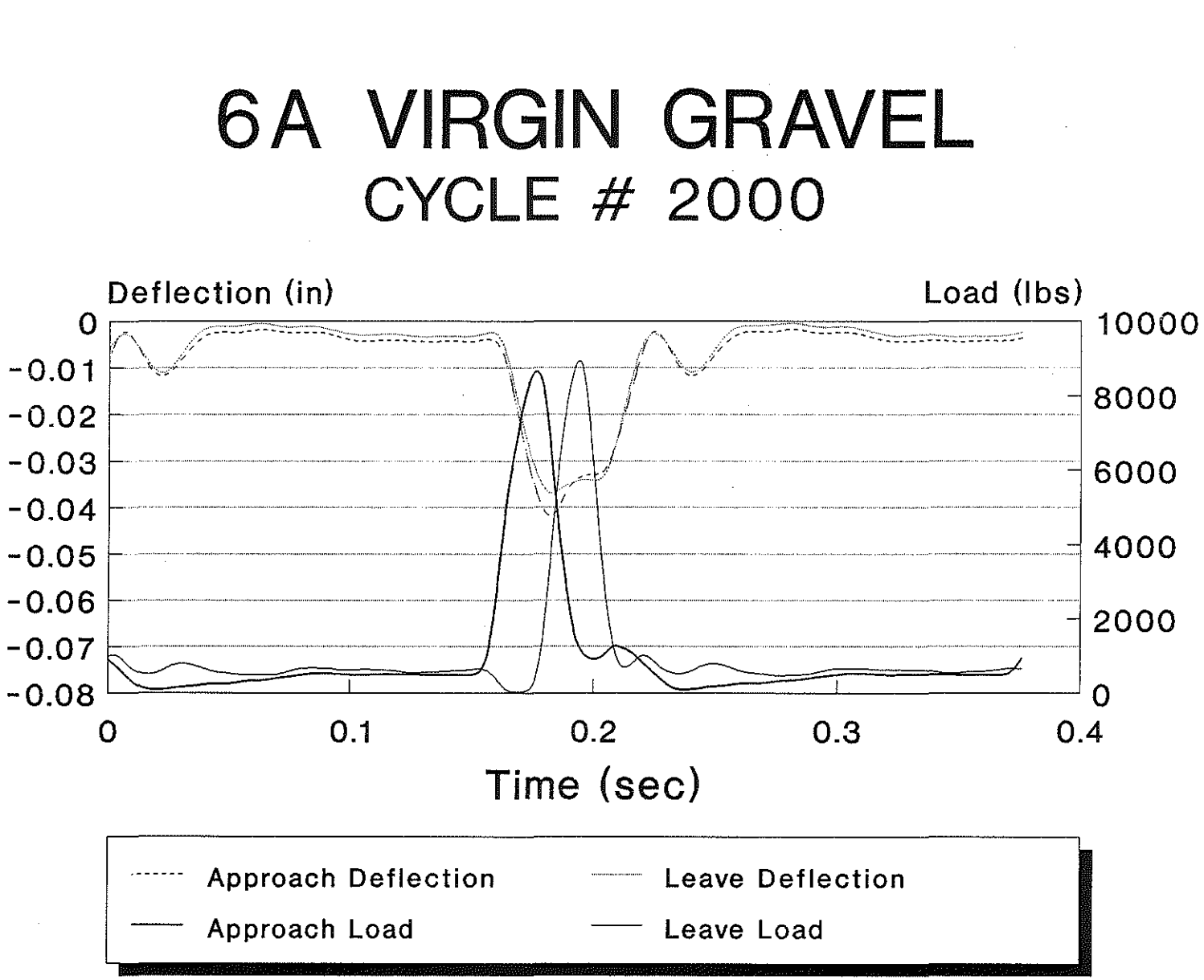

Figure A-3: Load and deflection curves for 6A virgin gravel slab after cycle # 2,000.

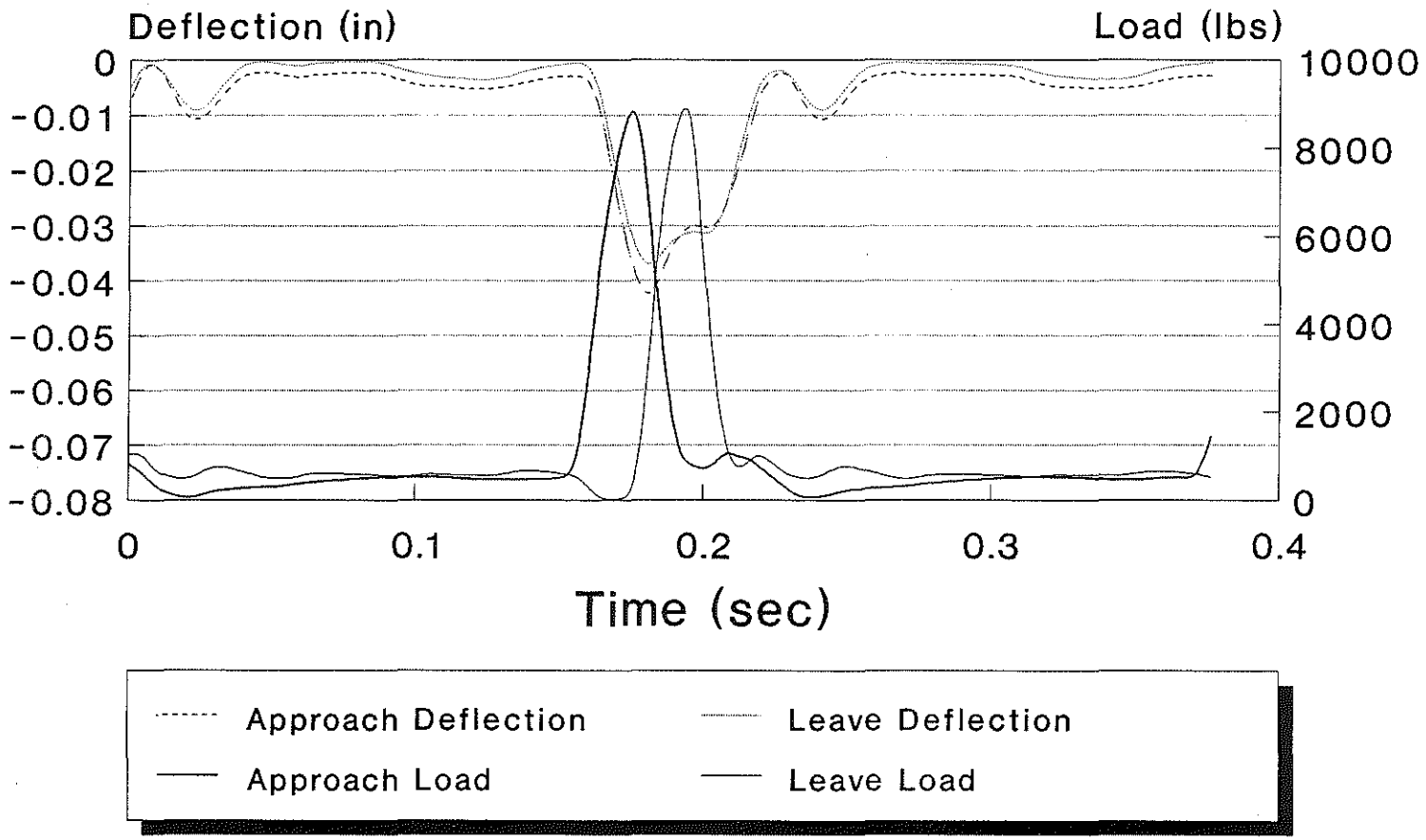

Figure A-4: Load and deflection curves for 6A virgin gravel slab after cycle # 5,000.

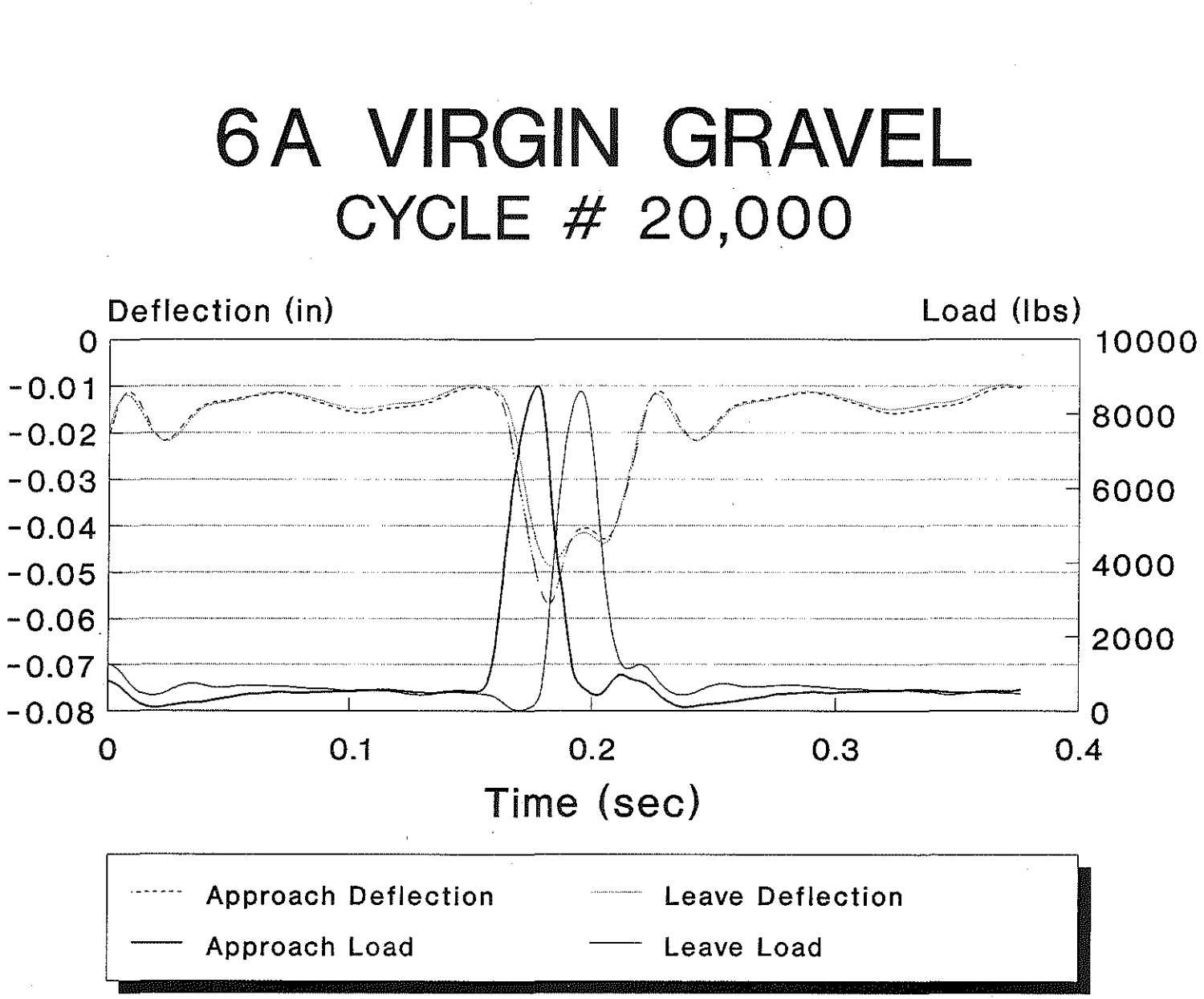

Figure A-5: Load and deflection curves for 6A virgin gravel slab after cycle # 20,000.

6A VIRGIN GRAVEL
CYCLE # 50,000

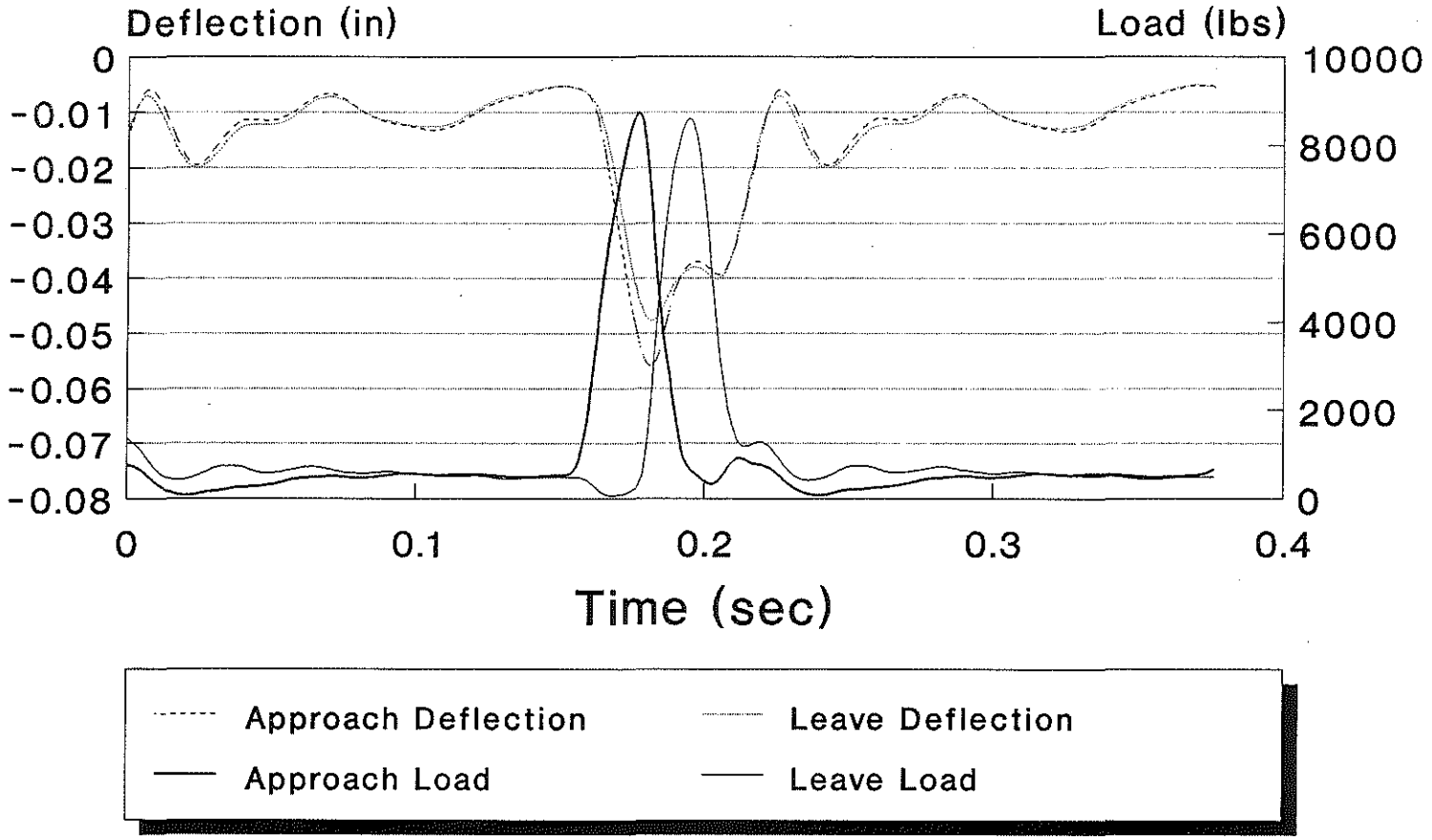

Figure A-6: Load and deflection curves for 6A virgin gravel slab after cycle # 50,000.

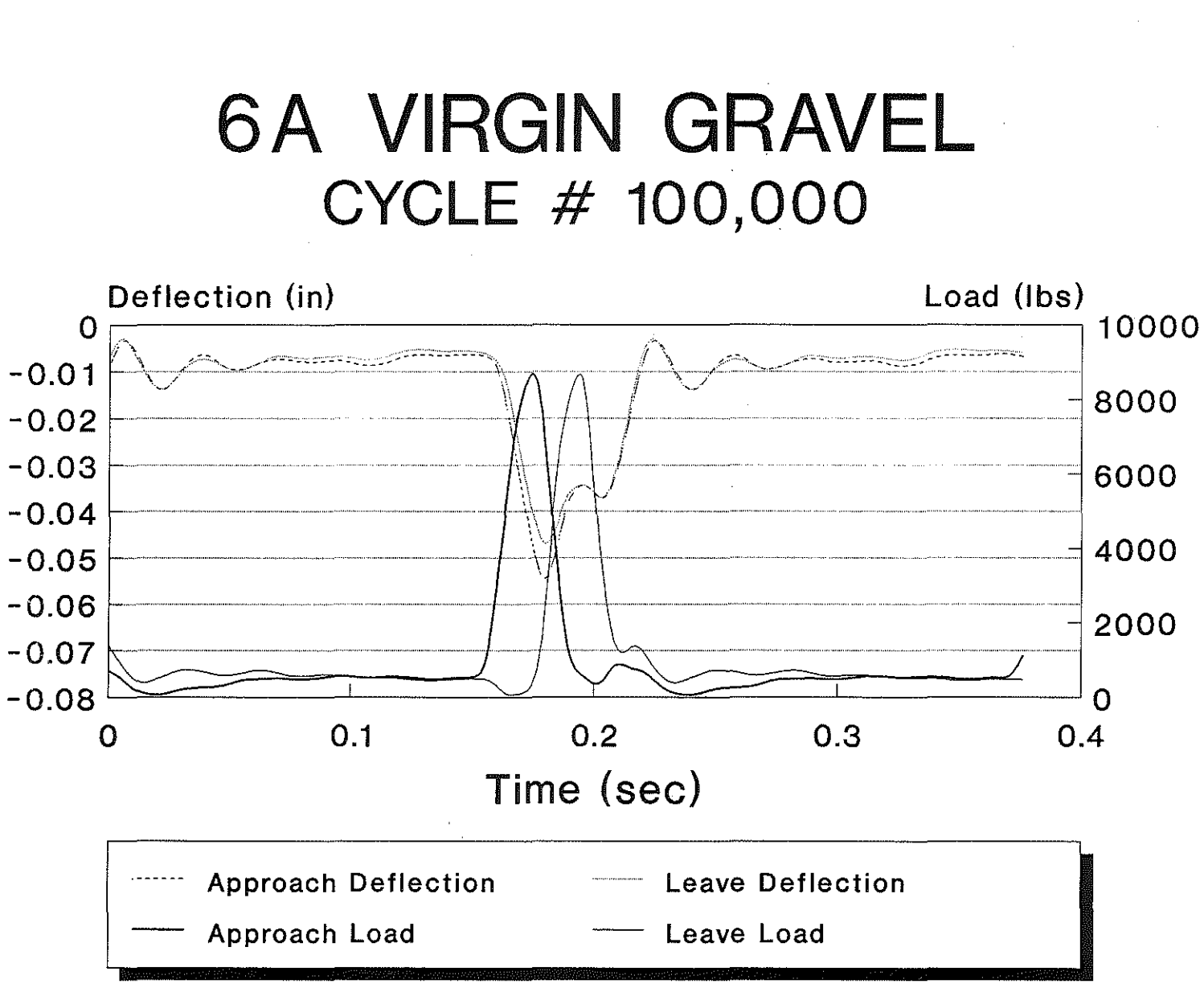

Figure A-7: Load and deflection curves for 6A virgin gravel slab after cycle # 100,000.

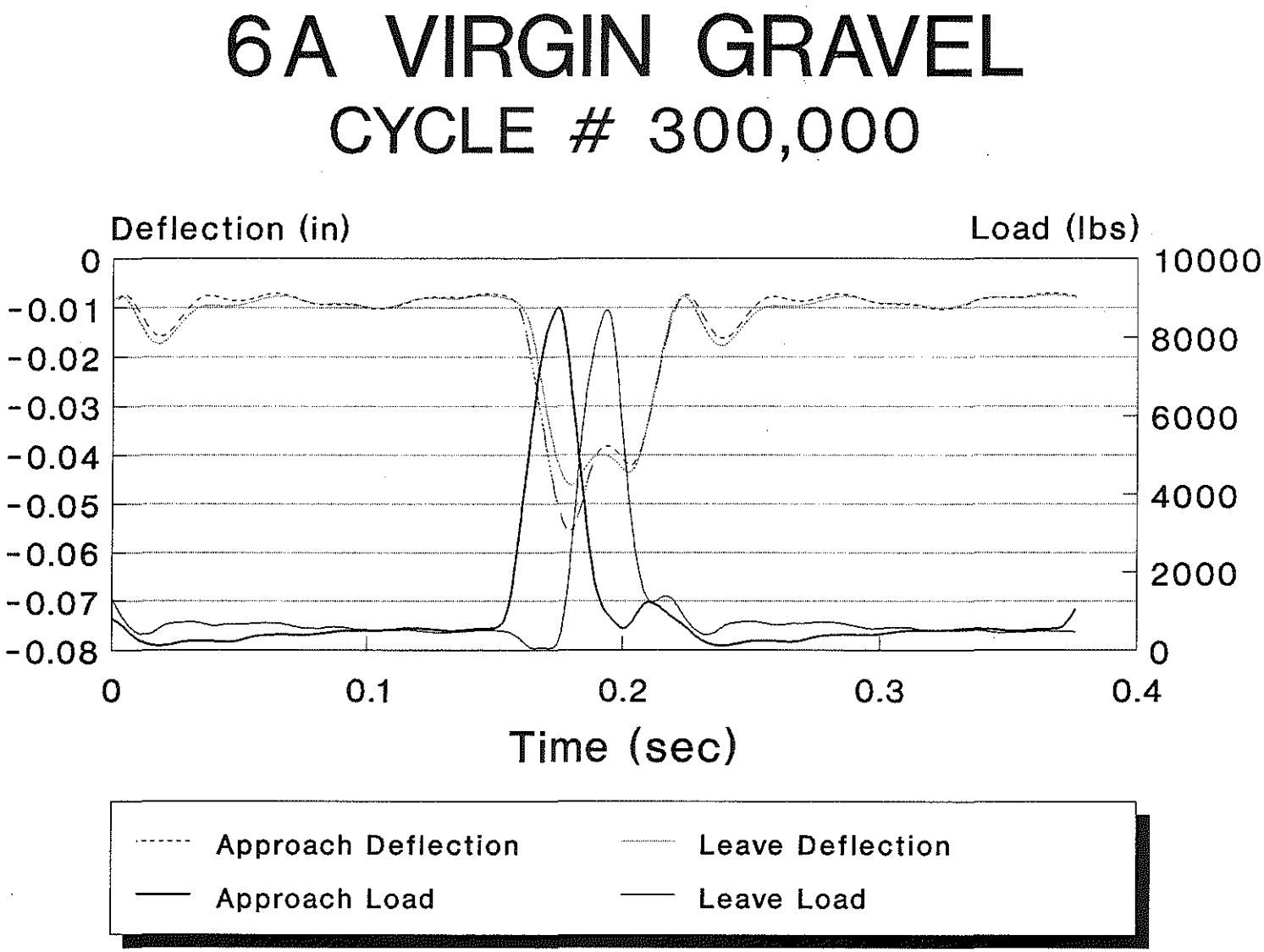

Figure A-8: Load and deflection curves for 6A virgin gravel slab after cycle # 300,000.

6A VIRGIN GRAVEL
CYCLE # 600,000

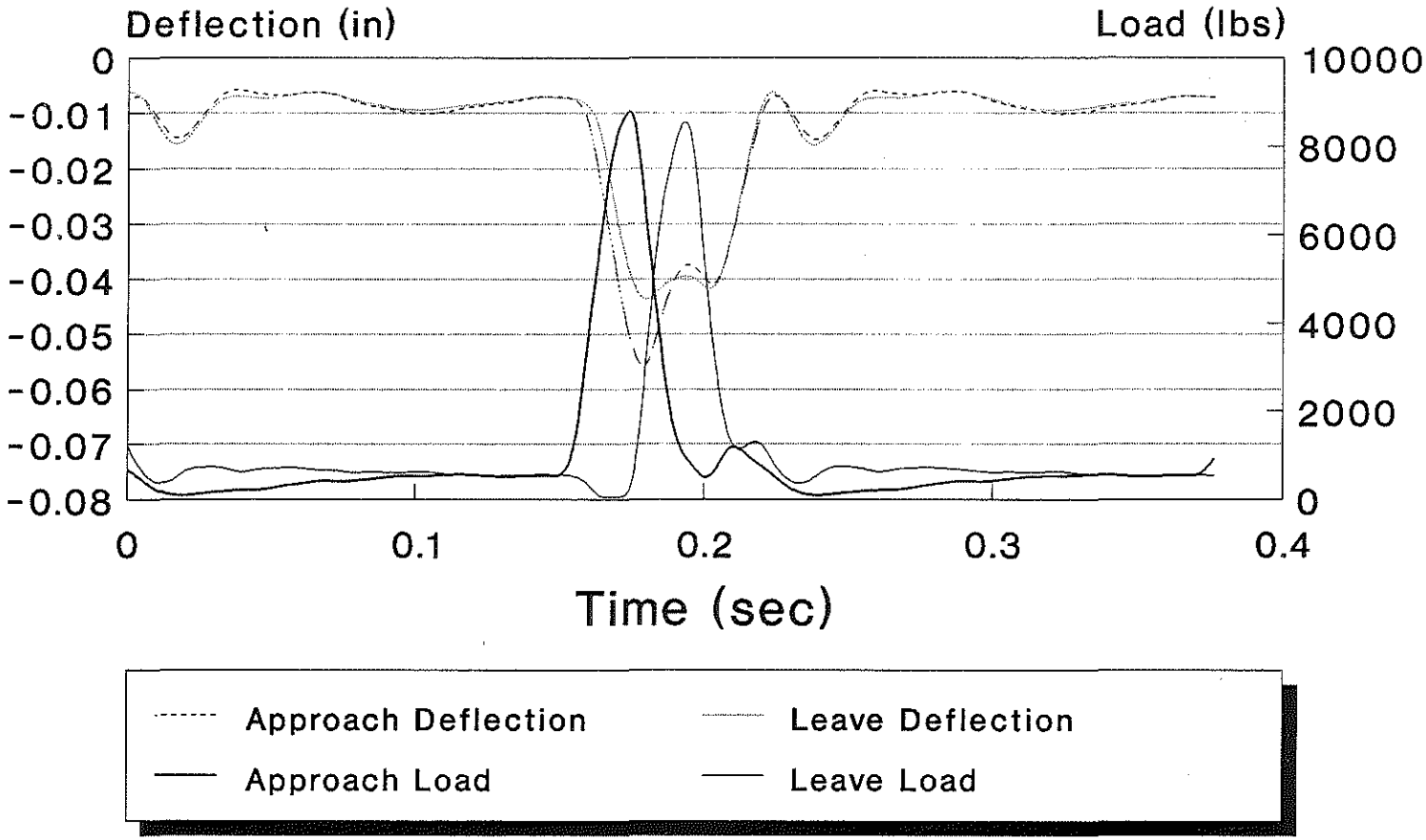

Figure A-9: Load and deflection curves for 6A virgin gravel slab after cycle # 600,000.

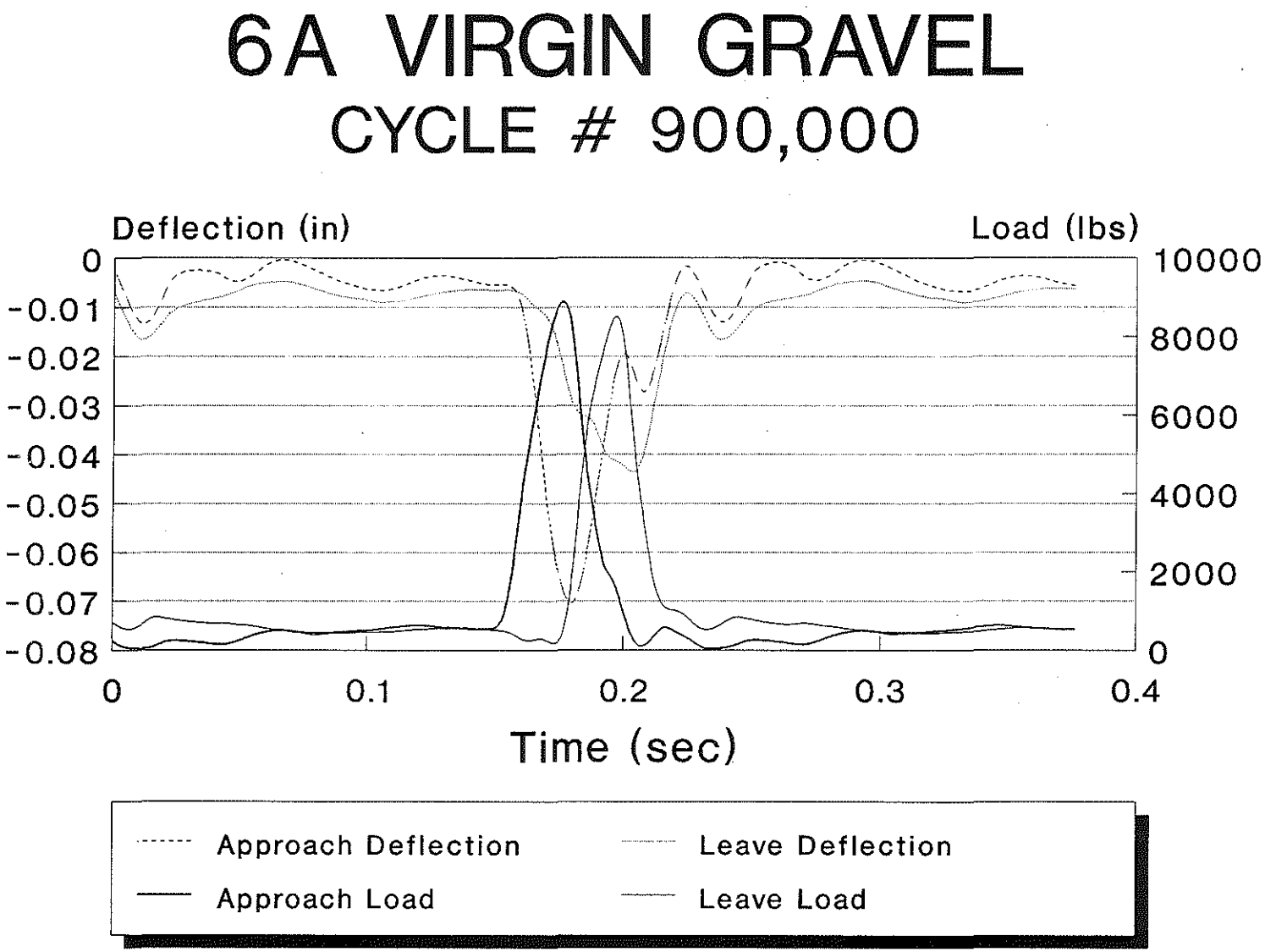

Figure A-10: Load and deflection curves for 6A virgin gravel slab after cycle # 900,000.

6A VIRGIN LIMESTONE
CYCLE # 1

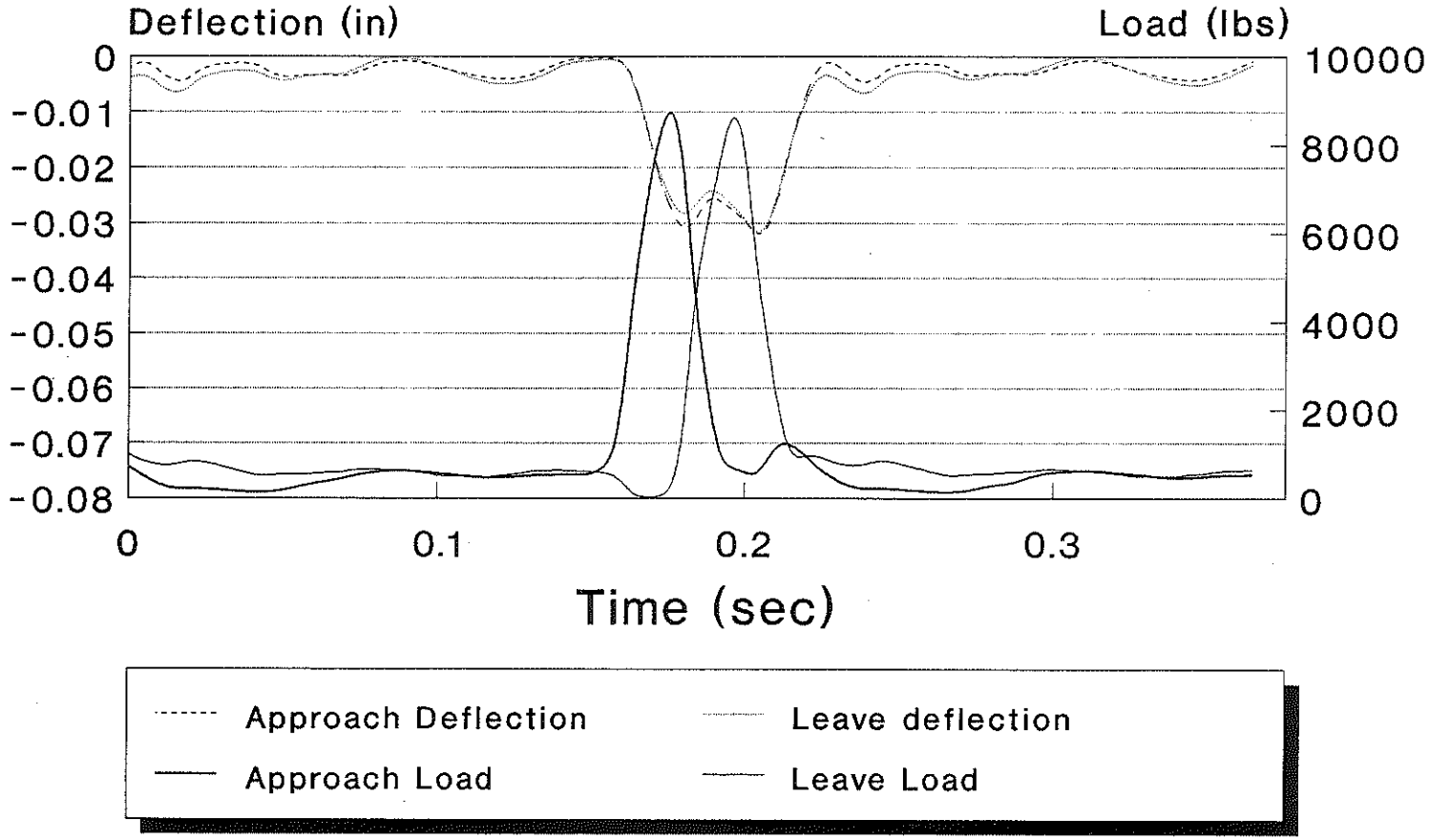

Figure A-11: Load and deflection curves for 6A virgin limestone slab after cycle # 1.

6A VIRGIN LIMESTONE
CYCLE # 1000

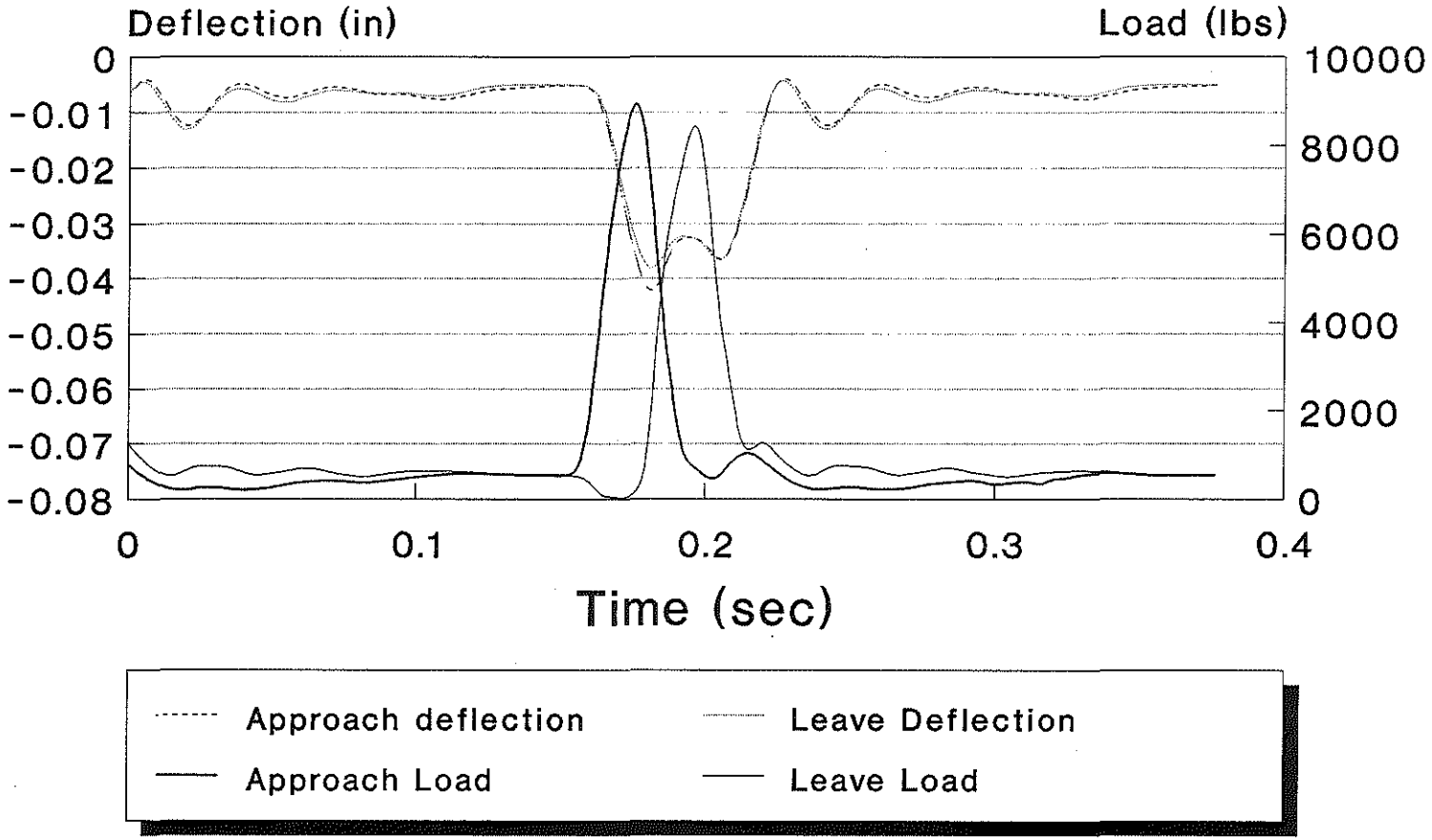

Figure A-12: Load and deflection curves for 6A virgin limestone slab after cycle # 1,000.

6A VIRGIN LIMESTONE
CYCLE # 2000

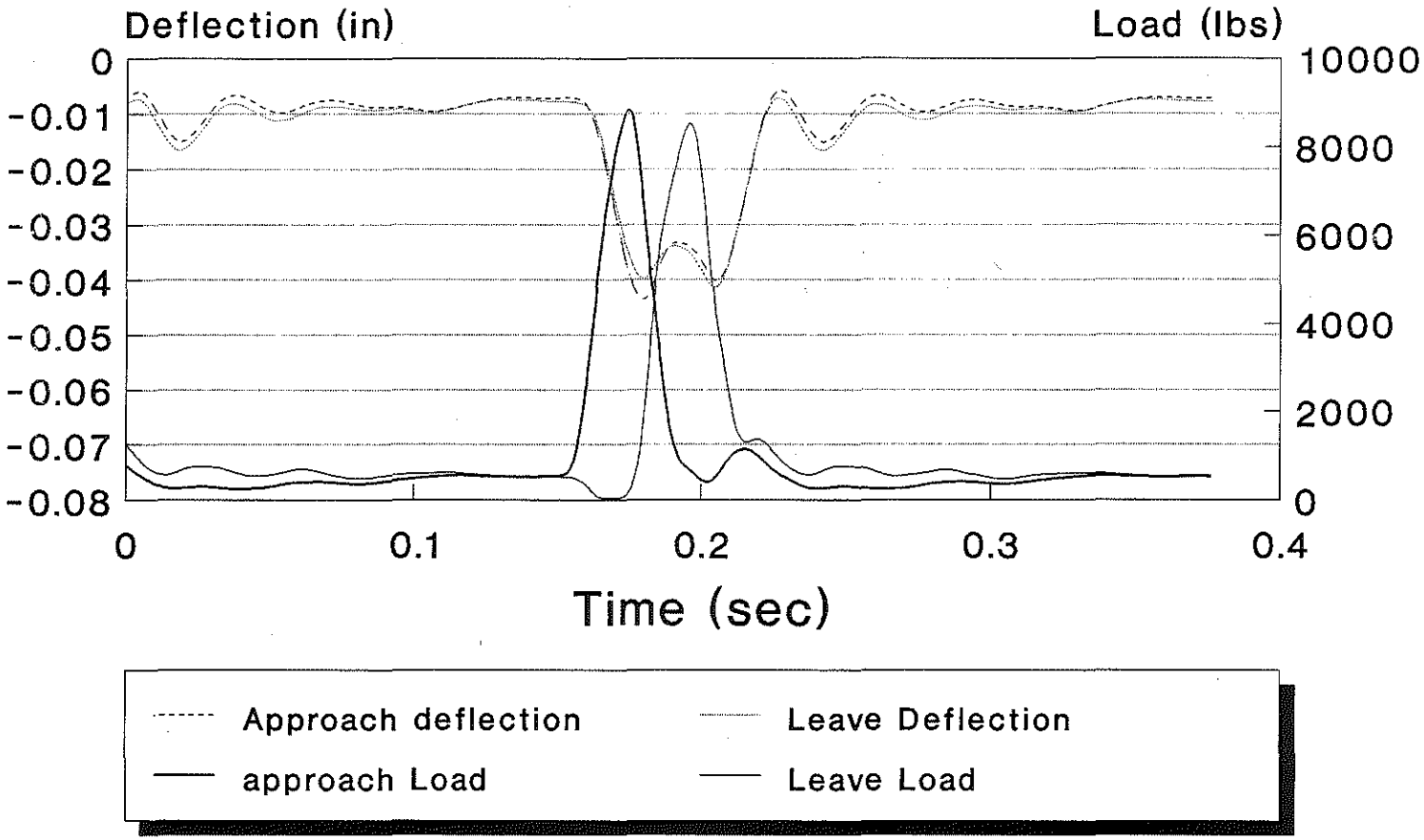

Figure A-13: Load and deflection curves for 6A virgin limestone slab after cycle # 2,000.

6A VIRGIN LIMESTONE
CYCLE # 5000

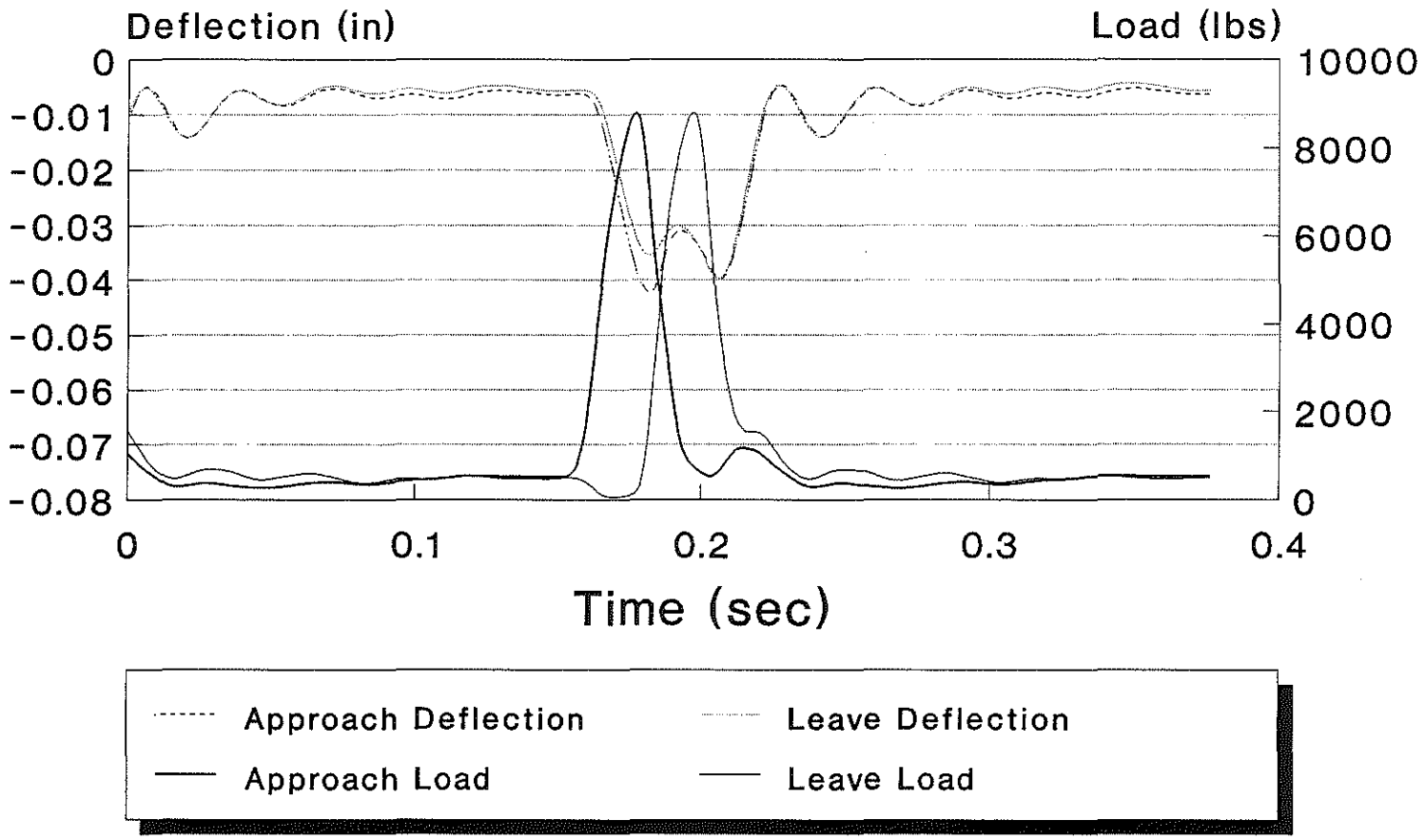

Figure A-14: Load and deflection curves for 6A virgin limestone slab after cycle # 5,000.

6A VIRGIN LIMESTONE
CYCLE # 10,000

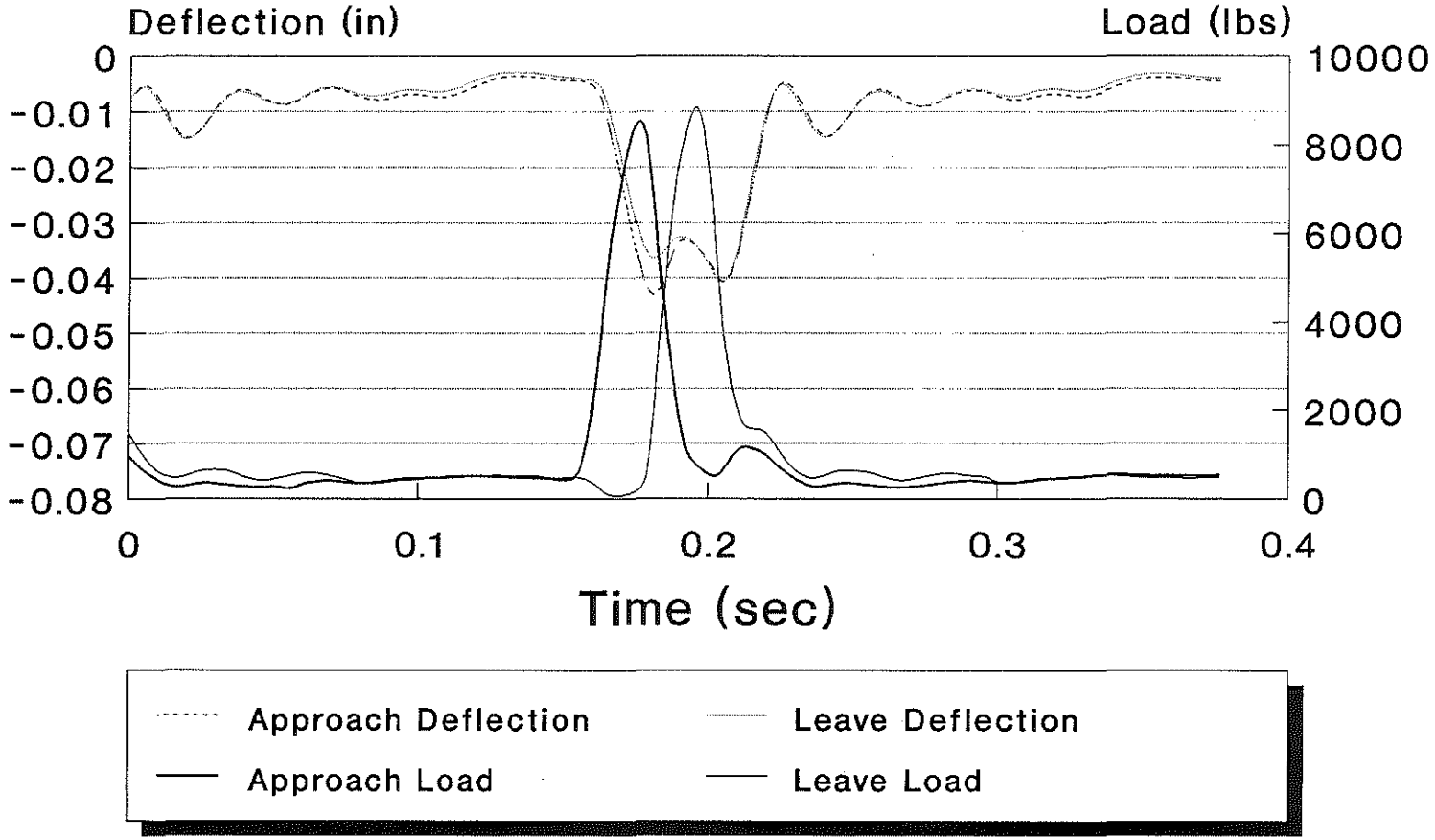

Figure A-15: Load and deflection curves for 6A virgin limestone slab after cycle # 10,000.

6A VIRGIN LIMESTONE
CYCLE # 20,000

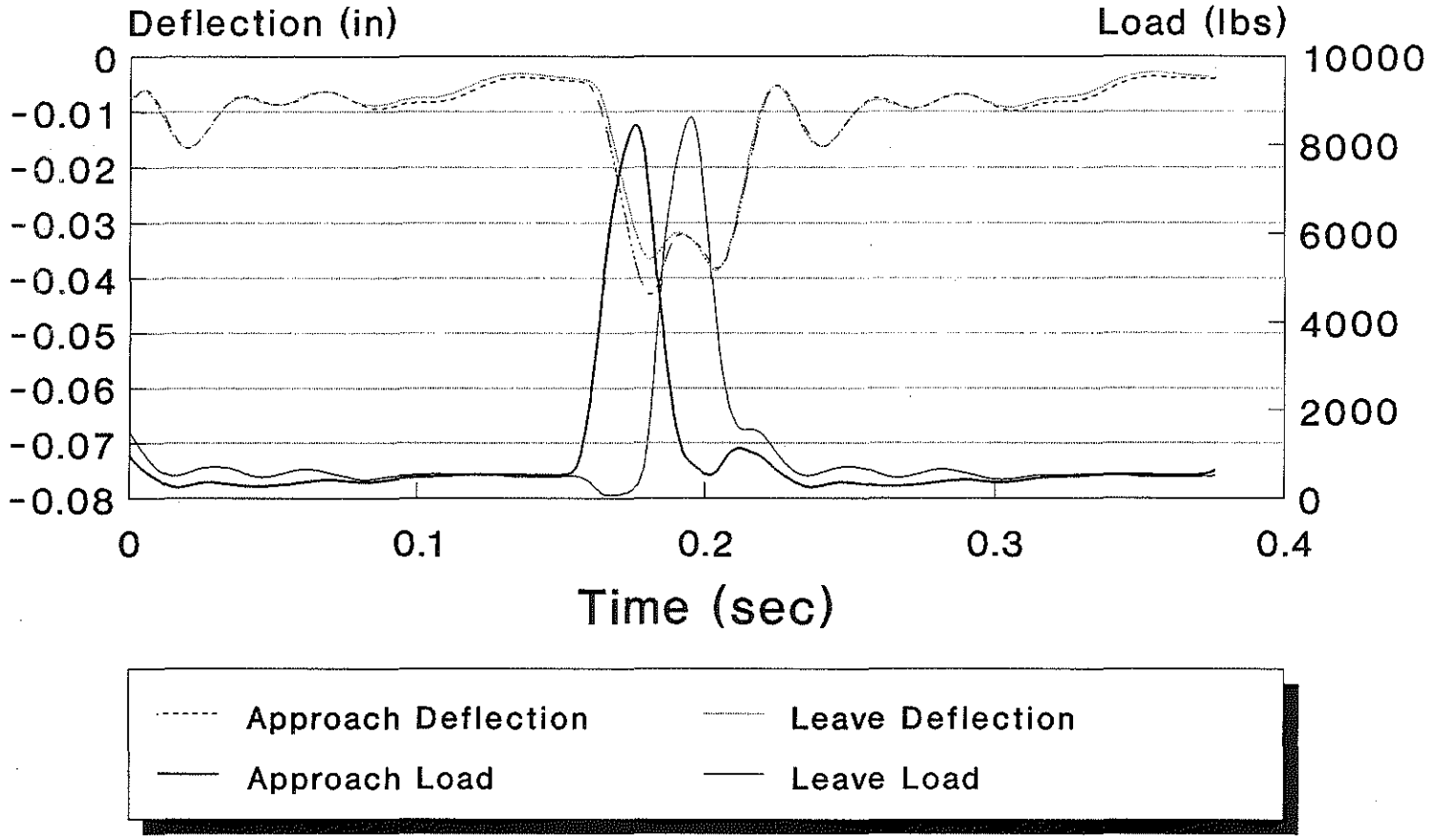

Figure A-16: Load and deflection curves for 6A virgin limestone slab after cycle # 20,000.

6A VIRGIN LIMESTONE
CYCLE # 50,000

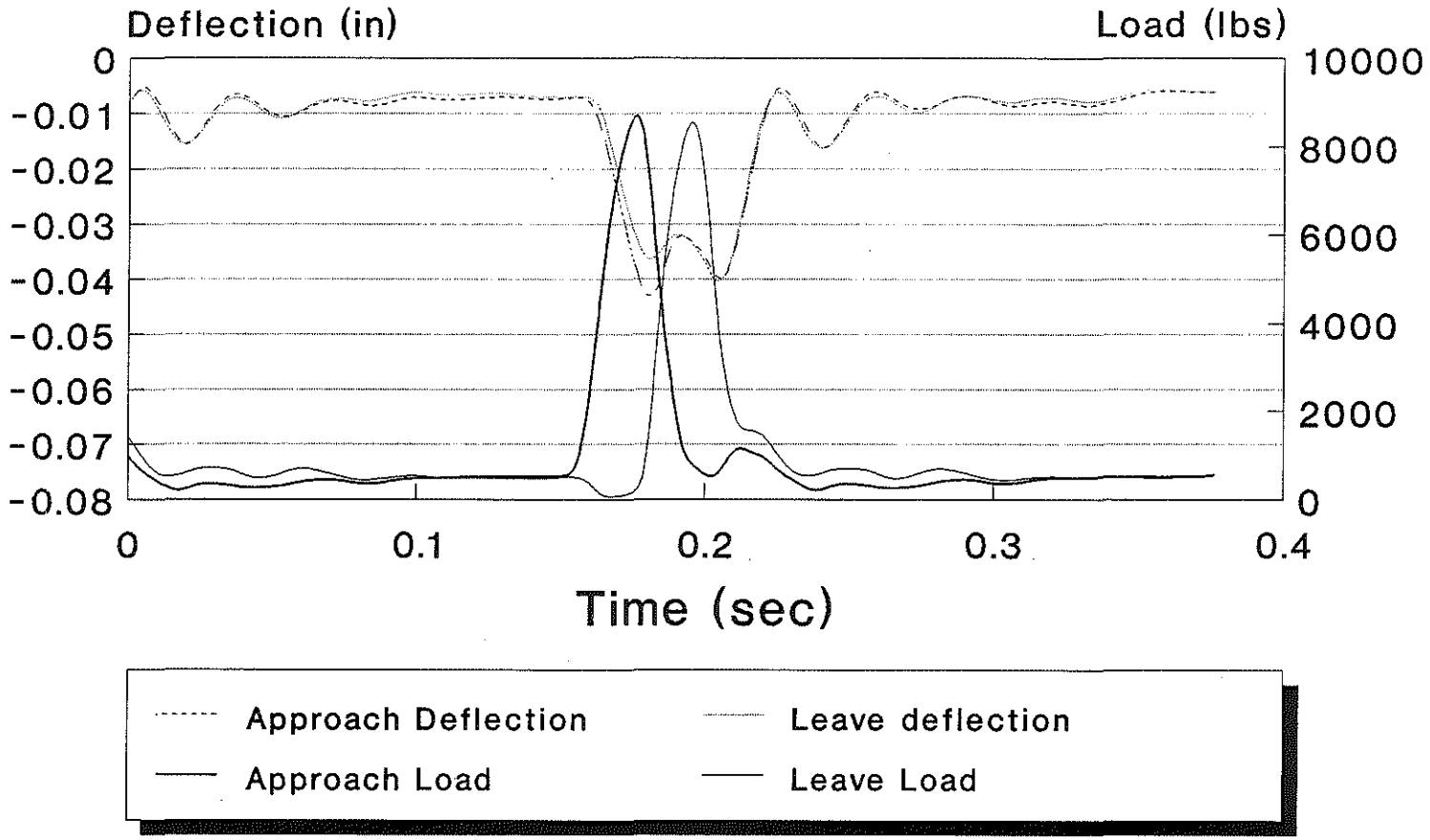

Figure A-17: Load and deflection curves for 6A virgin limestone slab after cycle # 50,000.

6A VIRGIN LIMESTONE
CYCLE # 100,000

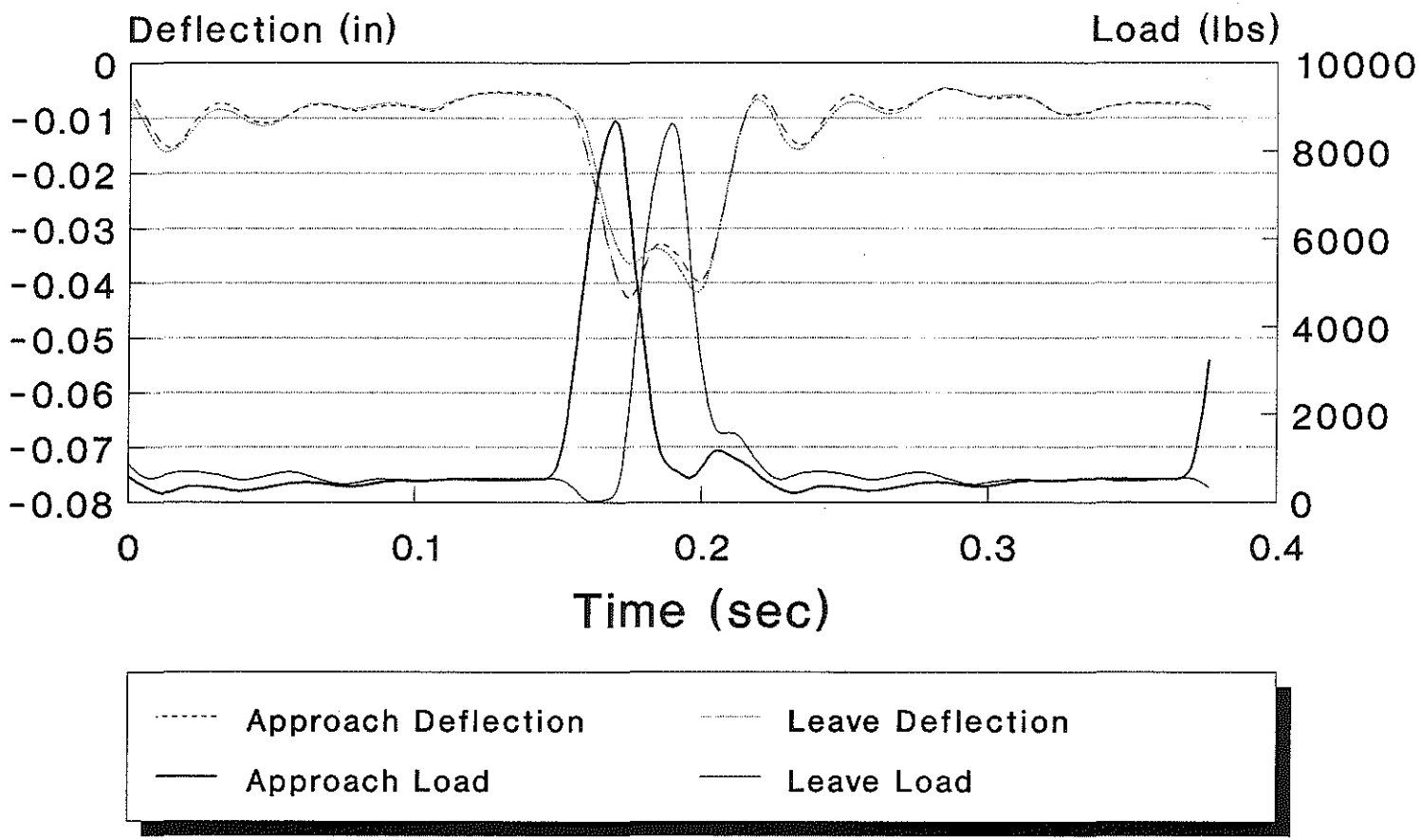

Figure A-18: Load and deflection curves for 6A virgin limestone slab after cycle # 100,000.

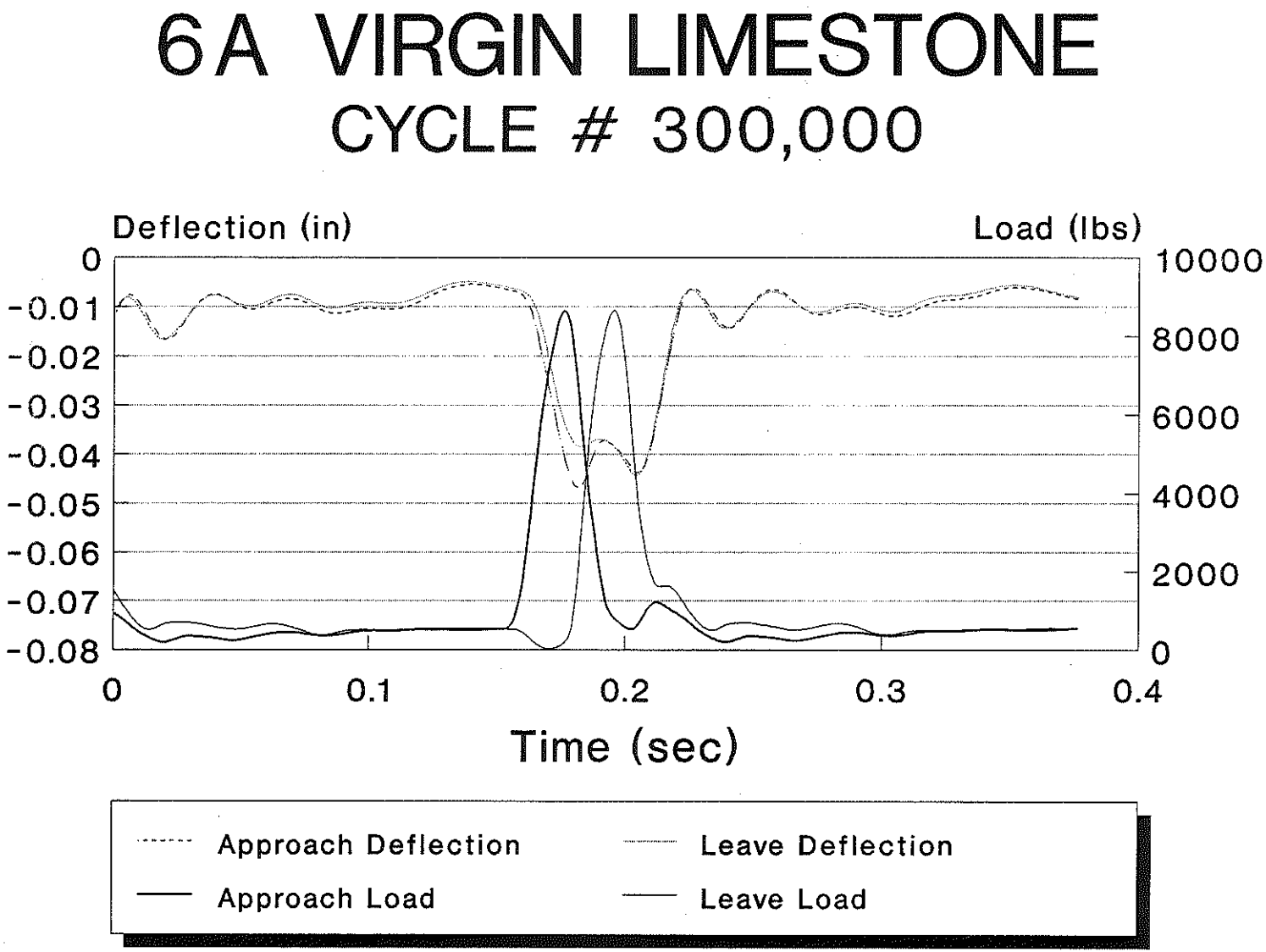

Figure A-19: Load and deflection curves for 6A virgin limestone slab after cycle # 300,000.

6A VIRGIN LIMESTONE
CYCLE # 600,000

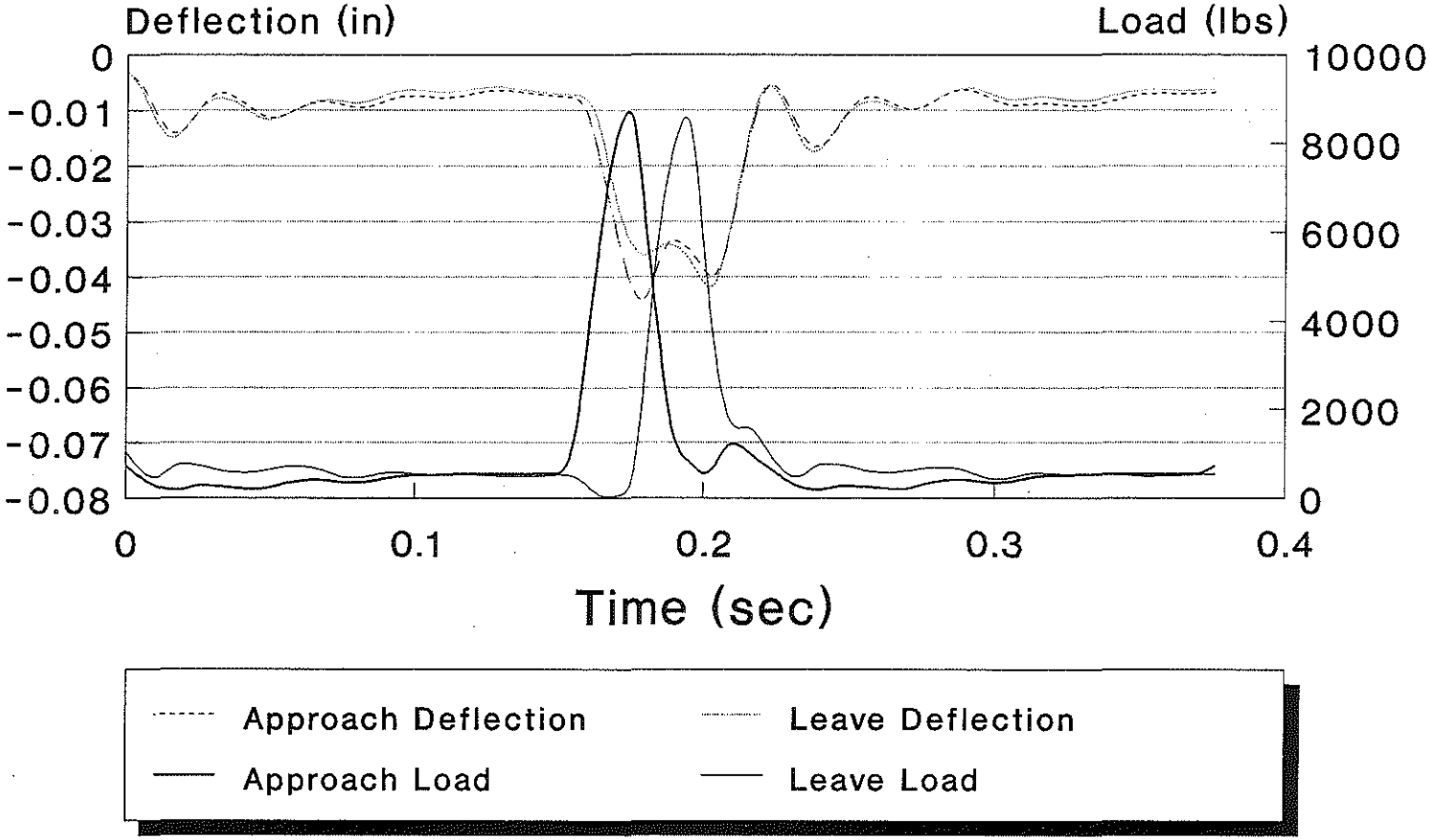

Figure A-20: Load and deflection curves for 6A virgin limestone slab after cycle # 600,000.

6A VIRGIN LIMESTONE
CYCLE # 900,000

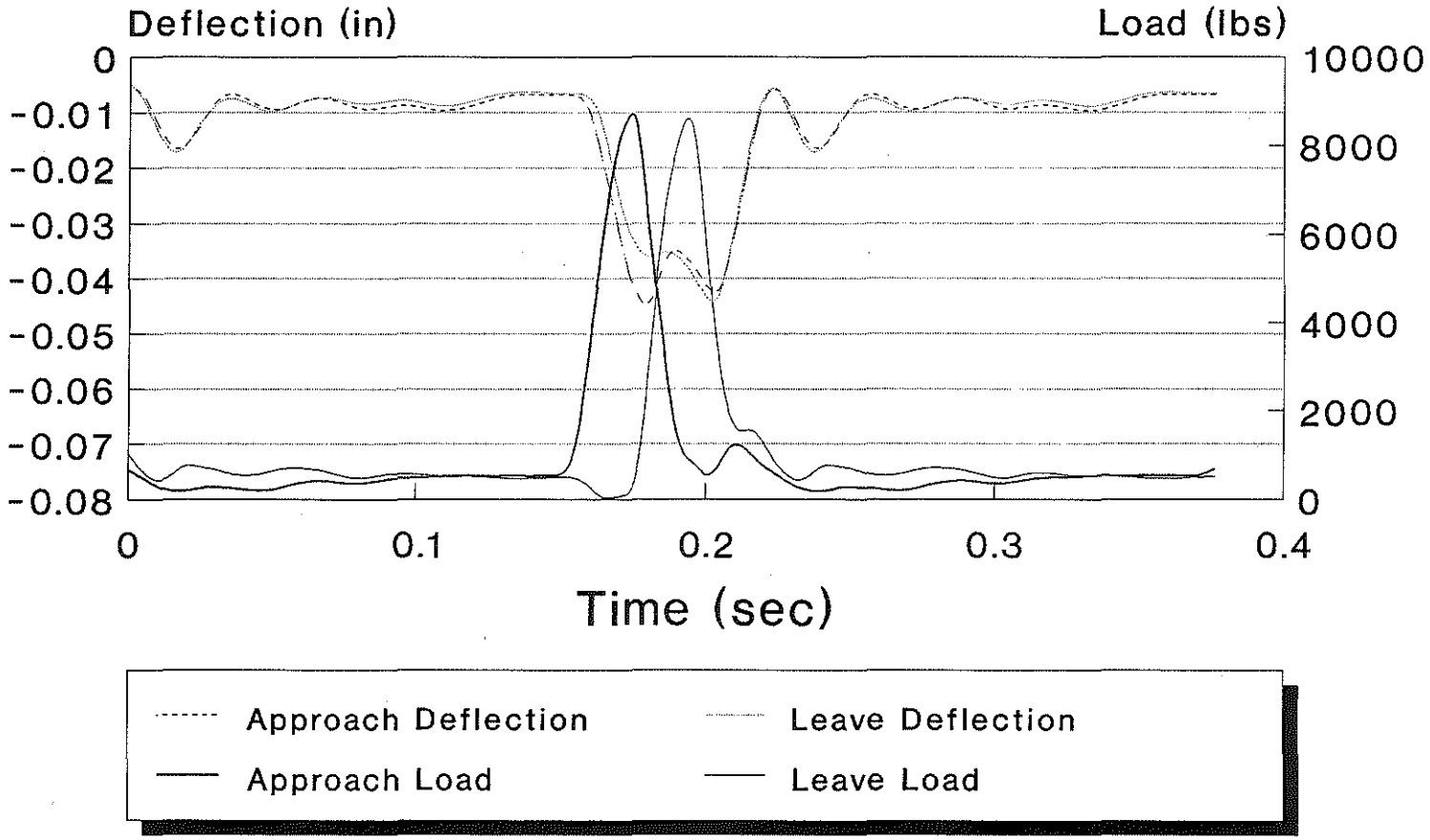

Figure A-21: Load and deflection curves for 6A virgin limestone slab after cycle # 900,000.

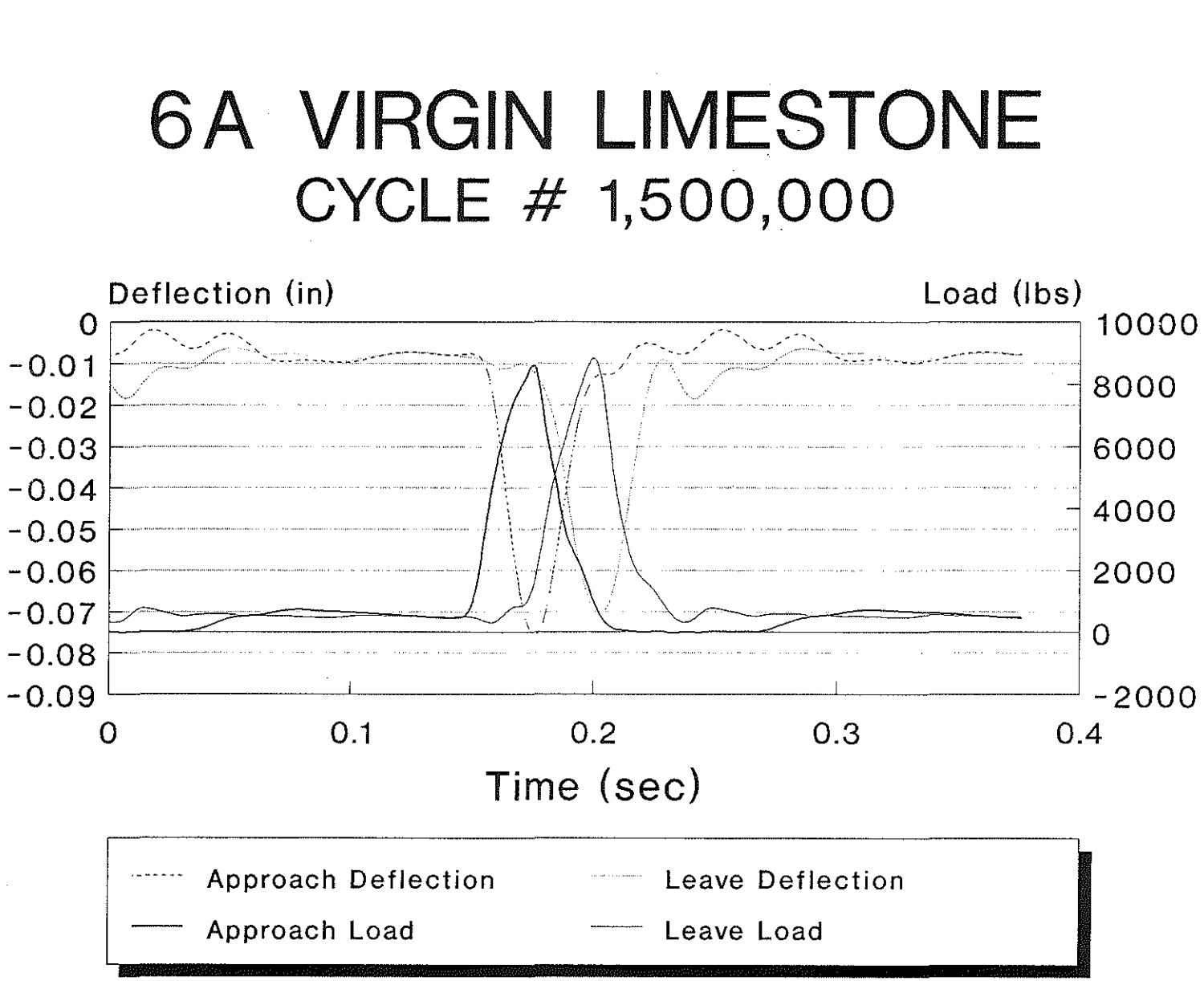

Figure A-22: Load and deflection curves for 6A Virgin limestone after cycle # 1,500,000.

6A VIRGIN SLAG
CYCLE # 1

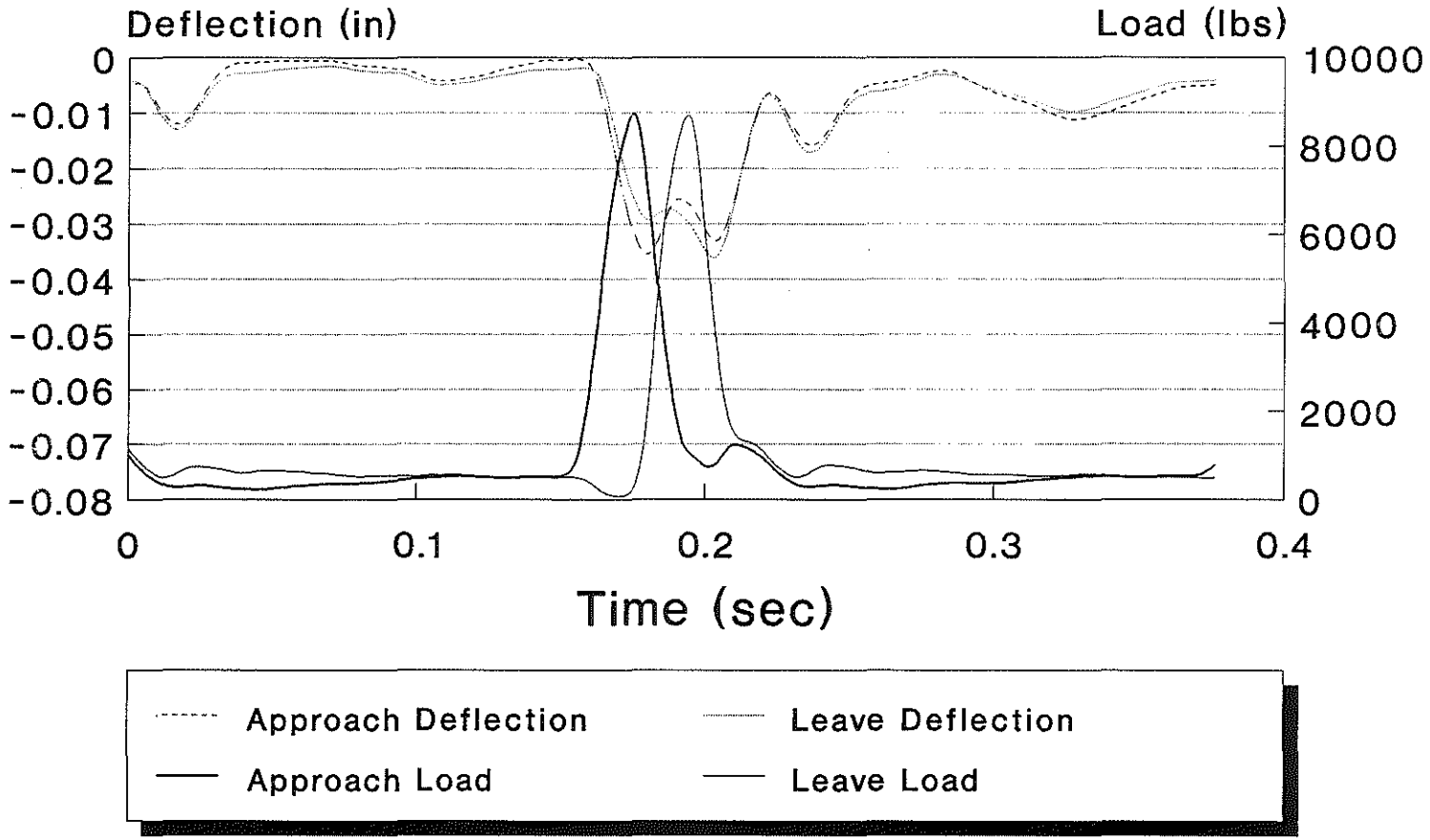

Figure A-23: Load and deflection curves for 6A virgin slag after cycle # 1.

6A VIRGIN SLAG
CYCLE # 1000

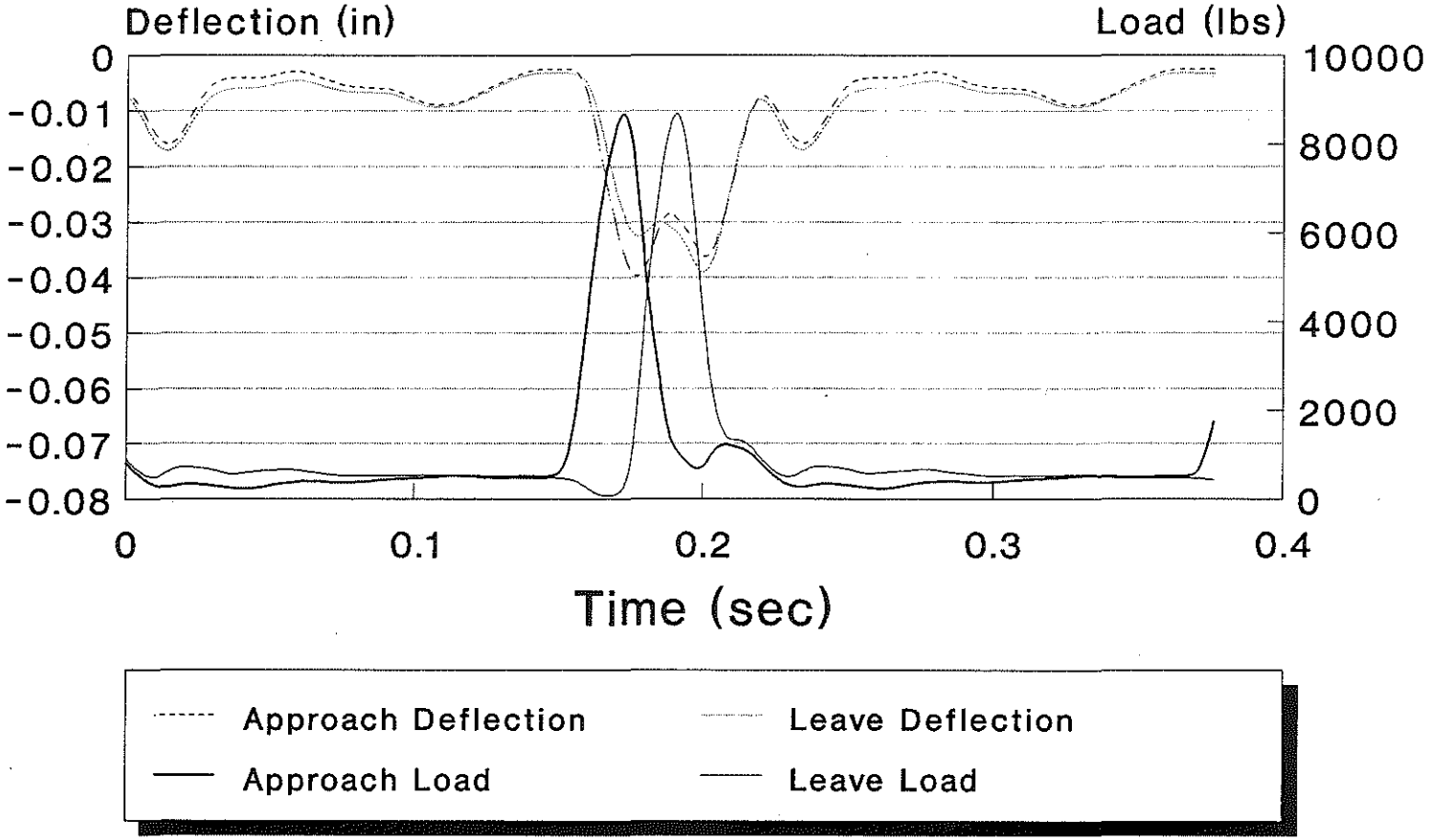

Figure A-24: Load and deflection curves for 6A virgin slag after cycle # 1,000.

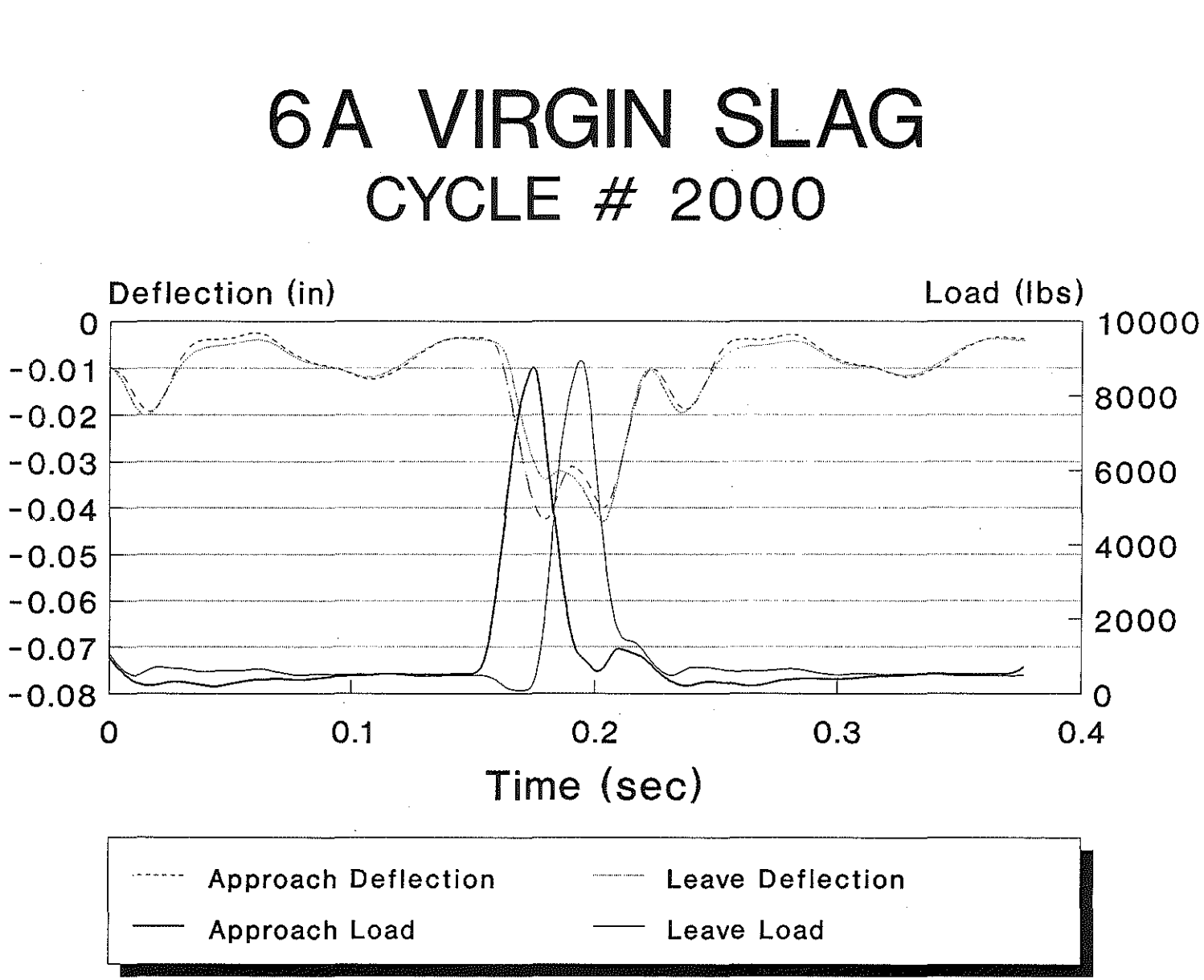

Figure A-25: Load and deflection curves for 6A virgin slag after cycle # 2,000.

6A VIRGIN SLAG
CYCLE # 5000

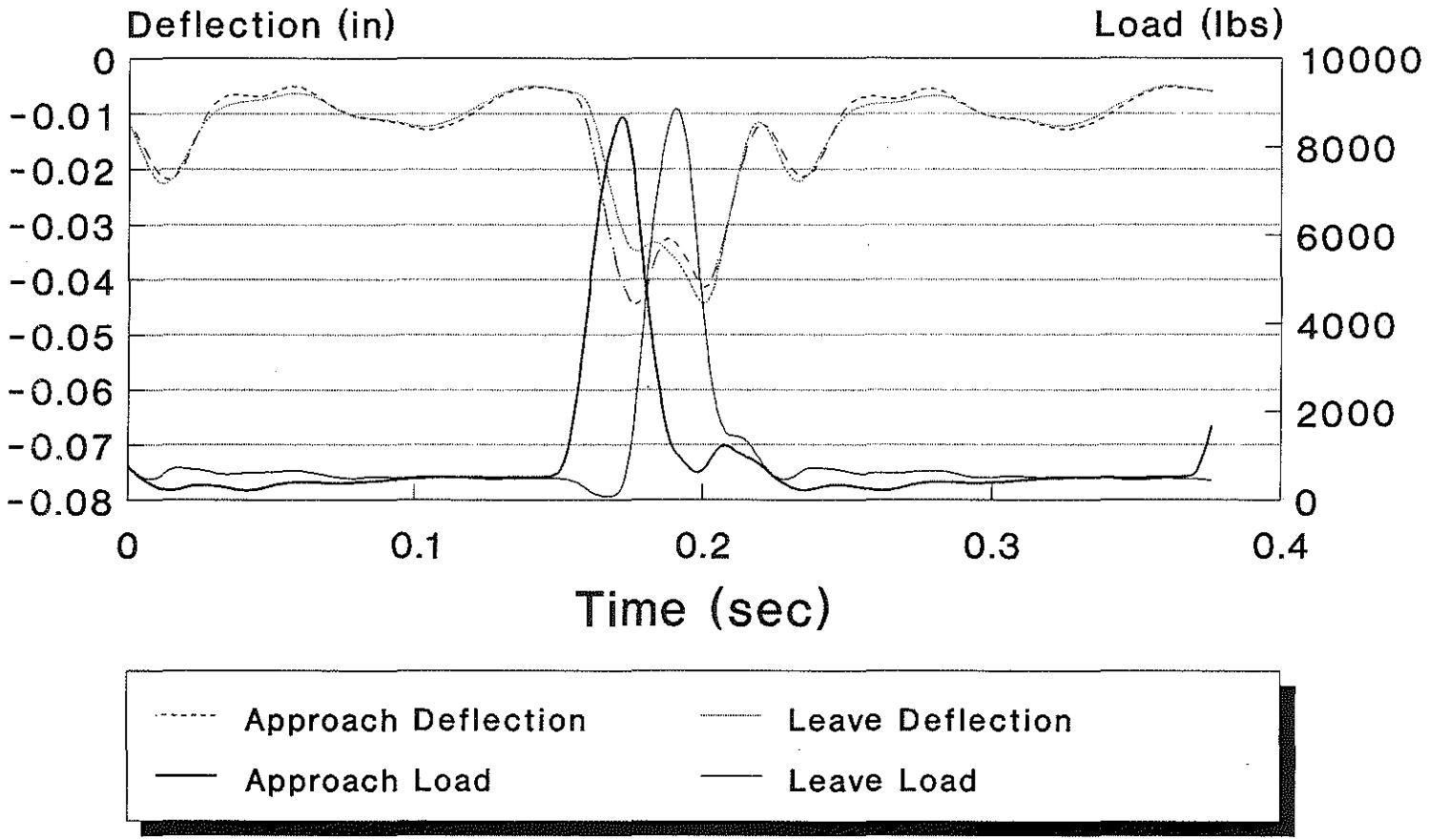

Figure A-26: Load and deflection curves for 6A virgin slag after cycle # 5,000.

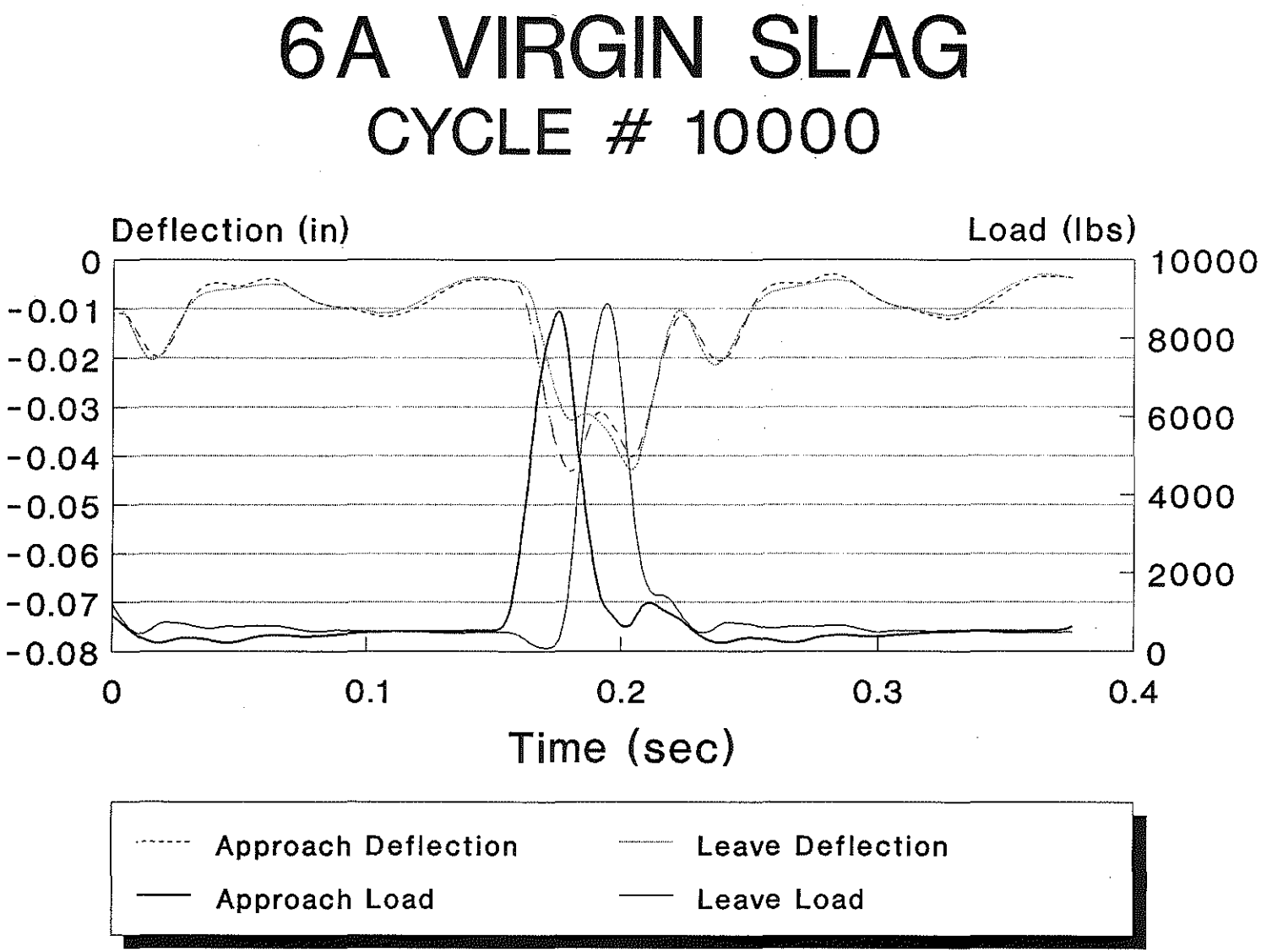

Figure A-27: Load and deflection curves for 6A virgin slag after cycle # 10,000.

6A VIRGIN SLAG
CYCLE # 20000

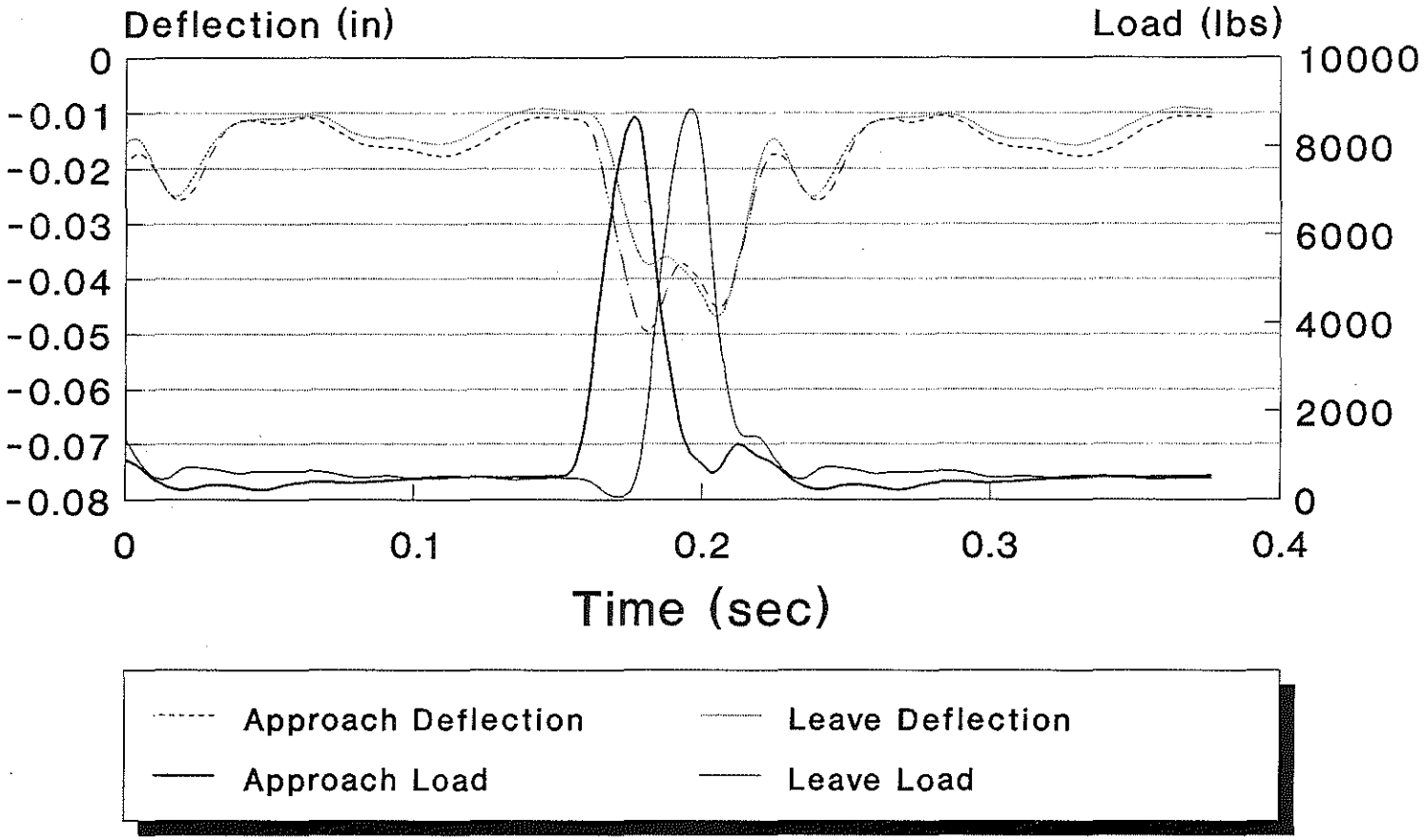

Figure A-28: Load and deflection curves for 6A virgin slag after cycle # 20,000.

6A VIRGIN SLAG
CYCLE # 50000

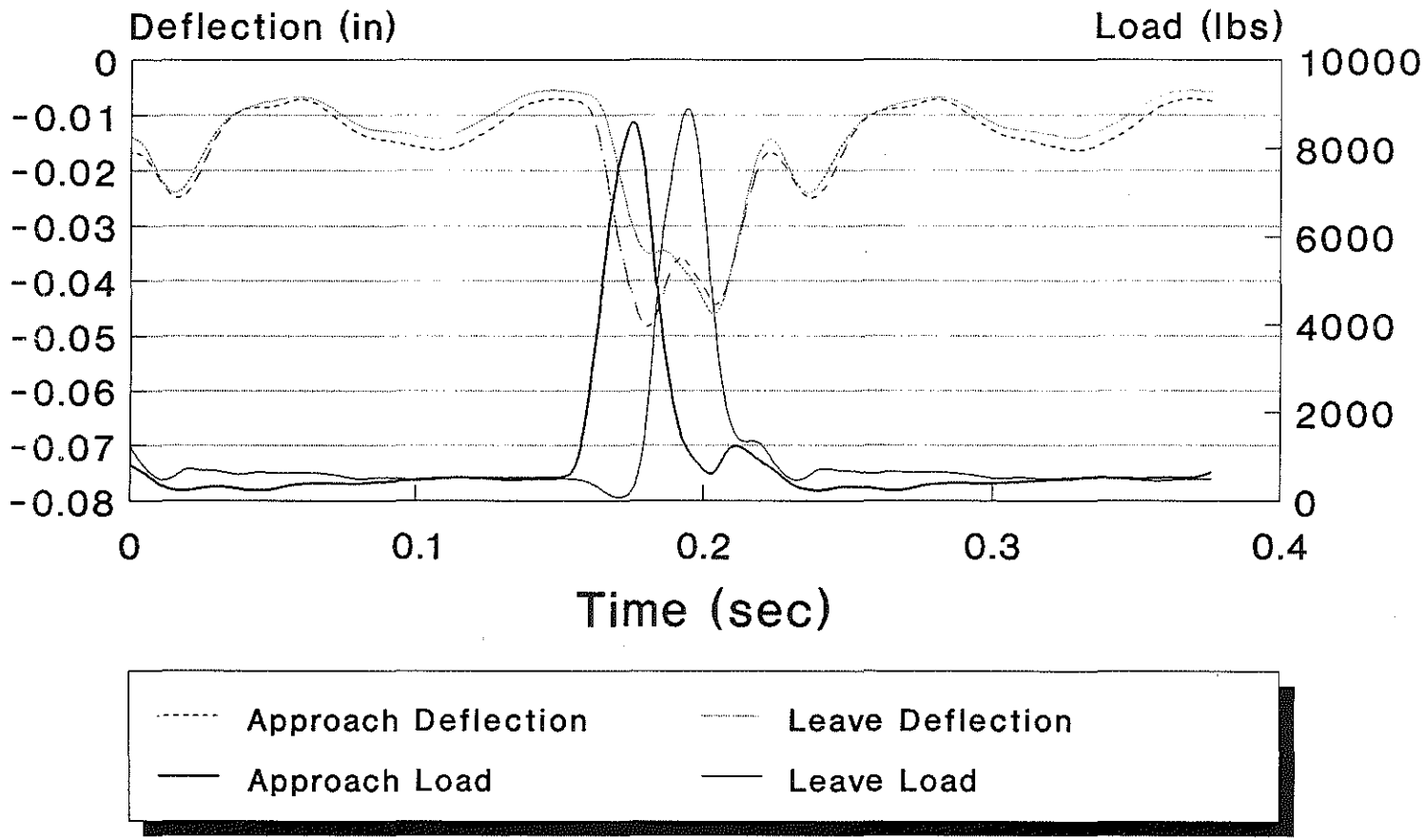

Figure A-29: Load and deflection curves for 6A virgin slag after cycle # 50,000.

6A VIRGIN SLAG
CYCLE # 100000

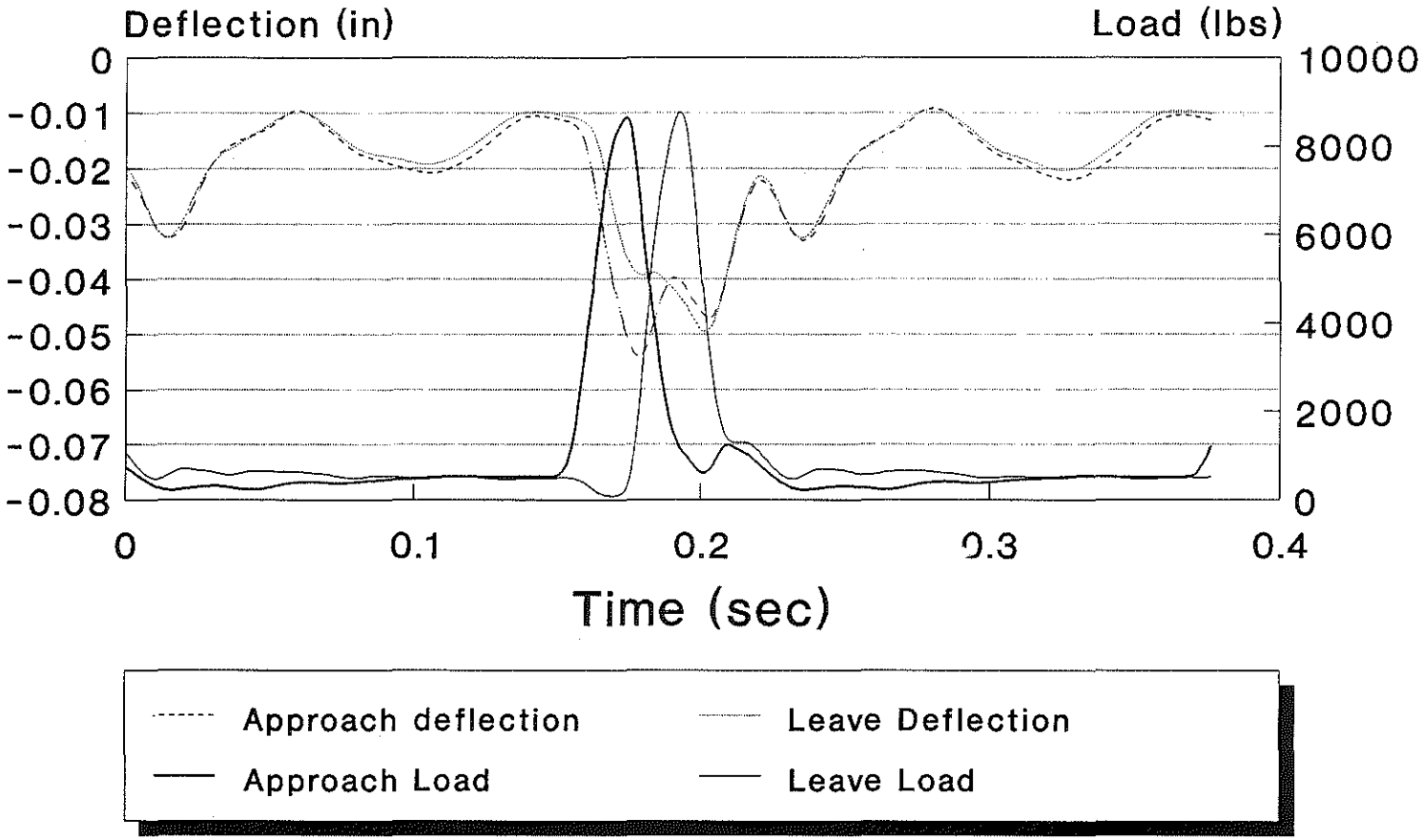

Figure A-30: Load and deflection curves for 6A virgin slag after cycle # 100,000.

6A VIRGIN SLAG
CYCLE # 250000

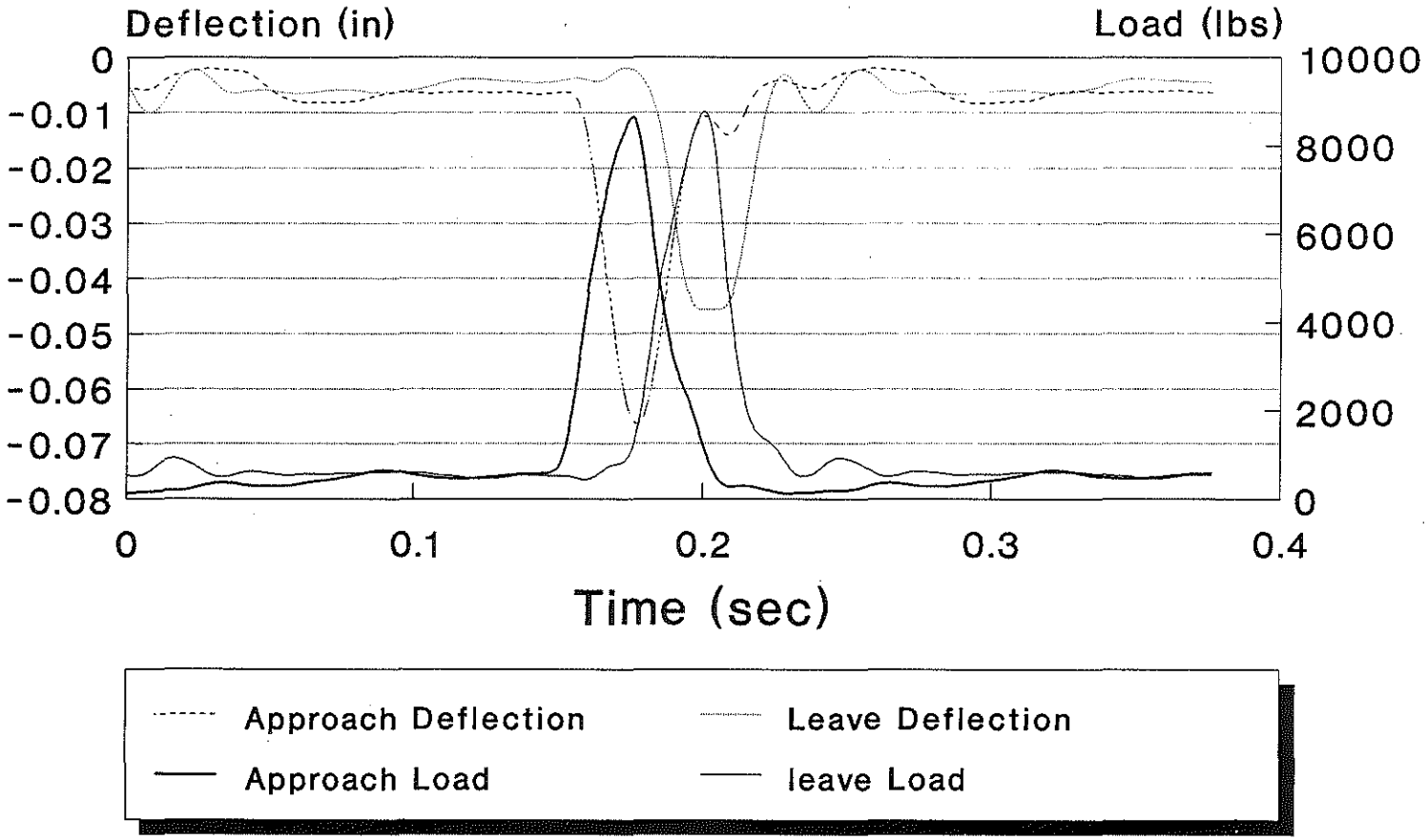

Figure A-31: Load and deflection curves for 6A virgin slag after cycle # 250,000.

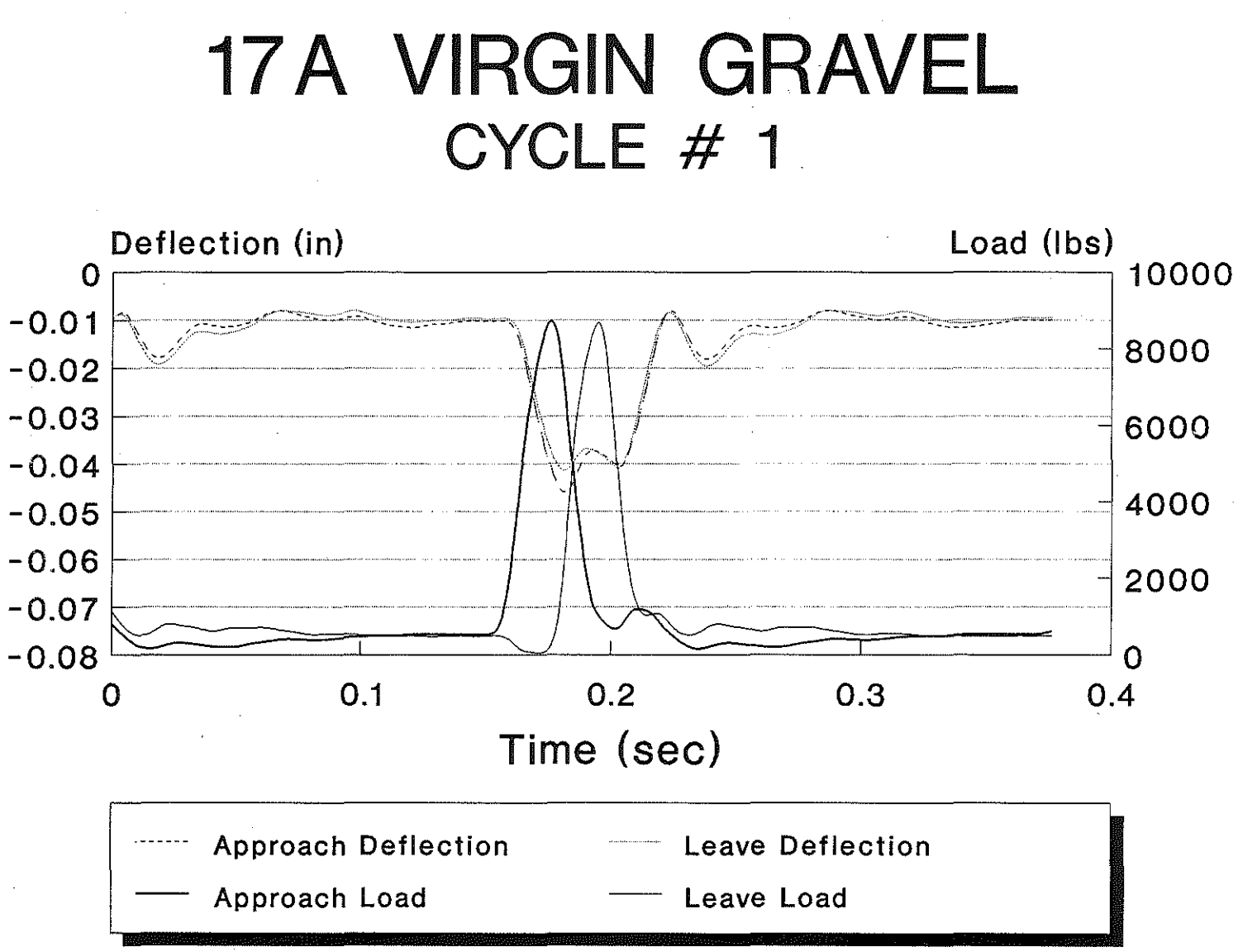

Figure A-32: Load and deflection curves for 17A virgin gravel after cycle # 1.

17A VIRGIN GRAVEL
CYCLE # 1000

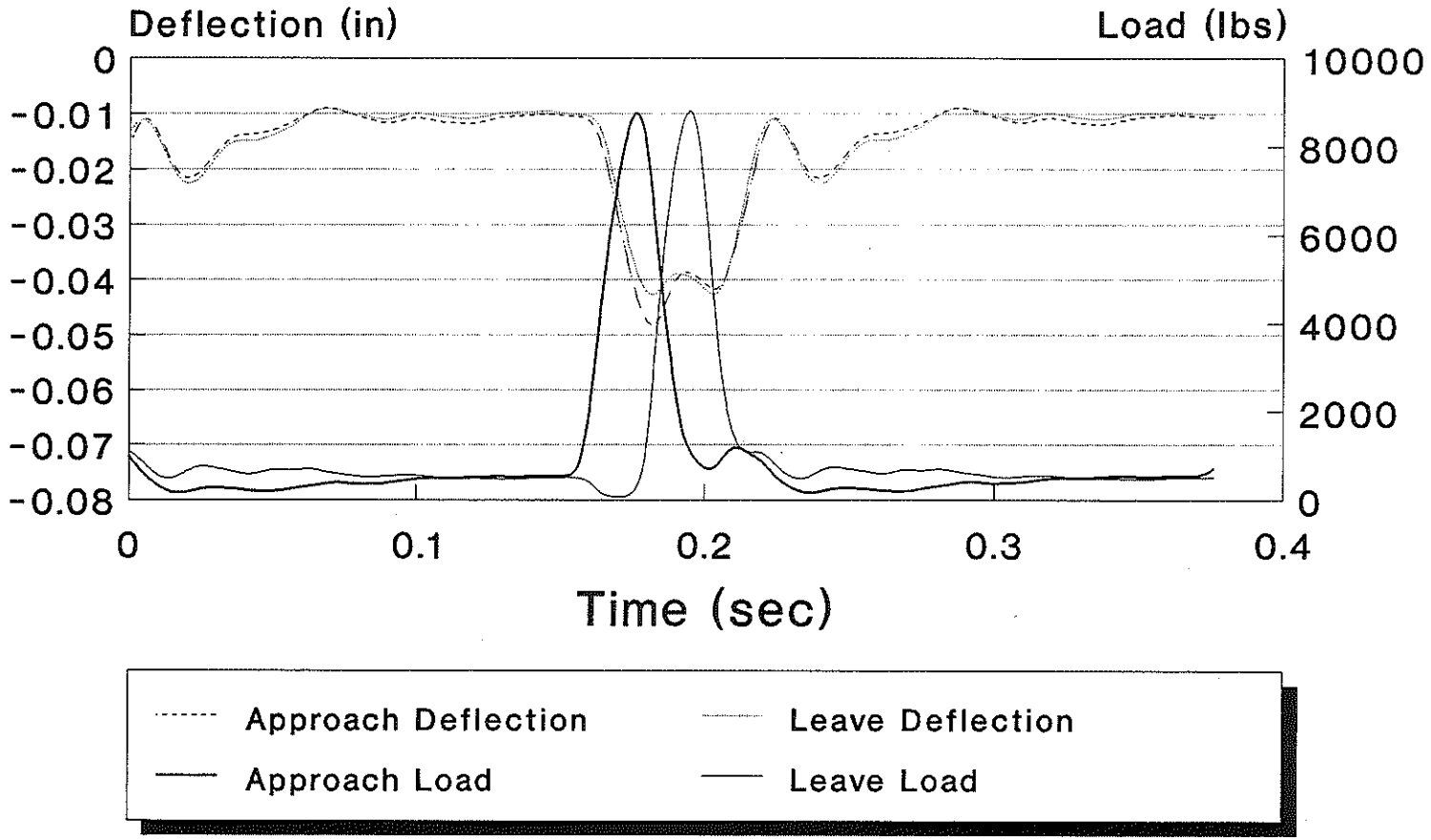

Figure A-33: Load and deflection curves for 17A virgin gravel after cycle # 1,000.

17A VIRGIN GRAVEL
CYCLE # 2000

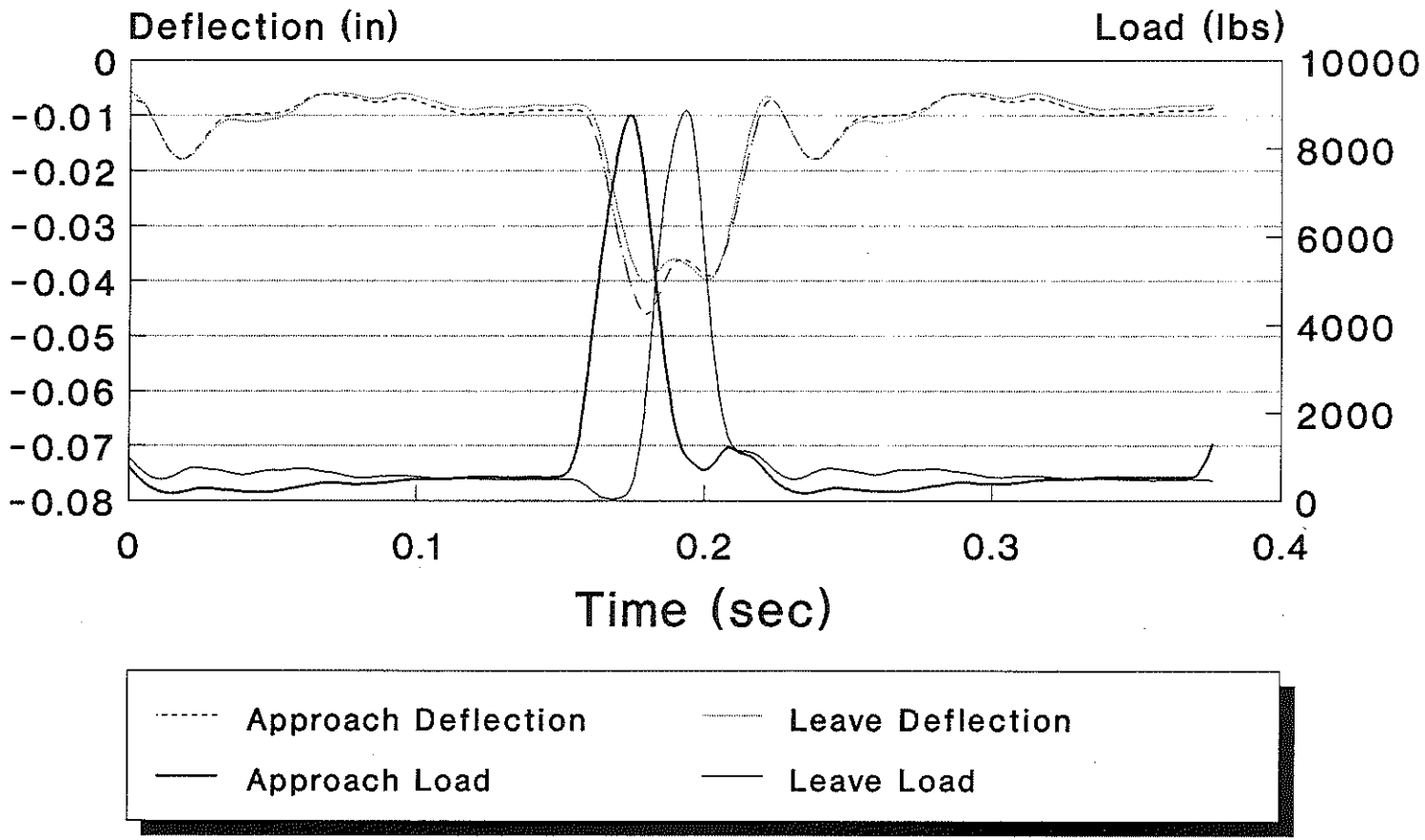

Figure A-34: Load and deflection curves for 17A virgin gravel after cycle # 2,000.

17A VIRGIN GRAVEL
CYCLE # 5000

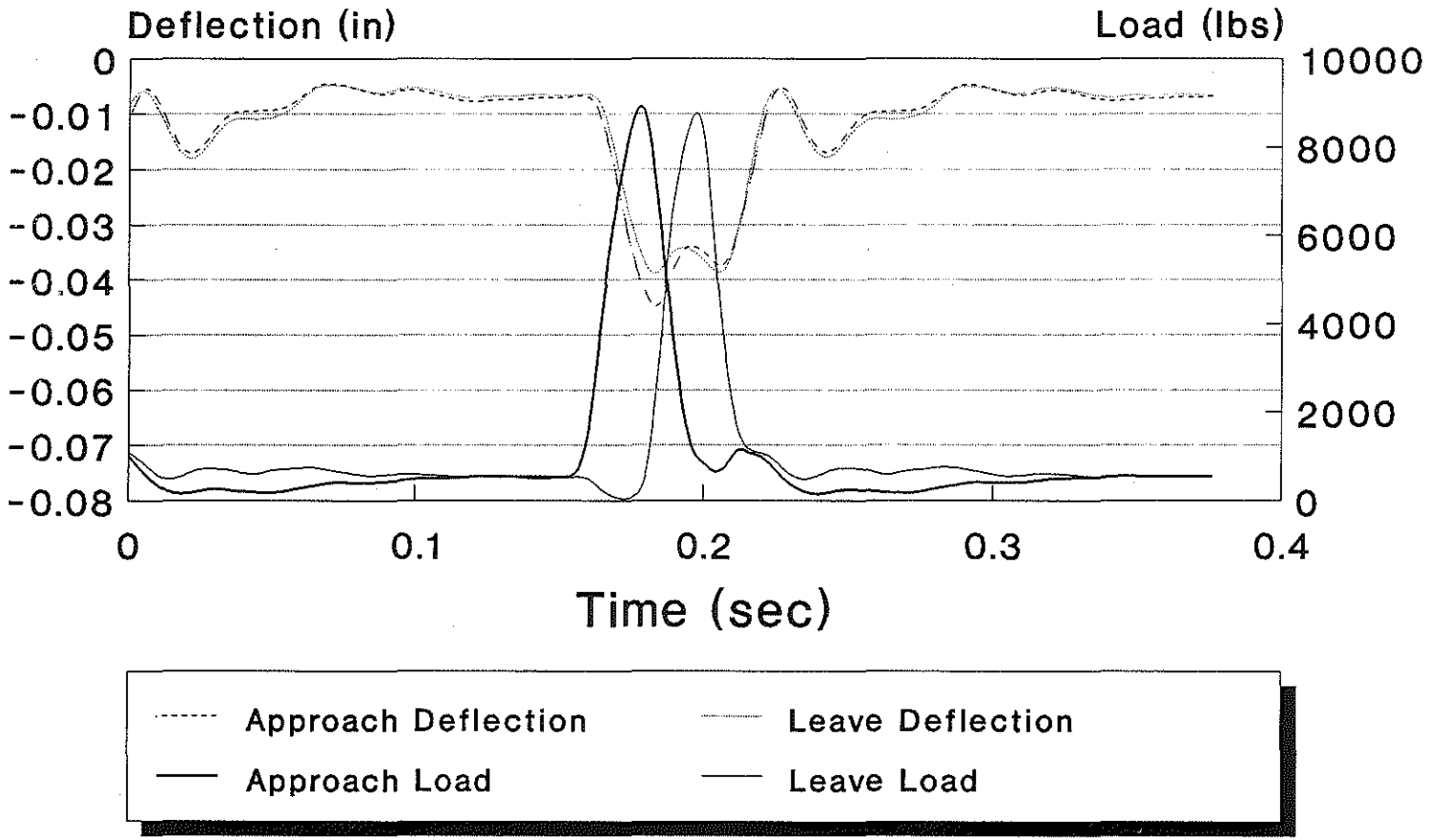

Figure A-35: Load and deflection curves for 17A virgin gravel after cycle # 5,000.

17A VIRGIN GRAVEL
CYCLE # 10000

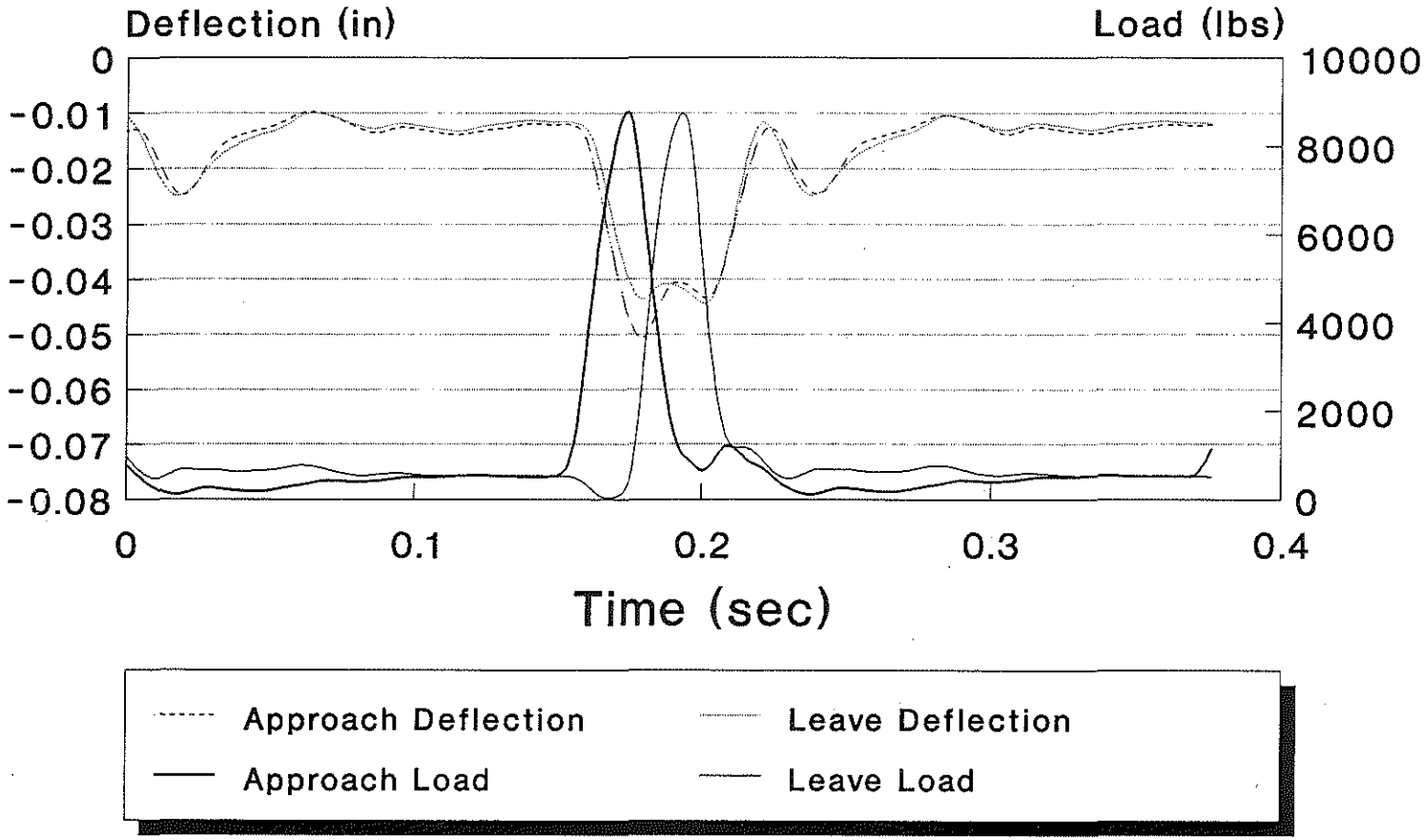

Figure A-36: Load and deflection curves for 17A virgin gravel after cycle # 10,000.

17A VIRGIN GRAVEL
CYCLE # 20000

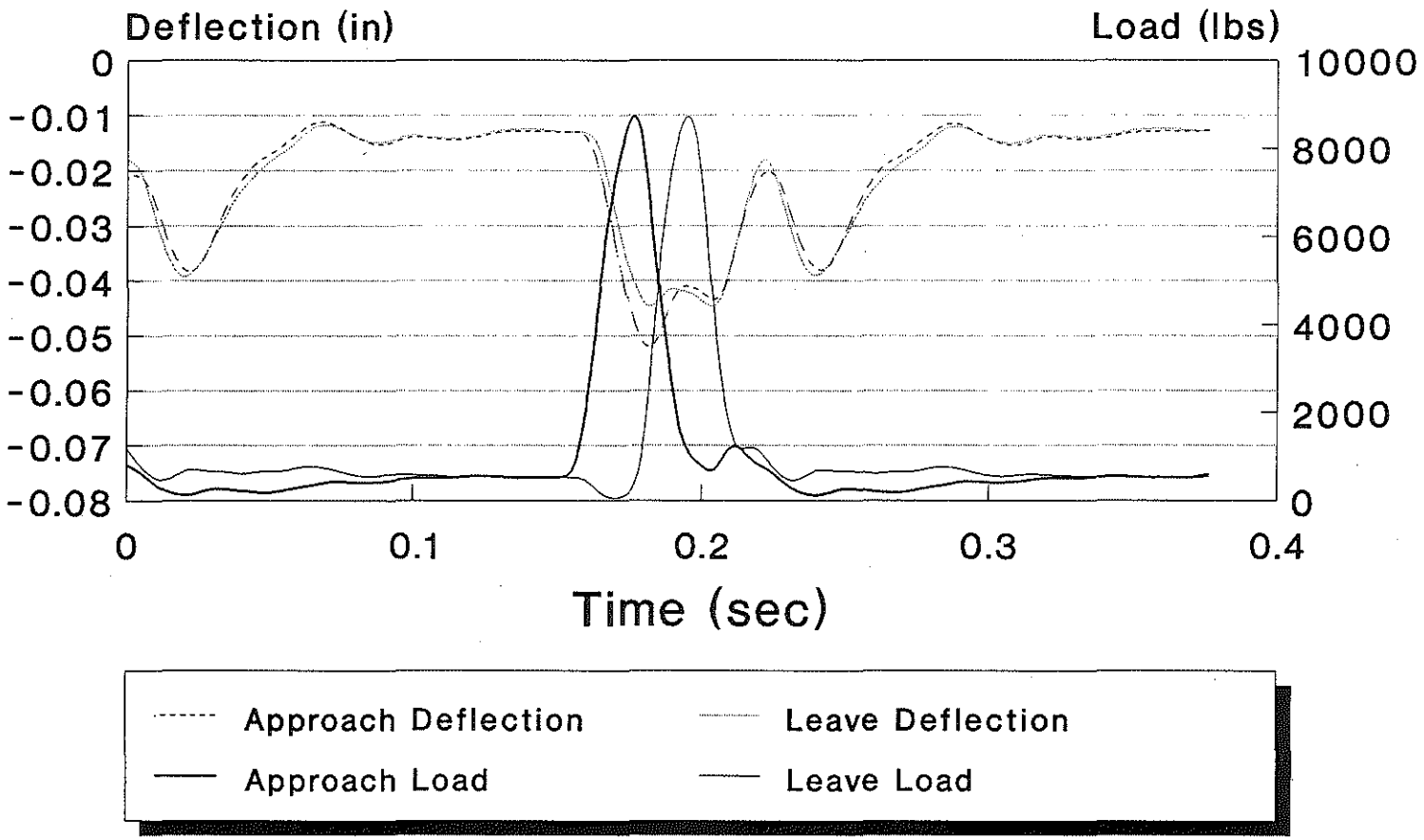

Figure A-37: Load and deflection curves for 17A virgin gravel after cycle # 20,000.

17A VIRGIN GRAVEL
CYCLE # 50000

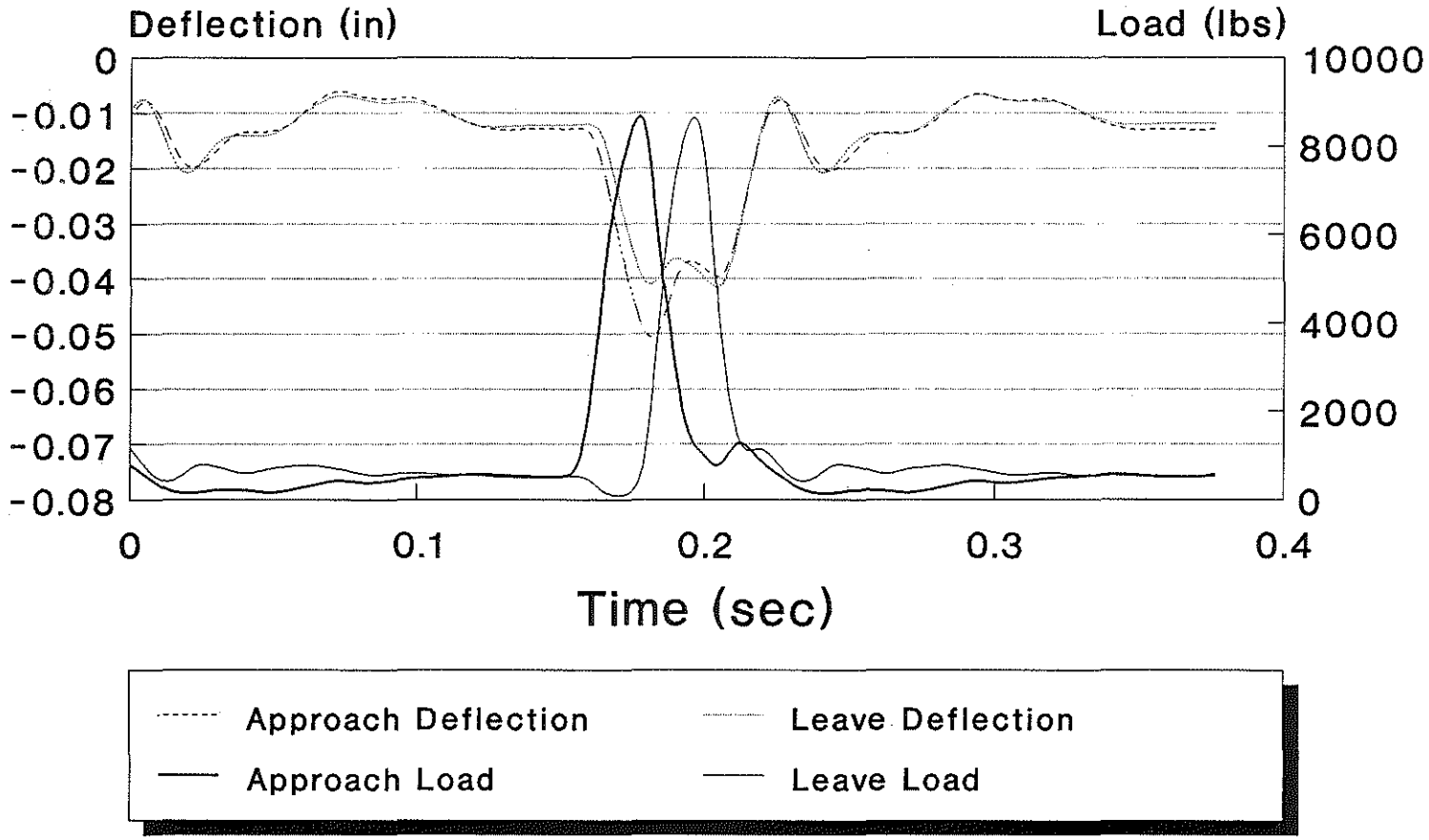

Figure A-38: Load and deflection curves for 17A virgin gravel after cycle # 50,000.

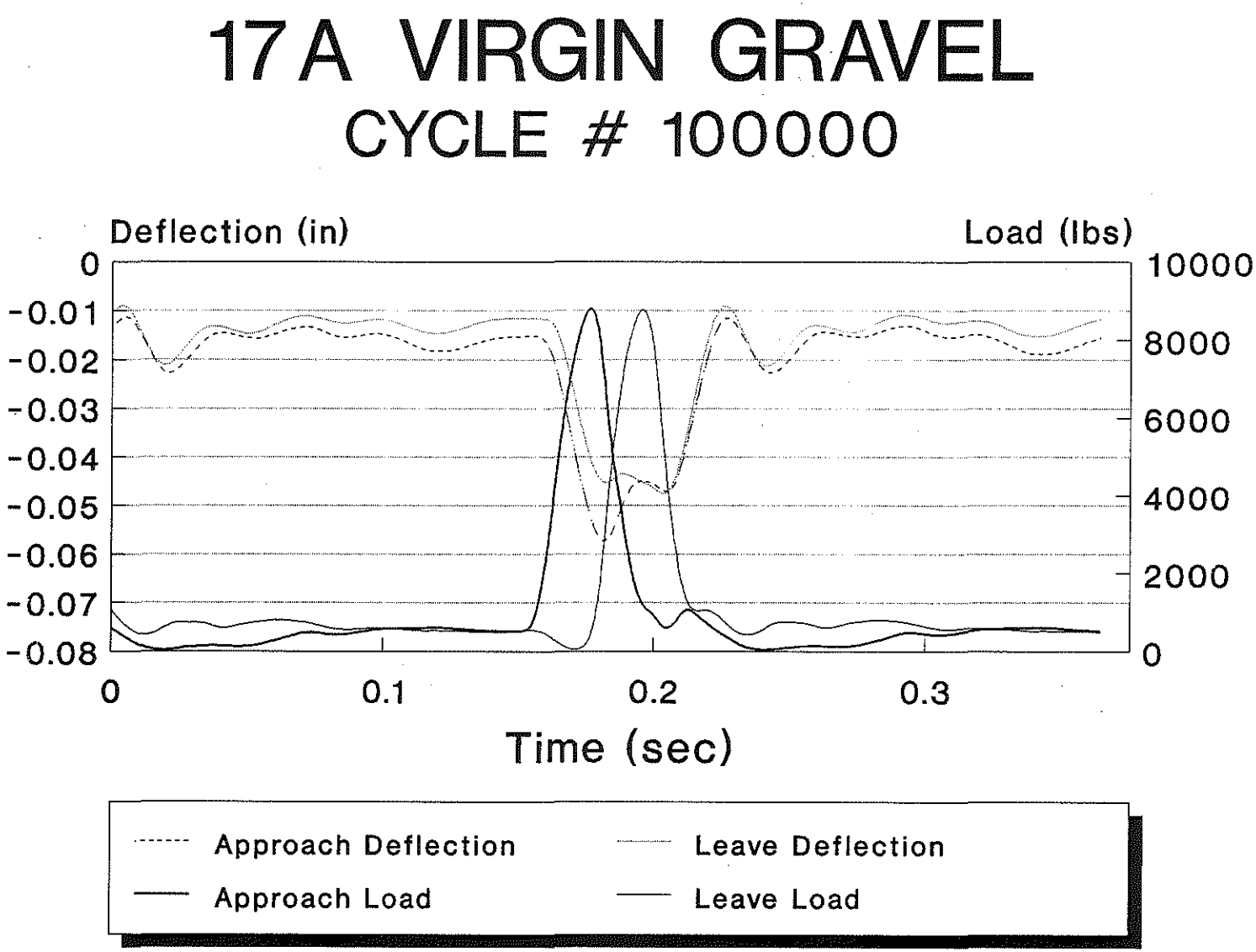

Figure A-39: Load and deflection curves for 17A virgin gravel after cycle # 100,000.

17A VIRGIN GRAVEL
CYCLE # 300000

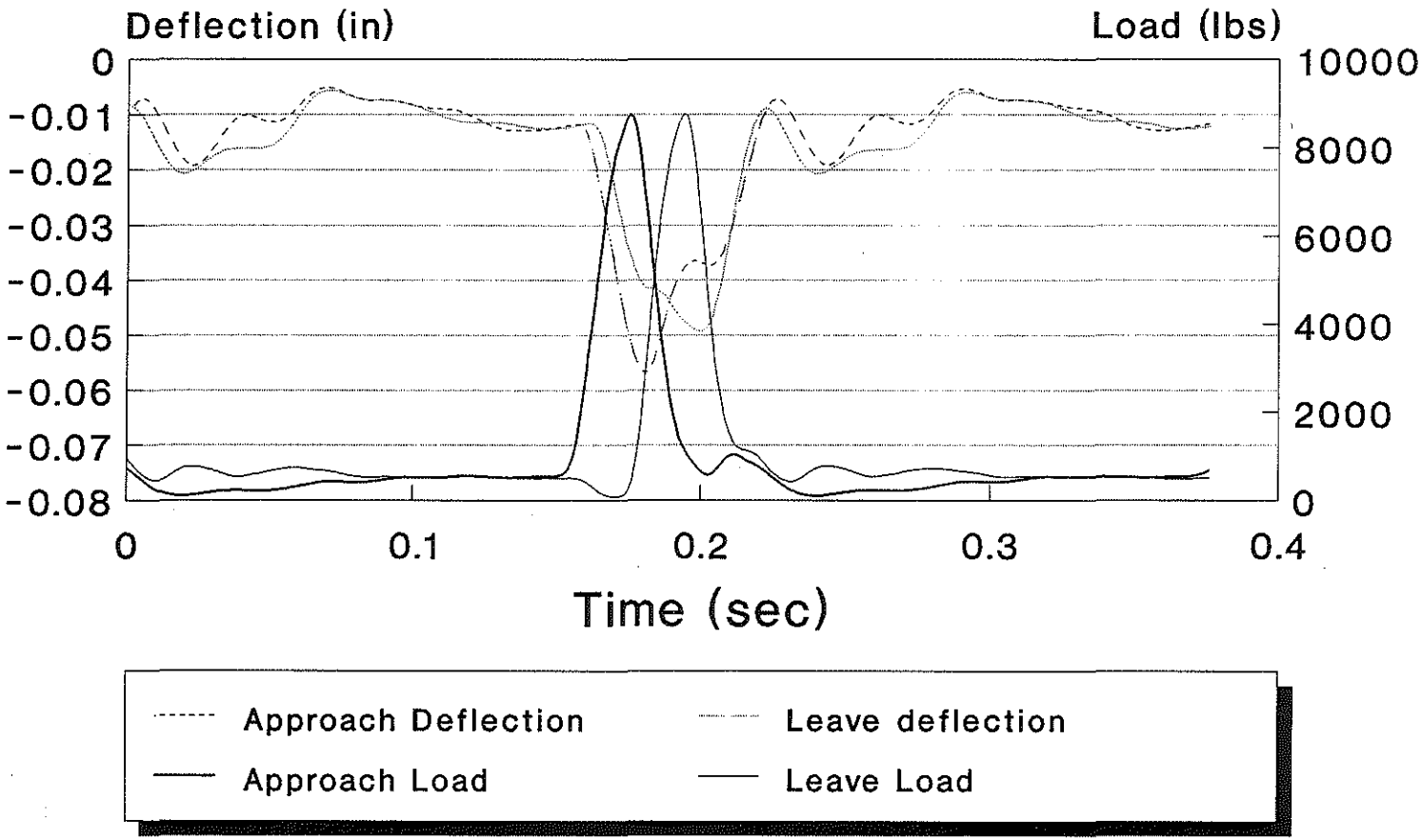

Figure A-40: Load and deflection curves for 17A virgin gravel after cycle # 300,000.

17A VIRGIN GRAVEL
CYCLE # 600000

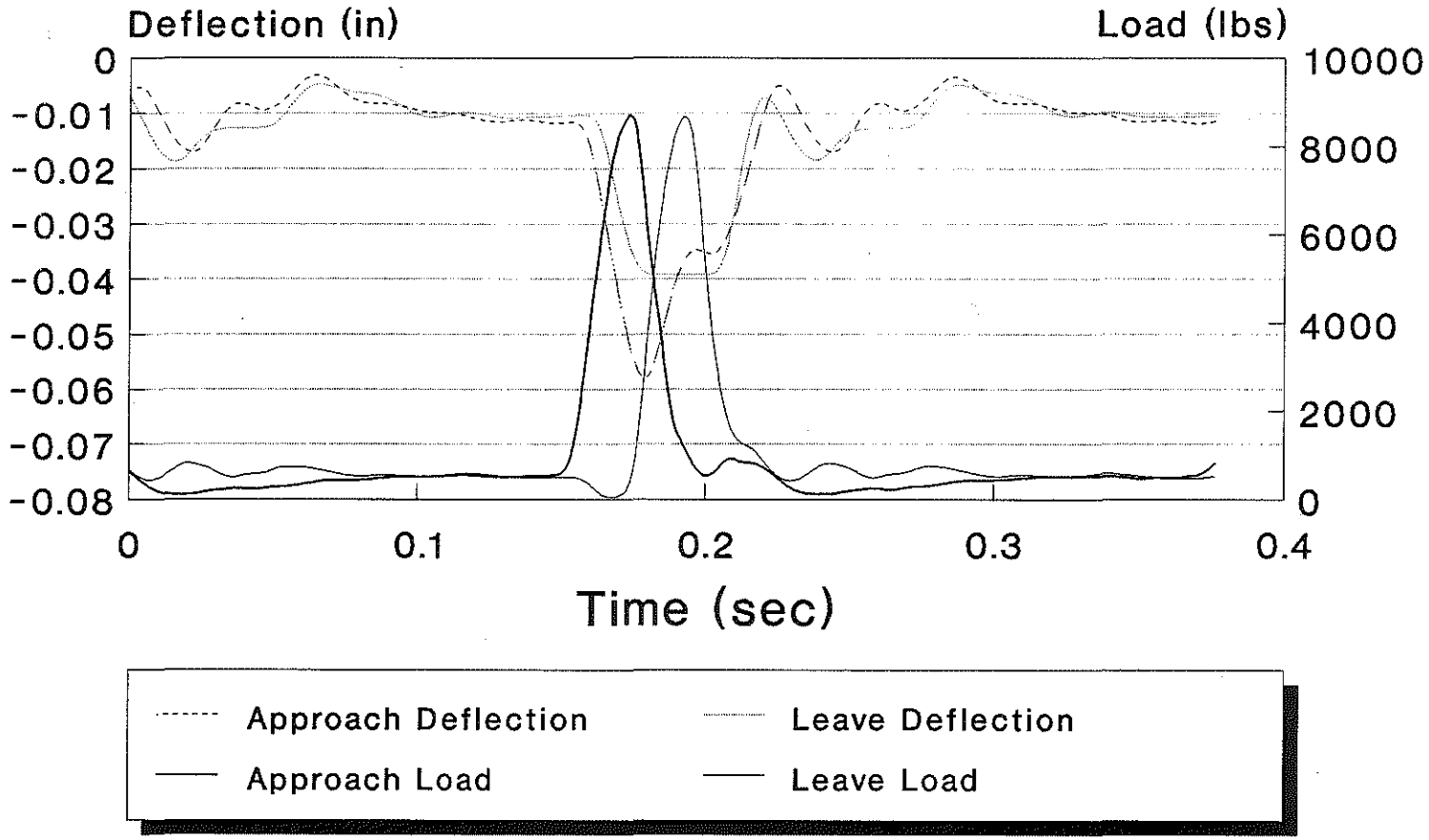

Figure A-41: Load and deflection curves for 17A virgin gravel after cycle # 600,000.

17A VIRGIN GRAVEL
CYCLE # 900000

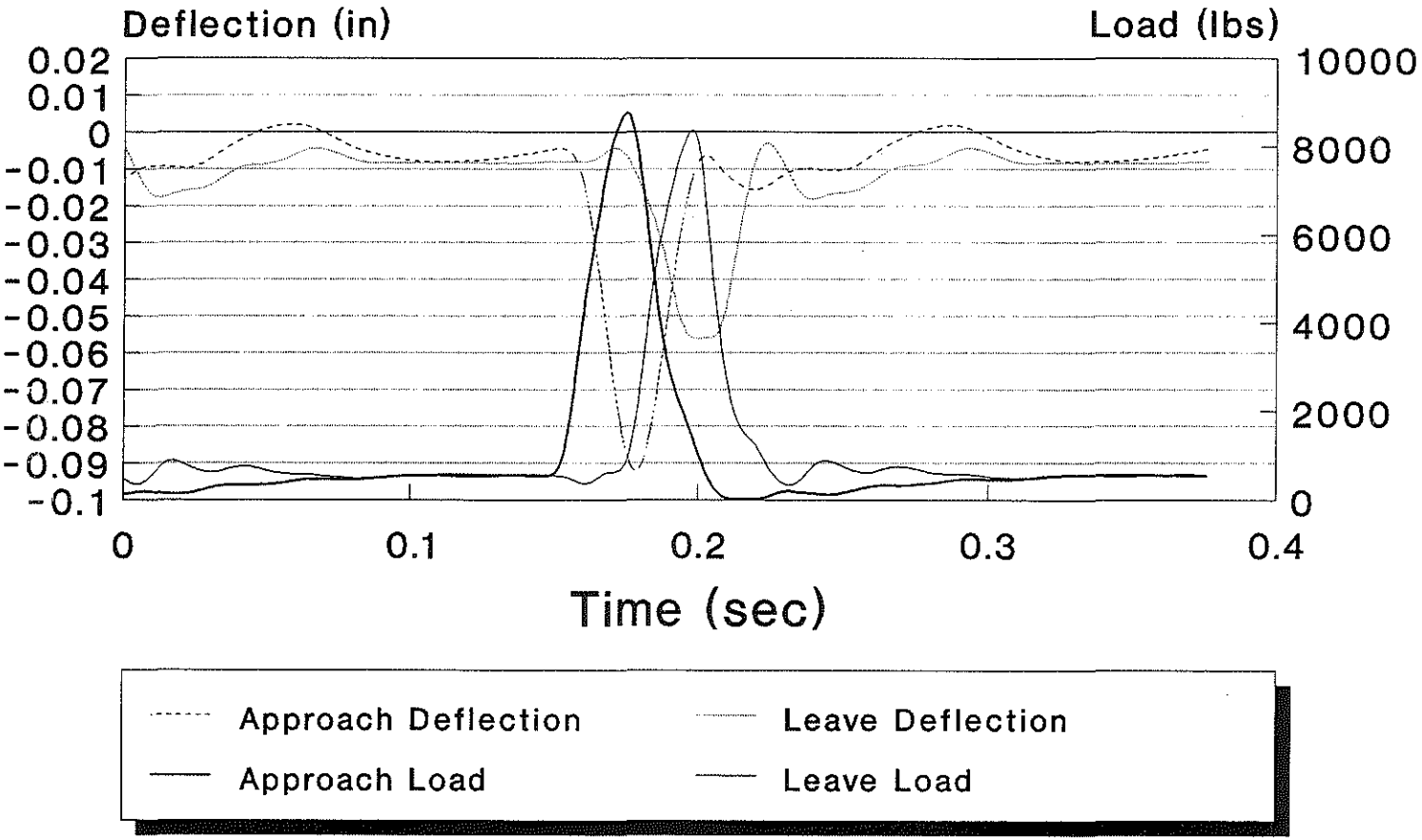

Figure A-42: Load and deflection curves for 17A virgin gravel after cycle # 900,000.

6A 100% RECYCLED GRAVEL
CYCLE # 1

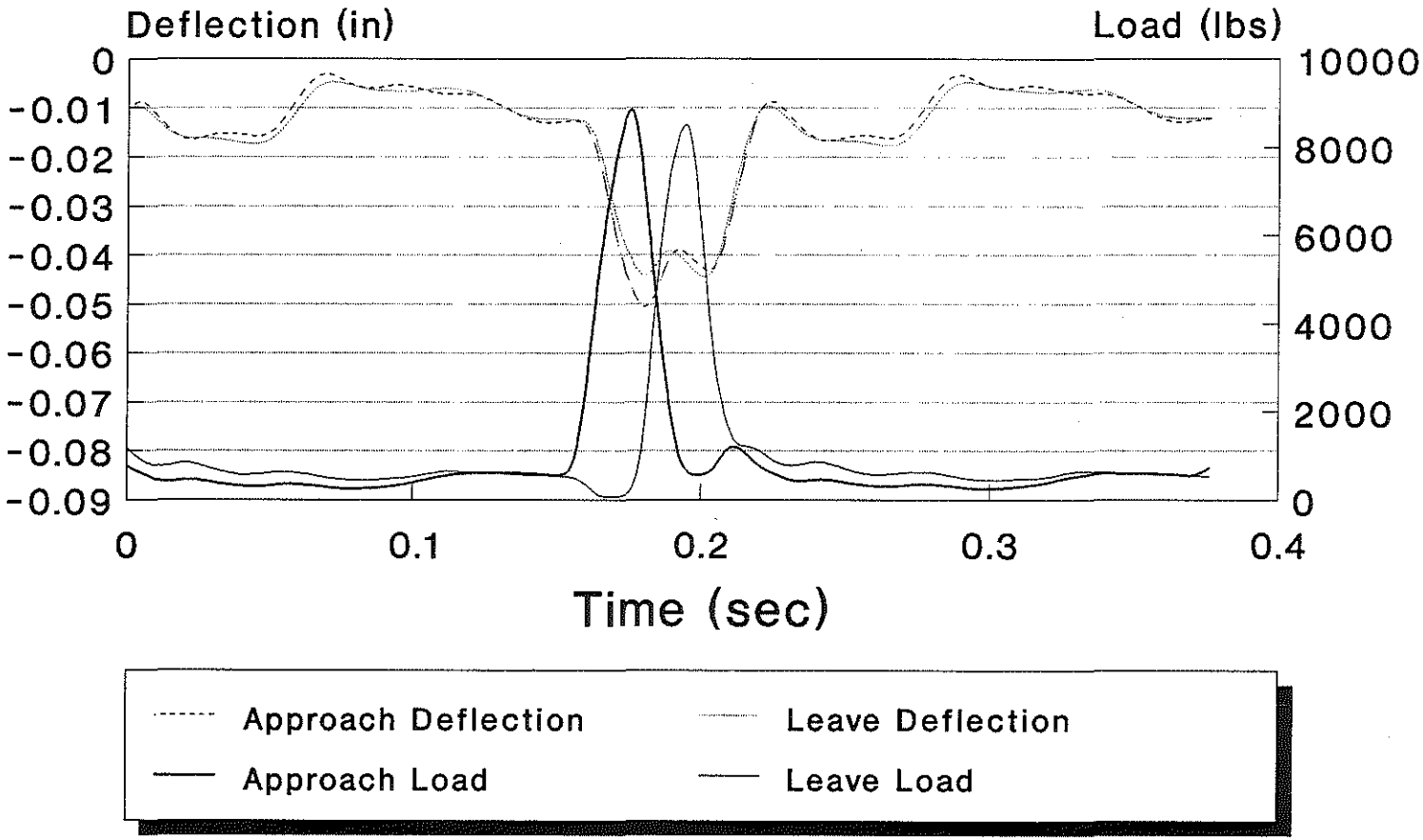

Figure A-43: Load and deflection curves for 6A 100% recycled gravel after cycle # 1.

6A 100% RECYCLED GRAVEL
CYCLE # 1000

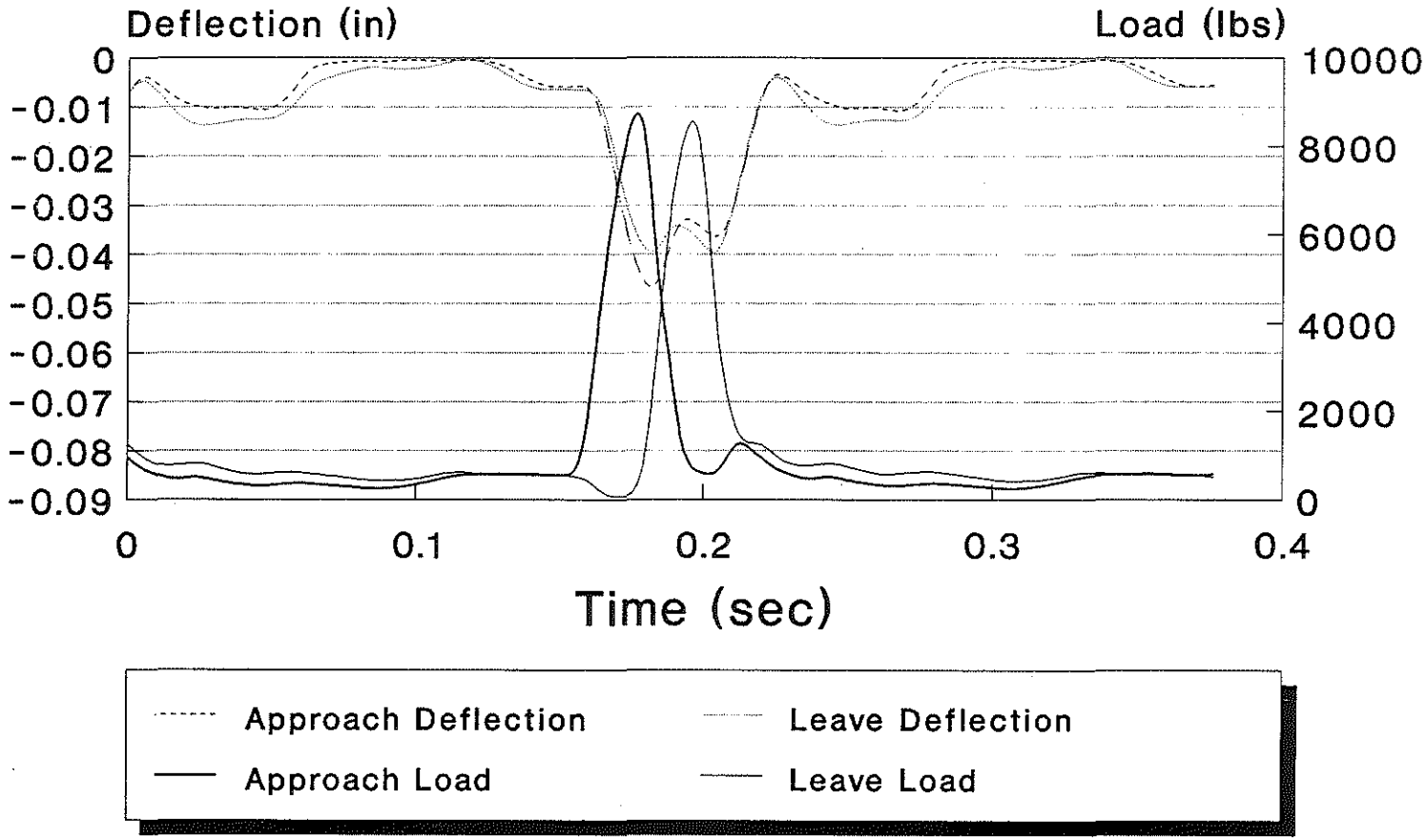

Figure A-44: Load and deflection curves for 6A 100% recycled gravel after cycle # 1,000.

6A 100% RECYCLED GRAVEL
CYCLE # 2000

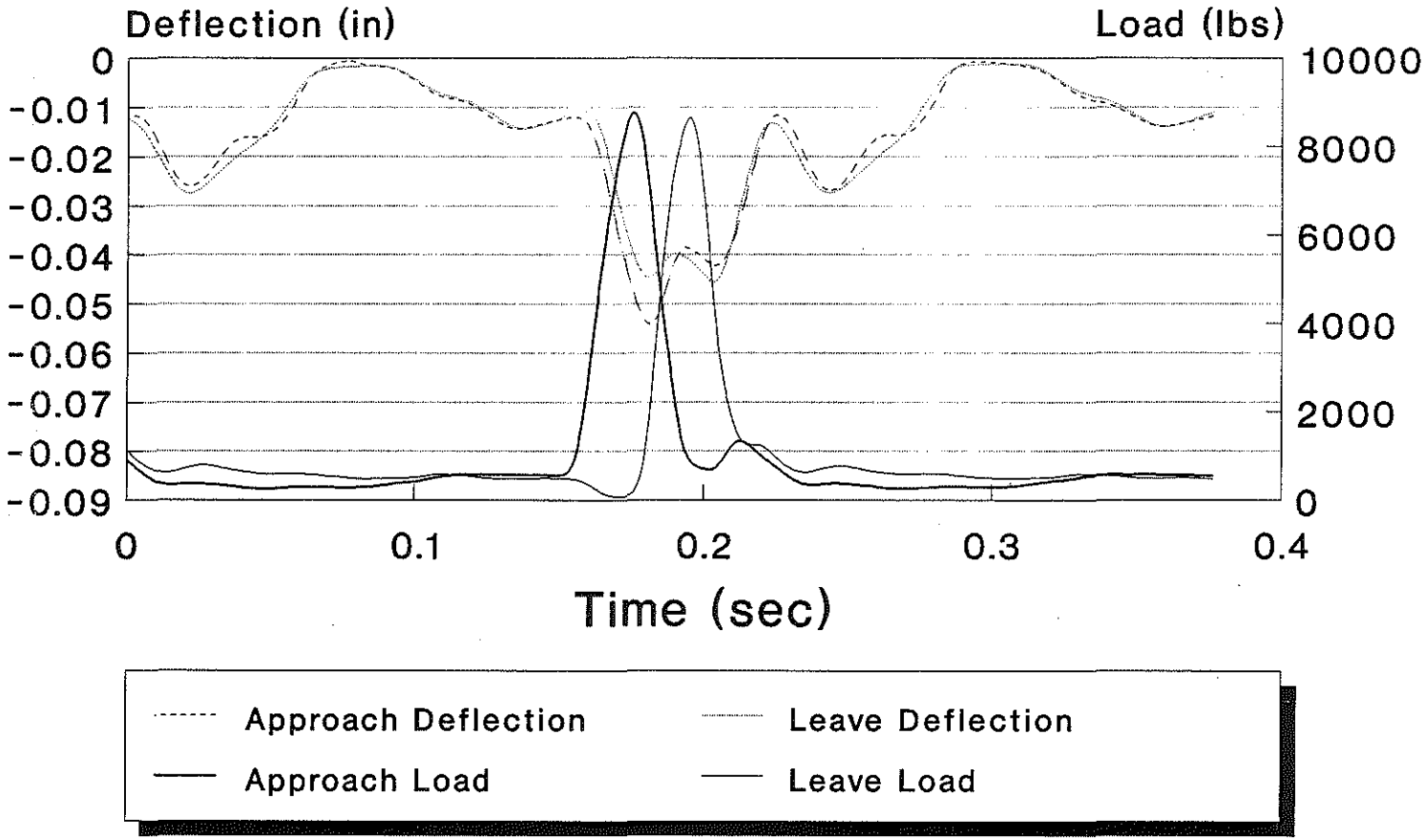

Figure A-45: Load and deflection curves for 6A 100% recycled gravel after cycle # 2,000.

6A 100% RECYCLED GRAVEL
CYCLE # 5000

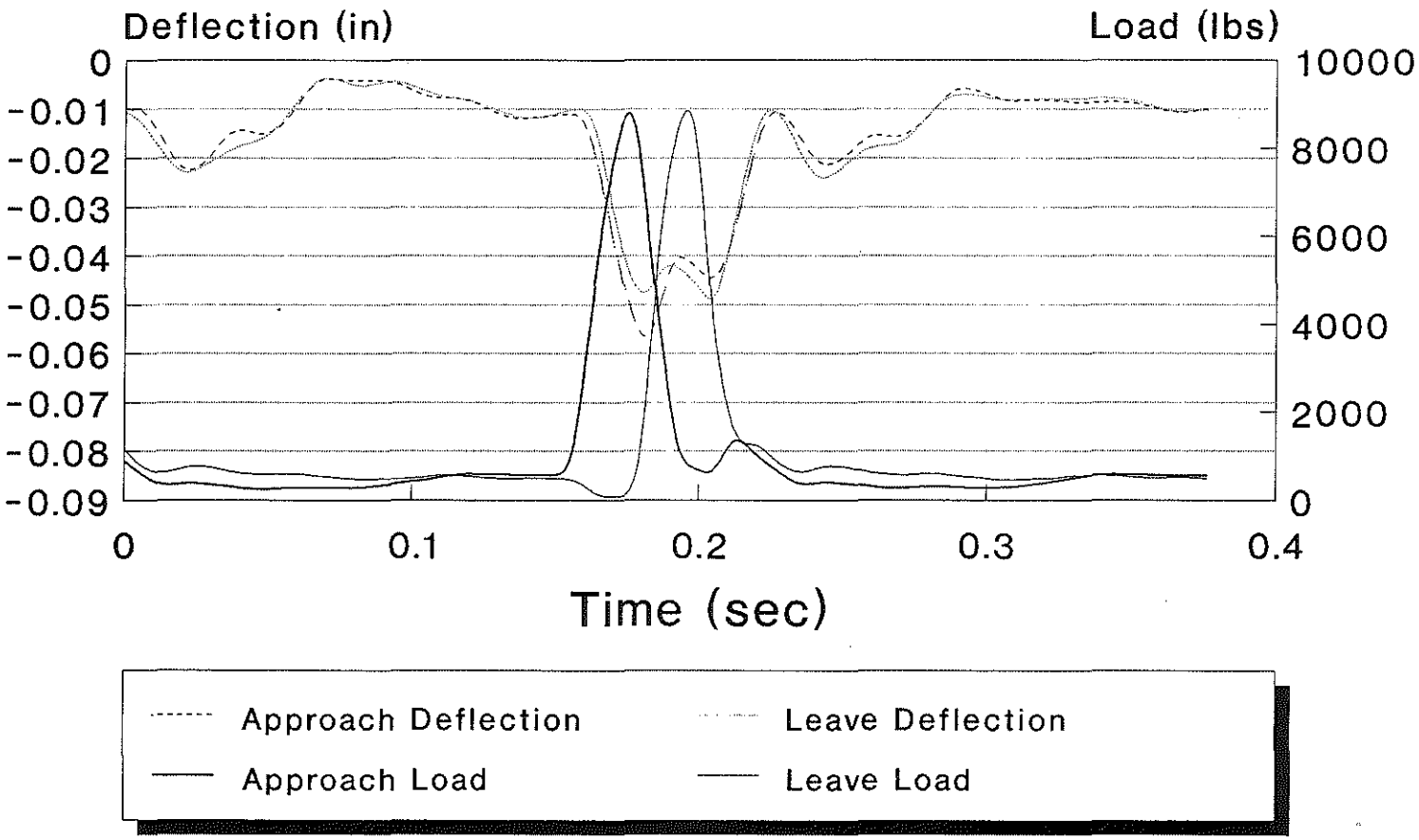

Figure A-46: Load and deflection curves for 6A 100% recycled gravel after cycle # 5,000.

6A 100% RECYCLED GRAVEL
CYCLE # 10000

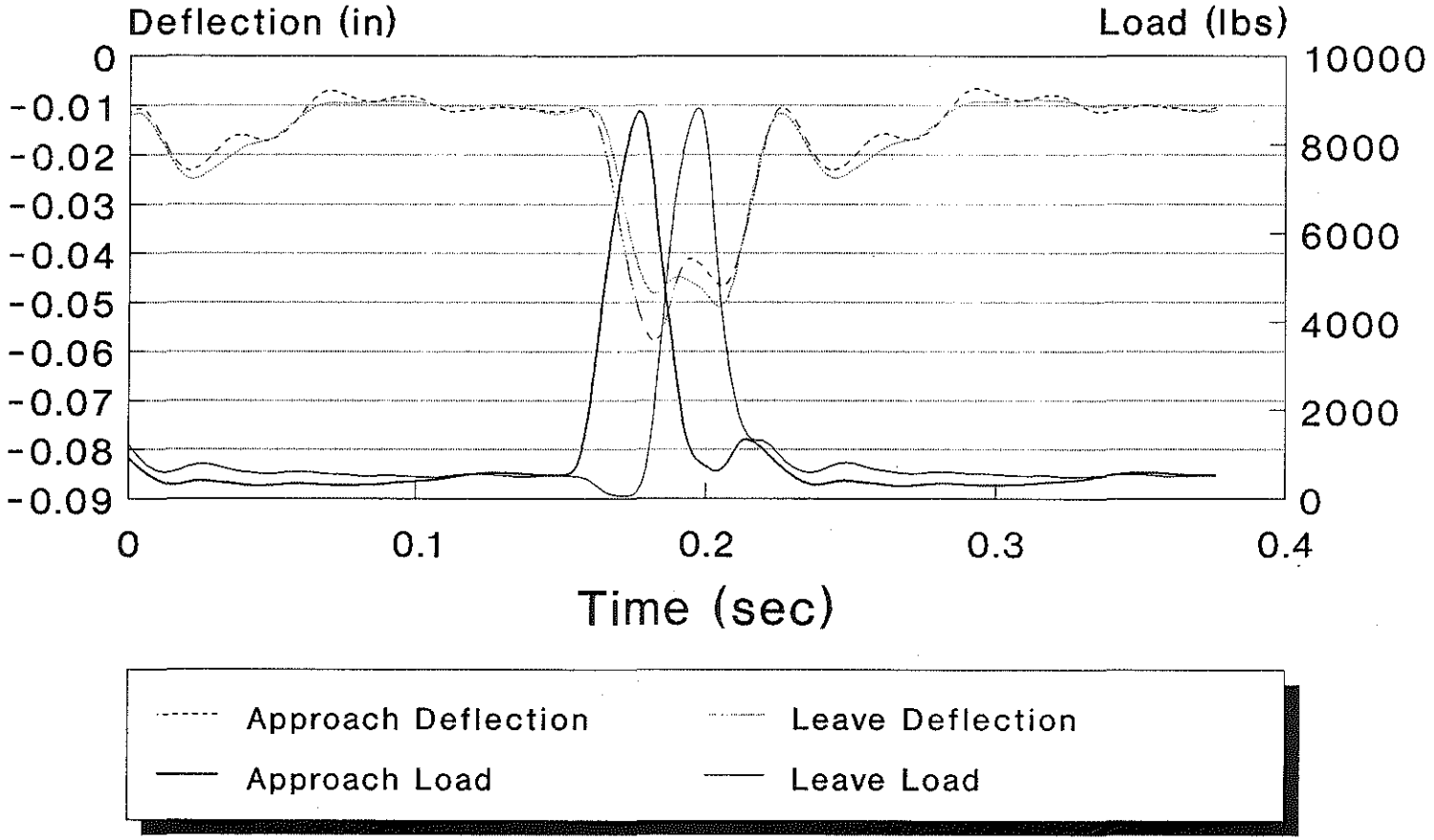

Figure A-47: Load and deflection curves for 6A 100% recycled gravel after cycle # 10,000.

6A 100% RECYCLED GRAVEL
CYCLE # 20000

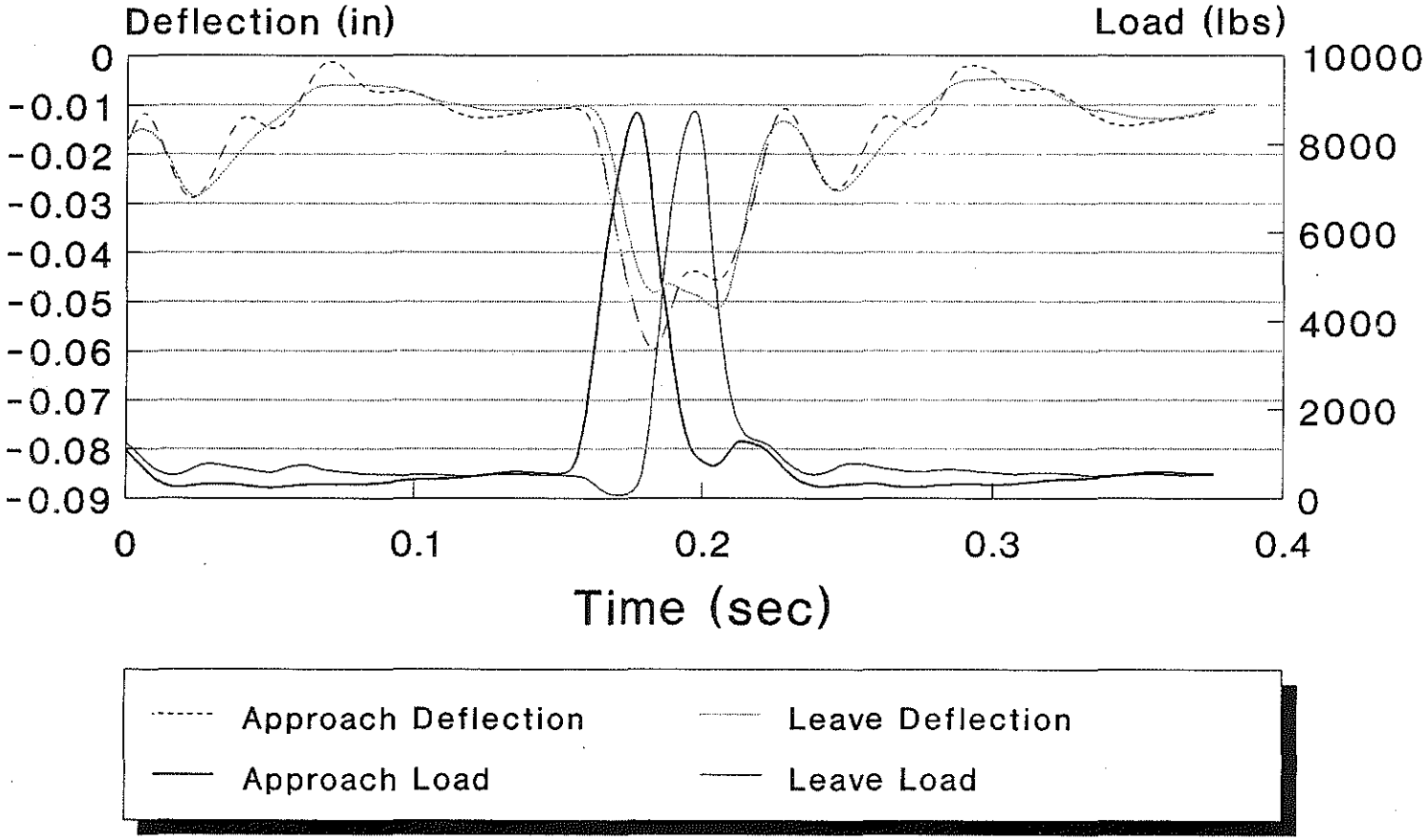

Figure A-48: Load and deflection curves for 6A 100% recycled gravel after cycle # 20,000.

6A 100% RECYCLED GRAVEL
CYCLE # 50000

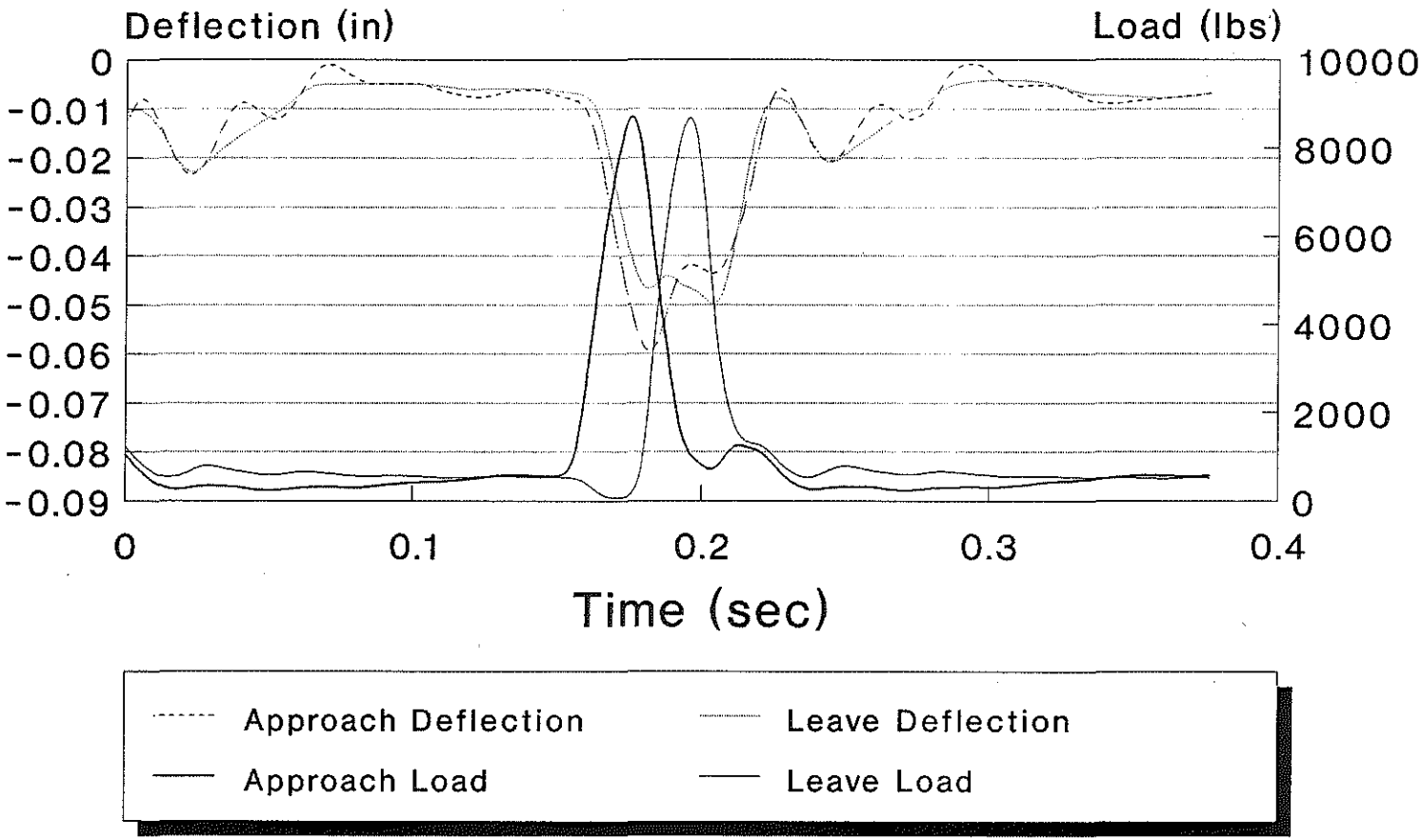

Figure A-49: Load and deflection curves for 6A 100% recycled gravel after cycle # 50,000.

6A 100% RECYCLED GRAVEL
CYCLE # 100000

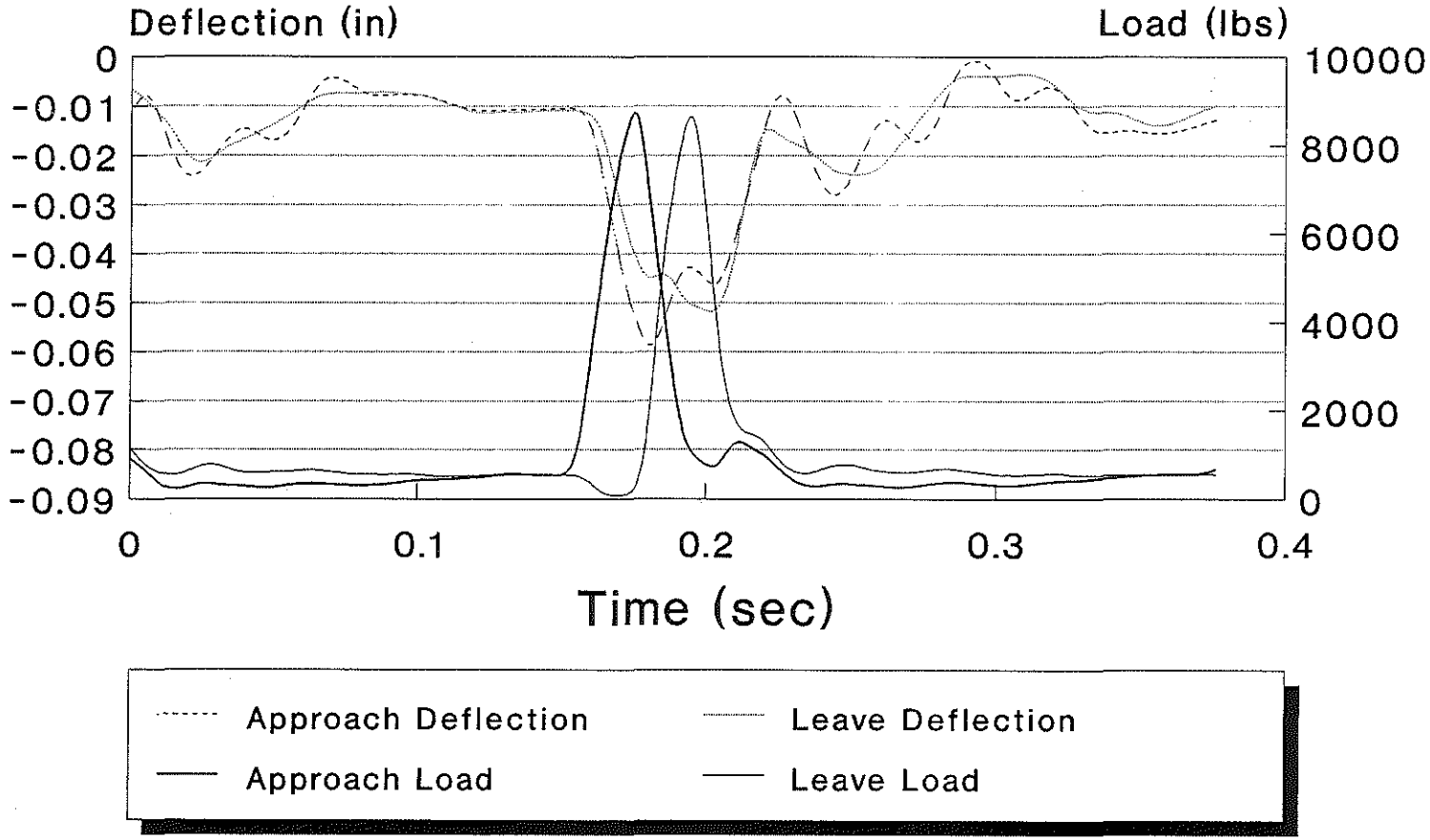

Figure A-50: Load and deflection curves for 6A 100% recycled gravel after cycle # 100,000.

6A 100% RECYCLED GRAVEL
CYCLE # 300000

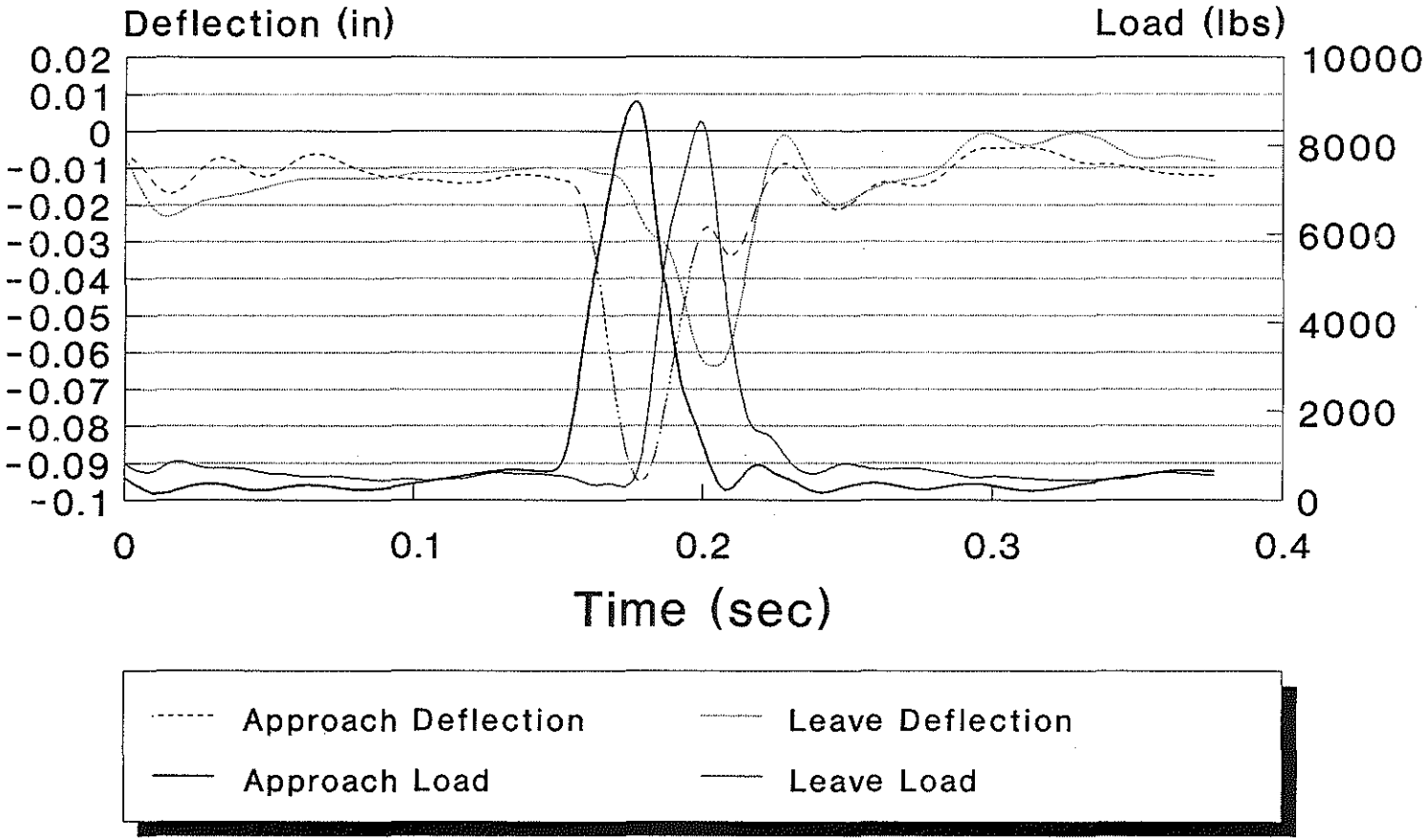

Figure A-51: Load and deflection curves for 6A 100% recycled gravel after cycle # 300,000.

50-50 RECYCLE BLEND
CYCLE # 1

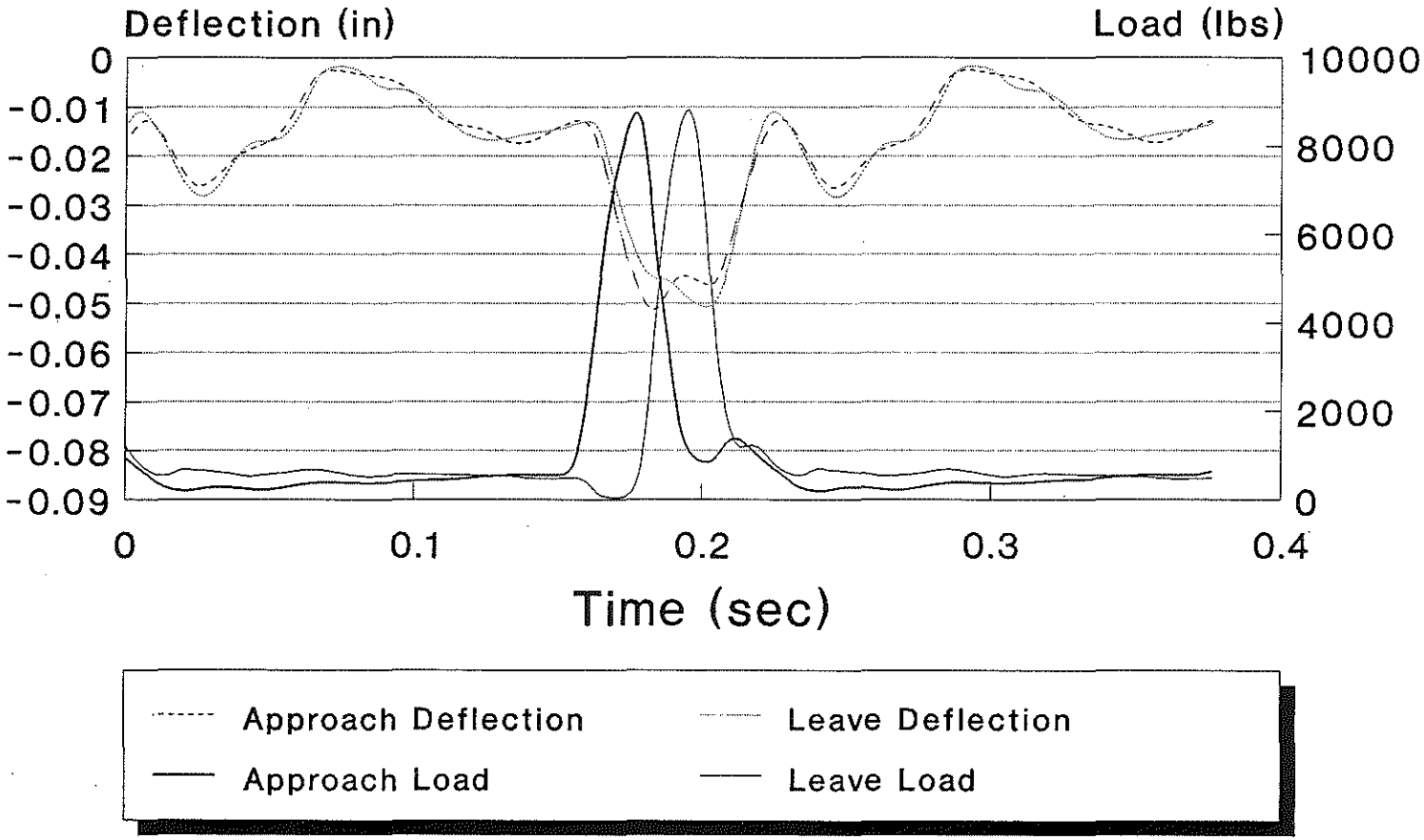

Figure A-52: Load and deflection curves for 50-50 recycled blend after cycle # 1.

50-50 RECYCLE BLEND
CYCLE # 1000

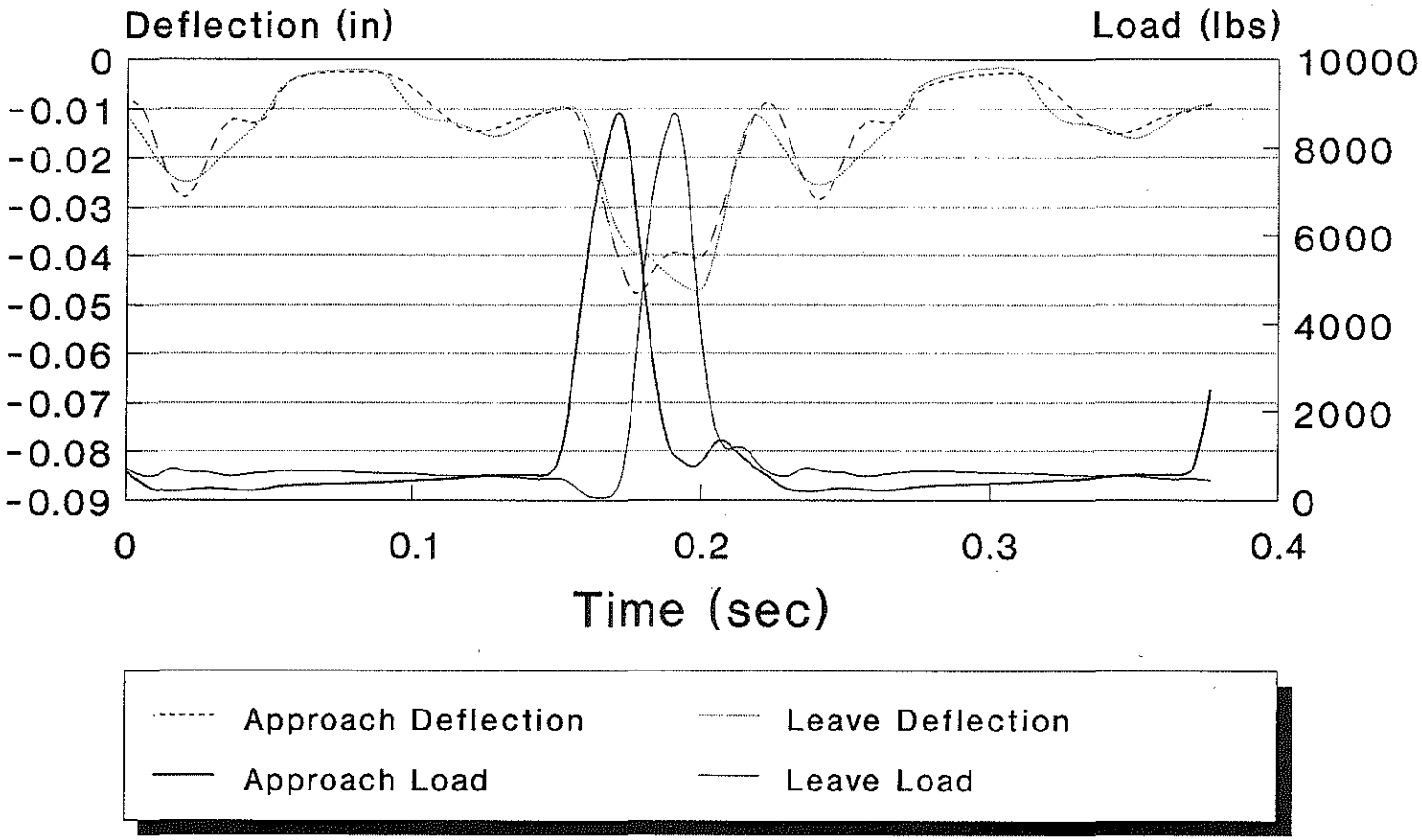

Figure A-53: Load and deflection curves for 50-50 recycled blend after cycle # 1,000.

50-50 RECYCLE BLEND
CYCLE # 5000

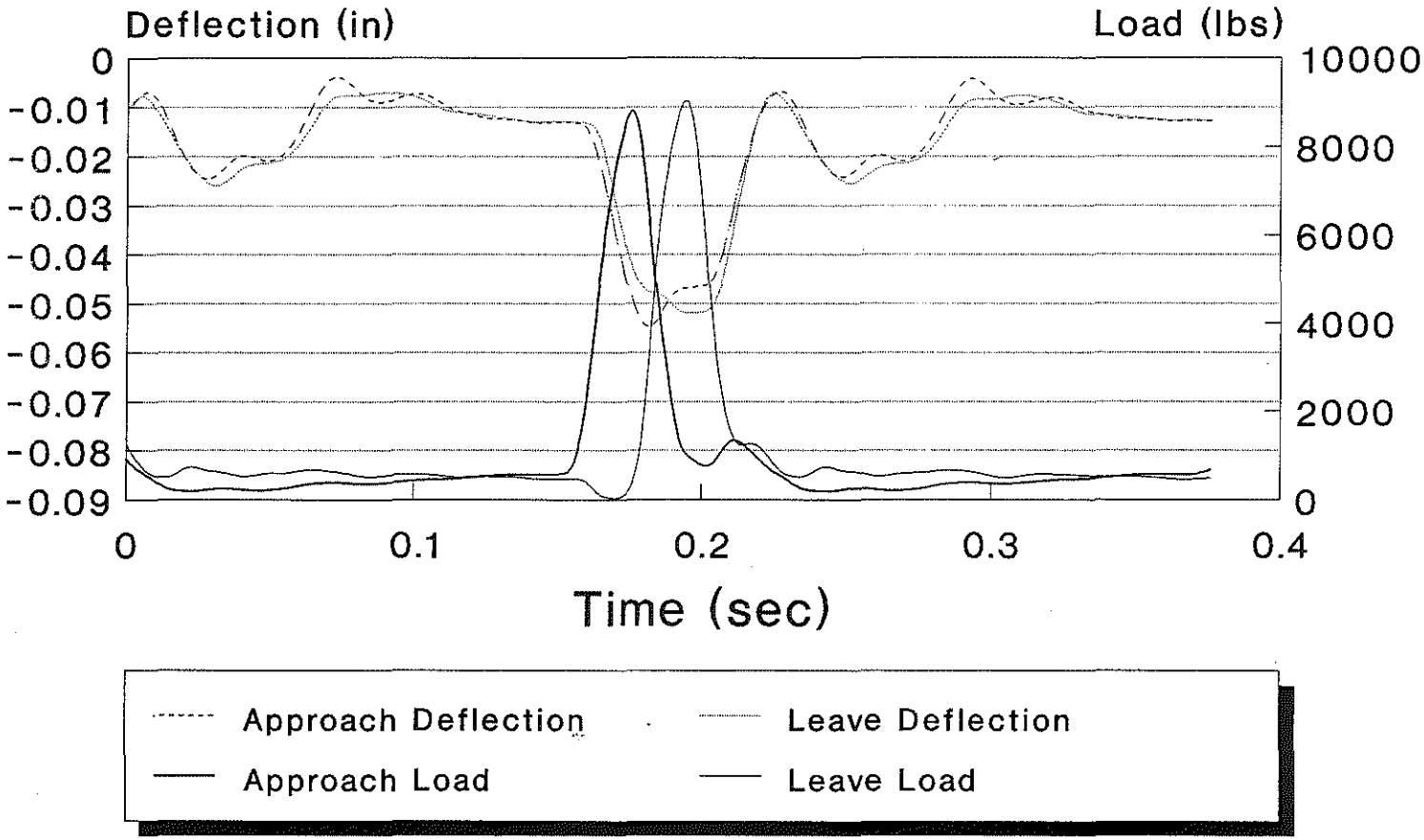

Figure A-54: Load and deflection curves for 50-50 recycled blend after cycle # 5,000.

50-50 RECYCLE BLEND
CYCLE # 10000

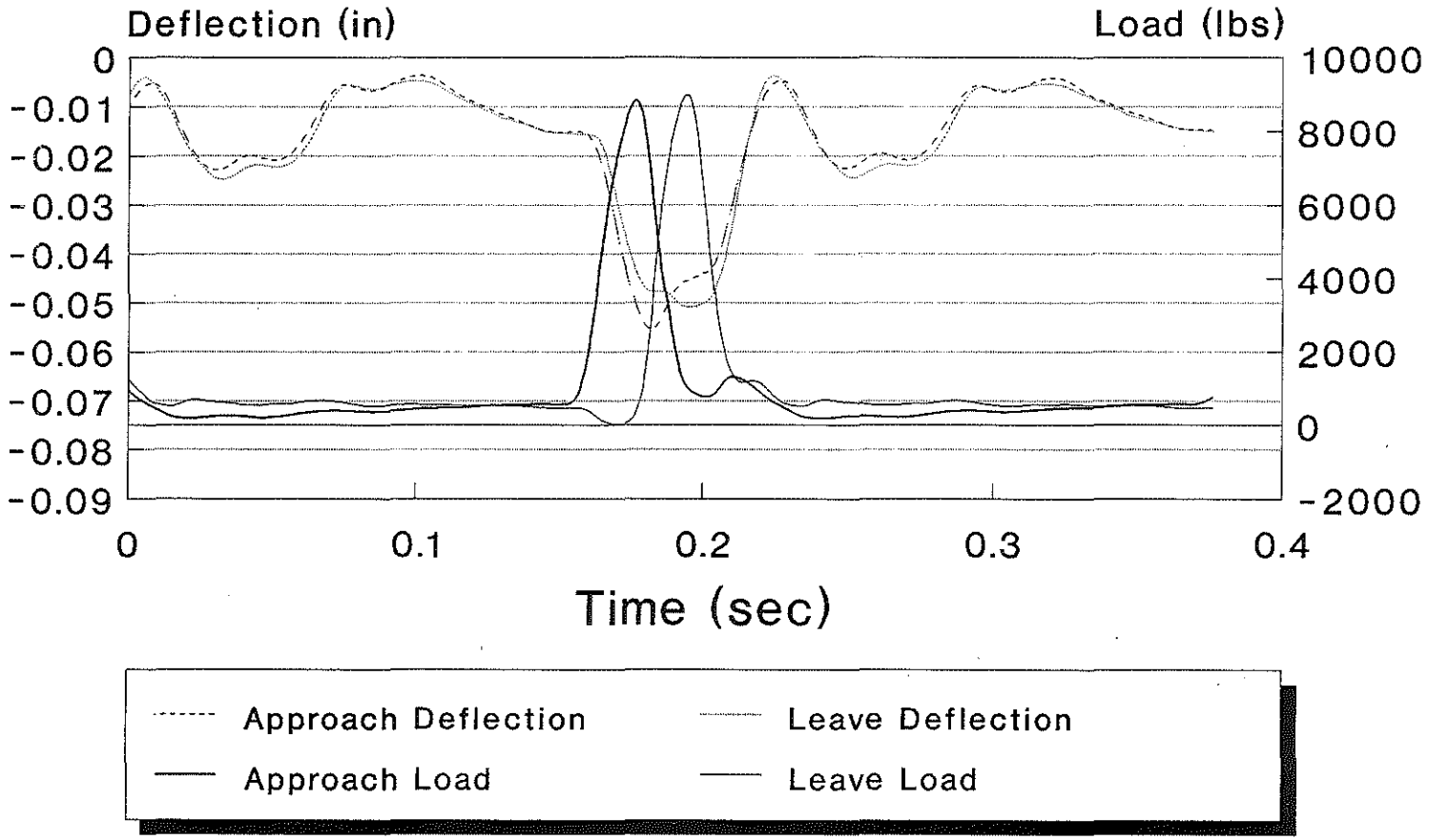

Figure A-55: Load and deflection curves for 50-50 recycled blend after cycle # 10,000.

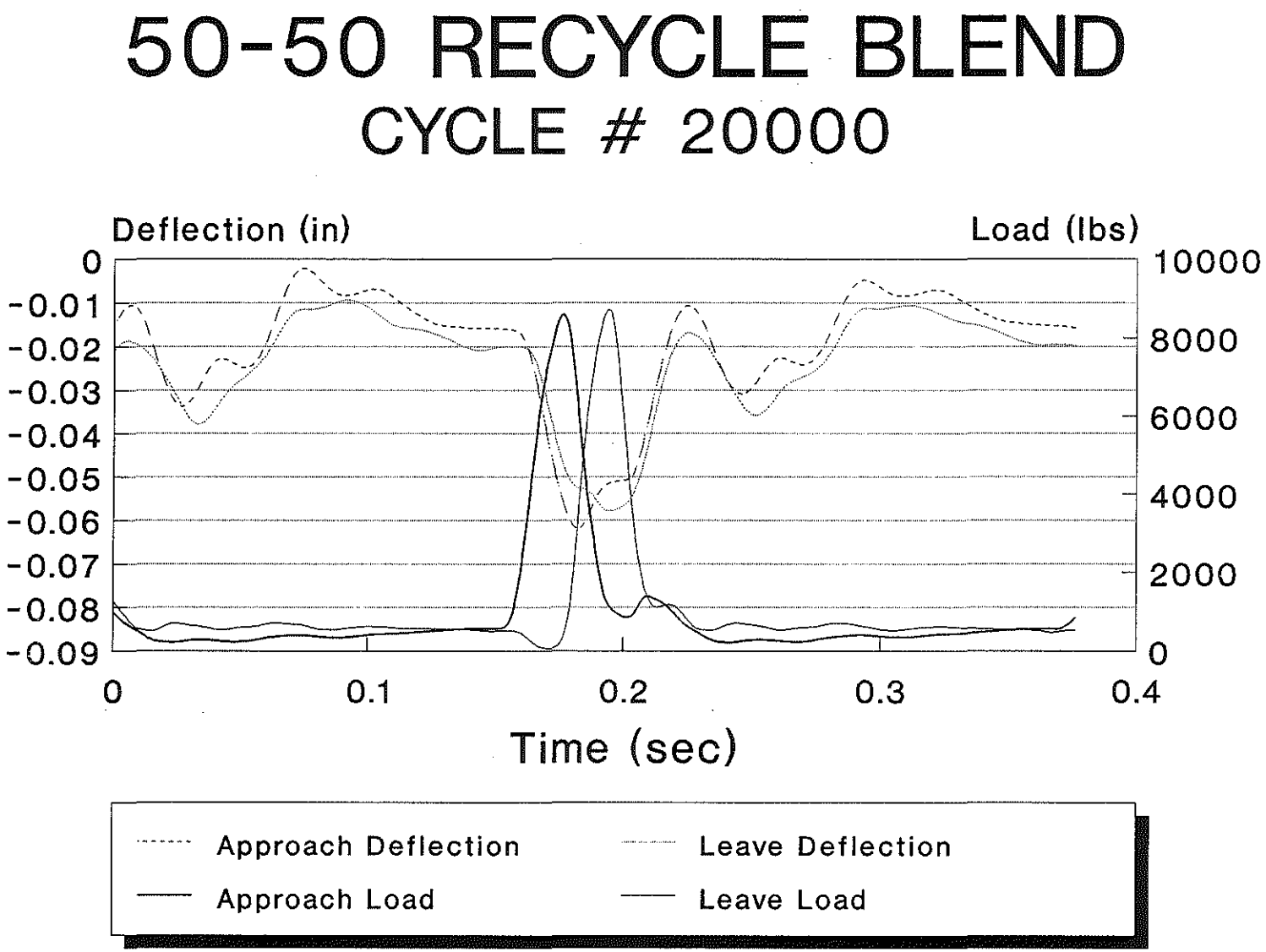

Figure A-56: Load and deflection curves for 50-50 recycled blend after cycle # 20,000.

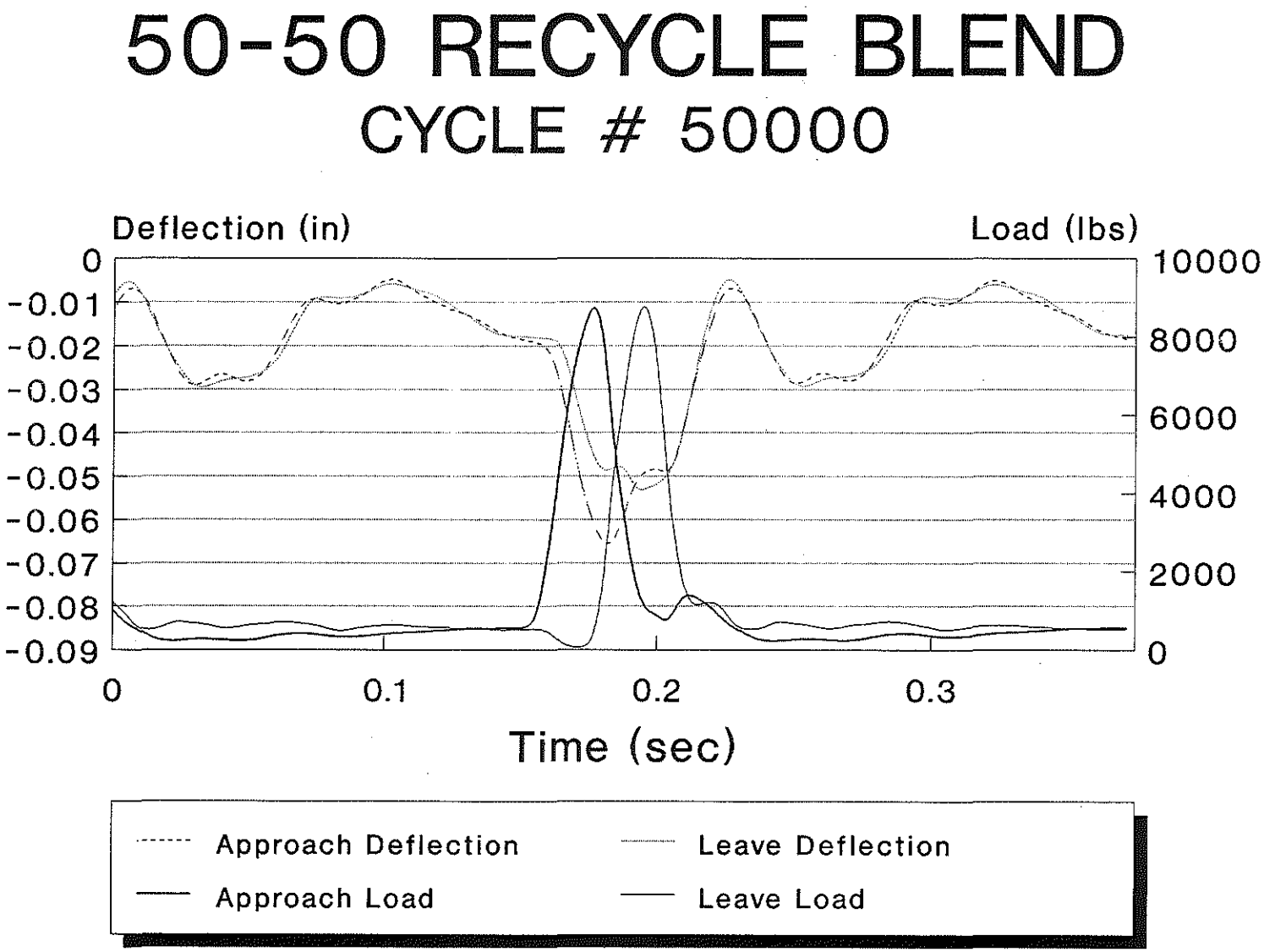

Figure A-57: Load and deflection curves for 50-50 recycled blend after cycle # 50,000.

50-50 RECYCLE BLEND
CYCLE # 100000

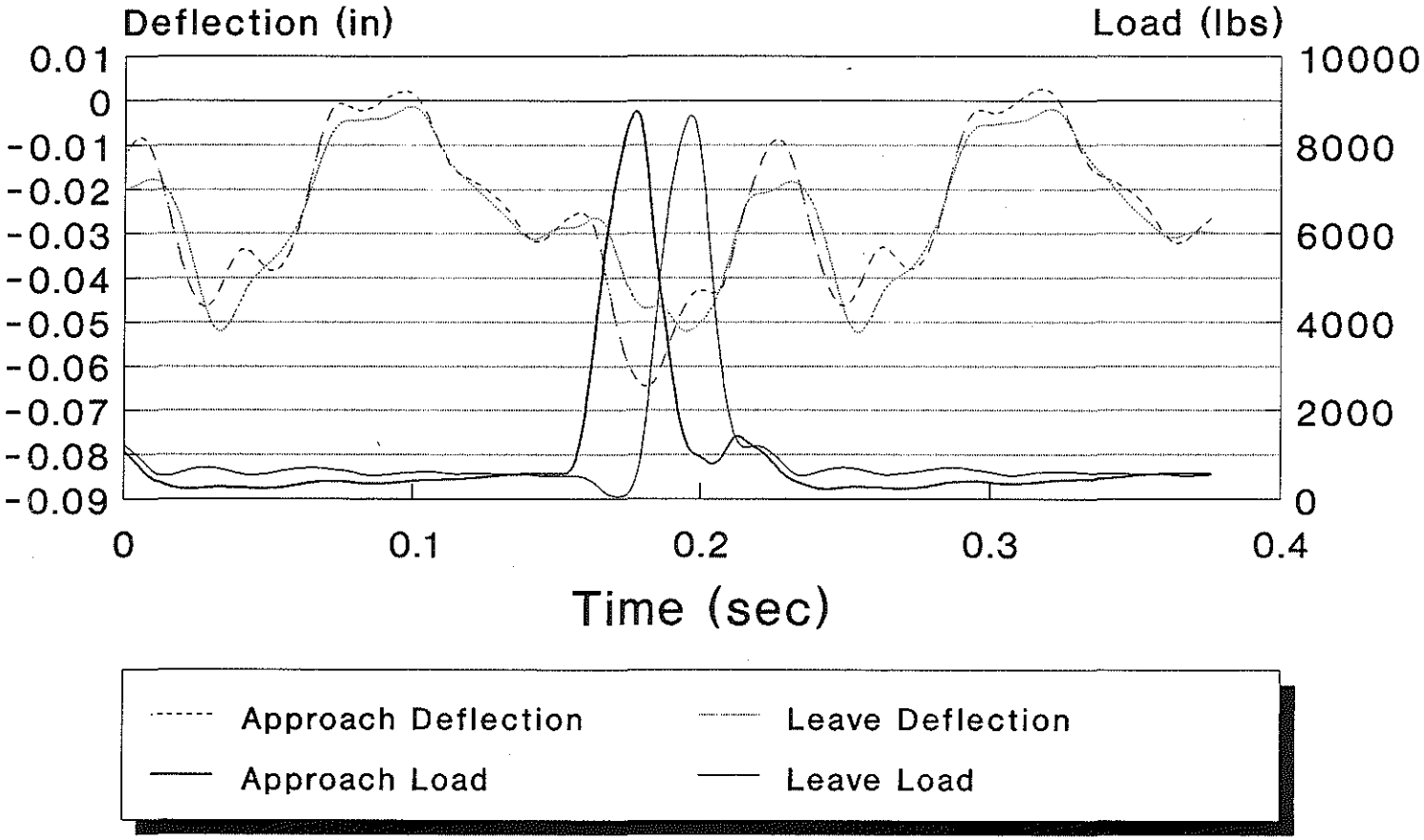

Figure A-58: Load and deflection curves for 50-50 recycled blend after cycle # 100,000.

50-50 RECYCLE BLEND
CYCLE # 300000

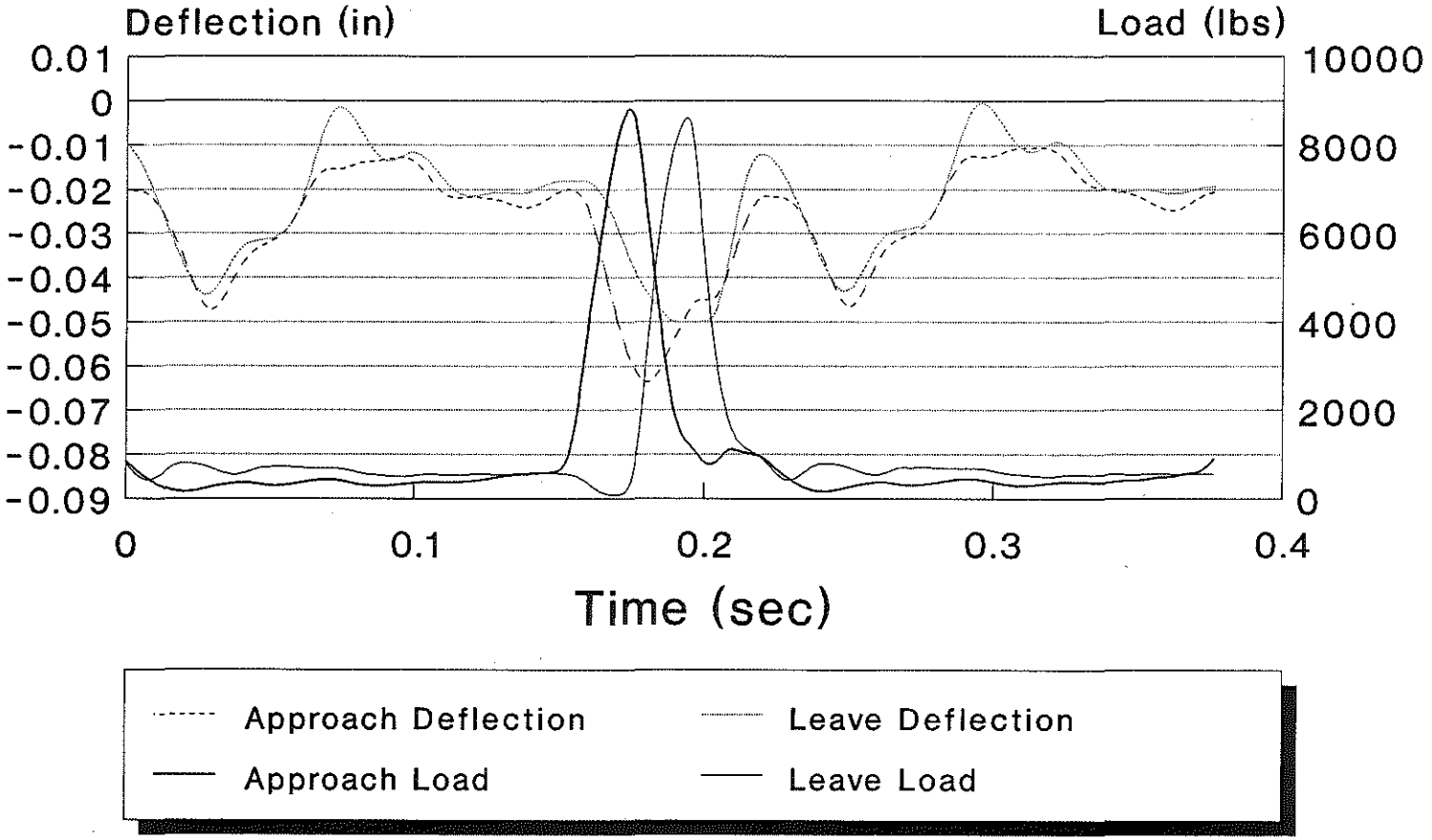

Figure A-59: Load and deflection curves for 50-50 recycled blend after cycle # 300,000.

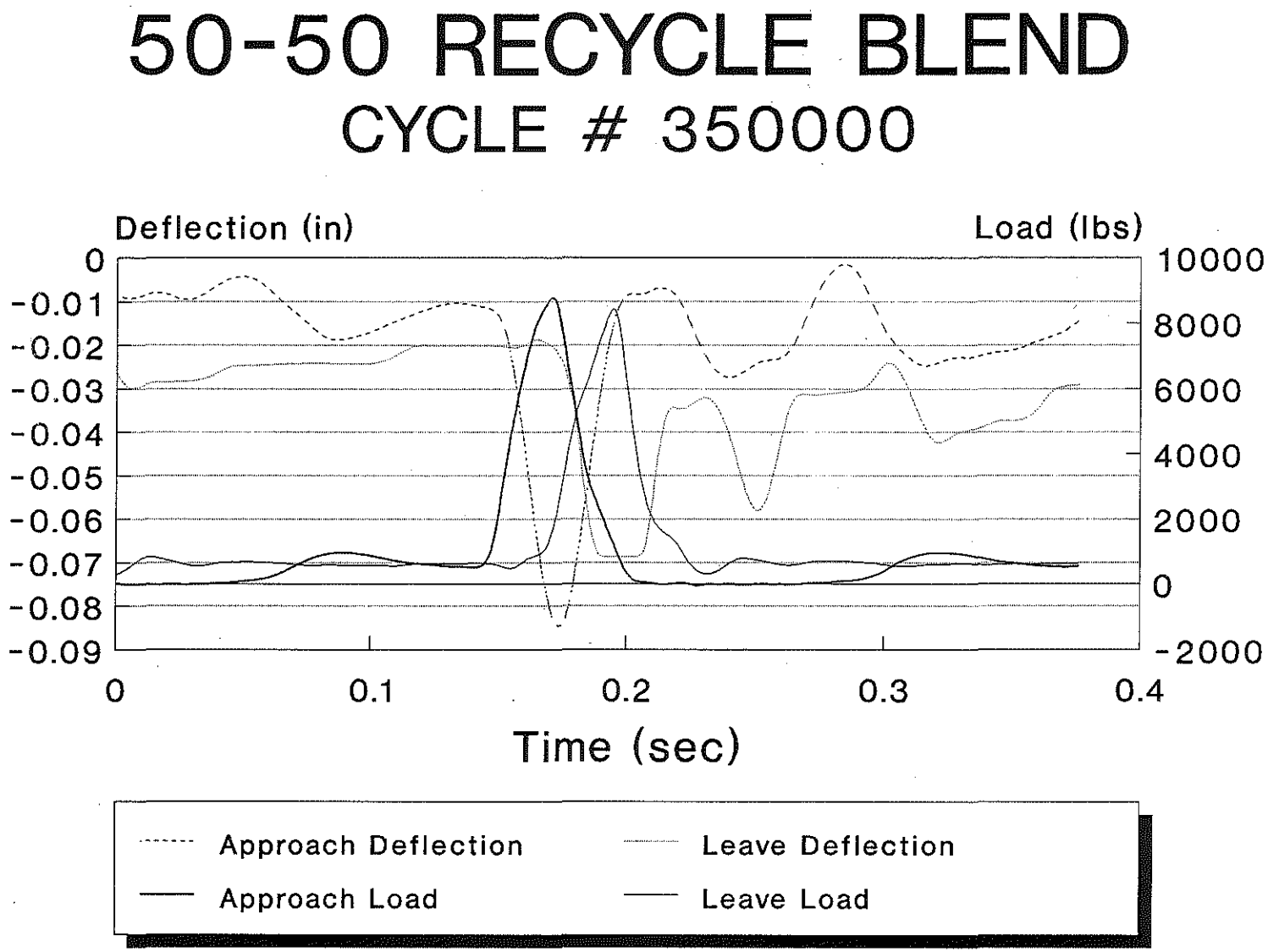

Figure A-60: Load and deflection curves for 50-50 recycled blend after cycle # 350,000.